DEVELOPING ANALYTICAL METHODS FOR TRACE LEVEL QUANTIFICATION OF DISINFECTION BY-PRODUCTS IN DESALINATED WATER AND BIOLOGICAL SAMPLE

BY

Abdulnaser Khaled Alsharaa

A Dissertation Presented to the

DEANSHIP OF GRADUATE STUDIES

KING FAHD UNIVERSITY OF PETROLEUM & MINERALS

DHAHRAN, SAUDI ARABIA

In Partial Fulfillment of the

Requirements for the Degree of

DOCTOR OF PHILOSOPHY

In

CHEMISTRY

MAY 2016

KING FAHD UNIVERSITY OF PETROLEUM & MINERALS

DHAHRAN- 31261, SAUDI ARABIA

DEANSHIP OF GRADUATE STUDIES

This thesis, written by Abdulnaser Khaled Alsharaa under the direction his thesis advisor and approved by his thesis committee, has been presented and accepted by the Dean of Graduate Studies, in partial fulfillment of the requirements for the degree of **DOCTOR OF PHILOSOPHY IN CHEMISTRY.**

Dr. Basheer Chanbasha
(Advisor)

22/5/2016

Dr. Abdulaziz Al-saadi
Department Chairman

Dr. Abdulla Abulkibash
(Member)

Dr. Salam A. Zummo
Dean of Graduate Studies

Dr. Abdel Nasser Kawde
(Member)

31/5/16

Date

Dr. Mazen Khaled
(Member)

Dr. Assad Thukair
(Member)

DEVELOPING ANALYTICAL METHODS FOR TRACE LEVEL QUANTIFICATION OF DISINFECTION BY-PRODUCTS IN DESALINATED WATER AND BIOLOGICAL SAMPLE

Ph.D. Student Name: Abdulnaser Khaled Alsharaa

Committee members

1. Advisor: Dr. Basheer Chanbasha
2. Dr. Abdulla Abulkibash
3. Dr. Abdel Nasser Kawde
4. Dr. Mazen Mohammad Khaled
5. Dr. Assad Thukair

Dedication

My parents: Thank you for your praying and unlimited support in all of my life especially with my studies. I love you.

My wife and son: Thank you for trusting and believing in me; for being with me and supporting me all the time during my PhD challenges. I love you.

My brothers and sisters: Thanks for every moment we spent together with love and support.

My Friend's: Thanks for your support and encouragement.

ACKNOWLEDGMENTS

With due gratitude to Allah (S.W.T.), The Best Planner, for making my long cherished dream a reality. I would like to acknowledge and thank King Fahd University of Petroleum & Minerals (KFUPM) for allowing me the opportunity toward this accomplishment and pursue the doctor of philosophy degree in chemistry. In this regard, I want to thank the administrators who have contributed in various ways in making this possible.

Also, it gives me great pleasure to thank my dissertation committee members who have guided me through the course of research and preparation of this thesis, they are warmly acknowledged: My advisor, Dr. Basheer Chanbasha, who has guided me through the courses of this research and preparation of this report, especial thanks for my master advisor and one of my PhD thesis committee Dr. Abdel Nasser Kawde, and warmly acknowledged to the remaining members of the committee Prof. Abdullah Abulkibash, Dr. Mazen Khaled and Dr. Assad Thukair for their efforts to improve this thesis in many different aspects.

In this regards I also want to thank National University of Singapore (NUS) where I spent summer (2015) for doing some parts of the work as a part of collaboration between KFUPM and NUS.

Finally, I would like to thank all faculty members and staff of chemistry department for their guidance and support.

TABLE OF CONTENTS

LIST OF FIGURES

LIST OF TABLES

LIST OF ABBREVIATIONS

GC-MS : Gas Chromatography Mass Spectrometry.

SPME : Solid Phase Microextraction

NAs : N-Nitrosoamines

HEs : Haloethers

FA-EE-SPME: Flow assisted Electro Enhanced Solid Phase Microextraction

LR : Linear Range

EF : Enrichment Factor

LOD : Limit of Detection

LOQ : Limit of Quantitation

R2 : Coefficient of Determination

R : Correlation Coefficient

RSD : Relative Standard Deviation

USEPA : United States Environmental Protection Agency

SPE : Solid Phase Extraction

LLE : Liquid Liquid Extraction

LPME : Liquid Phase Microextraction

HPLC : High Performance Liquid Chromatography

HF : Hollow Fiber

UA : Ultrasound Assisted

DBPs : Disinfection By Products

PDMS-DVB : Polydimethysiloxane-Divinylbenzene

PA : Poly Acrylate

FA : Flow Assisted

CW/DVB : Carbowax/Divinylbenzene

HS : Headspace

NDMA : N-nitosodimethelamine

CPPE : Chlorophenyl Phenyl Ether

BPPE : Bromophenyl Phenyl Ether

THMs : Trihalomethanes

HKs : Haloketones

HANs : Haloacetonitriles

HAAs : Haloacetic acids

MAE : Microwave Assisted Extraction

DSPE : Dispersive Solid-phase Extraction

LC-MS/MS : Liquid Chromatography-Mass Spectrometry/Mass Spectrometry

LDHs : Layer Double Hydroxides

MOS : Moringa Olifera Seeds

QS **:** Quartz Sand

US **:** Ultrasound

NFM **:** Nanofiltration Membrane

BPAC **:** Biological Powder-Activated Carbon

AOC : Assimilable Organic Carbon

SLME : Supported Liquid Microextraction

SDME : Single-Drop Microextraction

NA : Non-applicable

ND : Not Detectable

UPLC : Ultra Performance Liquid Chromatography

µ-SPE : Micro-Solid-Phase Extraction

ABSTRACT

Full Name : ABDULNASER KHALED ALSHARAA

Thesis Title : DEVELOPING ANALYTICAL METHODS FOR TRACE LEVEL QUANTIFICATION OF DISINFECTION BY-PRODUCTS IN DESALINATED WATER AND BIOLOGICAL SAMPLE

Major Field : ANALYTICAL CHEMISTRY

Date of Degree : May, 2016

Saudi Arabia does not have sufficient fresh water resources like other countries; 70% of its drinking water is from 27 desalination plants. Desalination has proven to be the most effective way of solving the country's water needs. The world's largest new desalination plant has now been completed in the Jubail, the Kingdom's Eastern Province. The existing desalination plants carry fresh water to Saudi cities by means of more than 4,000 kilometers of water pipes. The production of clean water, and its distribution requires huge amounts of electricity; yet it is critical since fresh water is crucial to the Kingdom's development, as well as its survival. Chlorination has been the most common disinfectant procedure for domestic drinking water produced by desalination. Chlorination dramatically reduces the incidence of waterborne diseases such as typhoid, cholera, and hepatitis, as well as gastrointestinal illness. However, chlorine can also react with natural materials in the raw water to form disinfection by-products (DBPs) that are hazardous to health. Long term exposure of these disinfection by-products may potentially increase the risk of cancer, apart from causing other adverse health effects. New research on human exposure to DBPs has revealed that oral ingestion is not the only major route of exposure. Inhalation while showering,

dermal absorption while bathing or during leisure activities such as swimming, can result in equivalent or even greater exposure to certain DBPs.

Interesting, no data on DBPs are available for Saudi Arabian water samples. Only limited studies have been conducted on DBPs in this region. Therefore, there is an urgent need to develop analytical methods and regularly monitor these DBPs in order to determine the composition of known and, more importantly, emerging DBPs from desalination and potable water samples to understand better the potential consequences arising from such exposure. We also need to study the bioaccumulation of these DBPs from biota samples closer to the desalination facilities to assess their impacts to biota.

Chapter 2: In this chapter, a new, highly efficient and simple extraction procedure in the determination of haloacetic acids (HAAs) in water samples has been established. Three different types of layered double hydroxides (LDHs) were synthesized and used as a sorbent in dispersive solid-phase extraction (DSPE). Due to the interesting behavior of LDHs in an acidic medium (pH<4), the analyte elution step was not needed; the LDHs are simply dissolved in acid immediately after extraction to release the analytes which are then directly introduced into a liquid chromatography-tandem mass spectrometry system for analysis. Several DSPE parameters were optimized to increase the efficiency of HAA extraction such as temperature, time of extraction and pH. Under optimum conditions, linearity was good over the concentration range of 0.05-100 µg/L, and detection limits in the range of 0.006-0.05 µg/L, with corresponding relative standard deviations of between 0.33 and 3.64% (n =6) were obtained. The proposed method was applied to different water samples collected from a drinking water plant to examine its feasibility.

Chapter 3: A single-step microwave assisted headspace liquid-phase microextraction (MA-HS-LPME) method was developed for determination of trihalomethanes (THMs), haloacwtonitrile (HANs) and haloketones (HKs) in biological samples. In this method, a porous membrane envelope was filled with few microliters of extraction solvent and then placed inside the microwave extraction vial. A PTFE ring was designed to support the membrane envelope over a certain height inside the vial. An optimum amount of biological sample was placed in the vial equipped with magnetic stirrer. After that nitric acid was added to the vial for digestion of biological sample. The sample was digested and the volatile THMs, HANs and HKs were extracted at headspace in the solvent containing porous membrane. After simultaneous digestion and extraction, the extract was injected to gas chromatography/mass spectrometry for analysis. Factors affecting the extraction efficiency were optimized to achieve higher extraction performance. Quantification was carried out over a concentration range of 0.3–100 ng/g for brominated compounds while for the chlorinated ones linear range was between 0.5–100 ng/g. Limit of detections (LODs) were ranged from 0.051 to 0.110 ng/g while limit of quantification (LOQ) were in the range of 0.175–0.351 ng/g. The relative standard deviations (RSDs) of the calibrations were ranged between 1.1 and 6.8%. The MA-HS-LPME was applied for the determination of trace level THMs, HANs and HKs in fish tissue and green alga samples.

Chapter 4: Haloethers represent a special class of disinfection byproducts which pose serious harms to humans and are carcinogenic at parts per billion levels. Flow-assisted electro-enhanced solid-phase microextraction (FA-EE-SPME) method was developed for the determination of 4-chlorophenyl phenyl ether (CPPE) and 4-bromophenyl phenyl ether (BPPE) in large volumes of water samples. Within the extraction system, different commercial SPME fibers were exposed into a 100 mL sample flowing at a rate of 50 mL/min via direct immersion mode for extraction of target

analytes. The major factors affecting the extraction efficiency such as absorption time, pump flow rate, ionic strength, applied potential, sample pH and SPME fiber type were optimized using one factor at-a-time approach. After extraction, the SPME fiber was desorbed in the injector port of gas chromatography–mass spectrometry (GC–MS). The proposed method combines advantages of electrical potential and flow system together to enhance extraction efficiency of SPME. Quantification was carried out over a concentration range of 0.5–100 µg/L and good linearity was obtained with detection limits of 0.05 and 0.07 µg/L, respectively, for CPPE and BPPE. The relative standard deviation of the calibrations was in the range of 1.1 and 3.6 %. Application of FA-EE-SPME was tested for various drinking and tap water samples collected from Eastern Province of Saudi Arabia and the method performance was compared with reported literature values.

Chapter 5: Studies have been conducted to investigate the hypothesis that *N*-nitrosodimethylamine (NDMA), one of nitrosamines, can be produced after the addition of disinfectant (involving monochloramine (MCA)) in the water treatment process. Experiments were conducted using dimethylamine (DMA) as a model precursor in presence of humic acid. NDMA was formed from the reaction between DMA and MCA indicating that it should be considered a potential DBP. The formation of NDMA increased with increased MCA concentration and showed maximum in yield when DMA was varied at fixed MCA concentrations. Addition of 0.05 and 0.5 mM of preformed MCA to a treated wastewater at pH 7.2 also resulted in the formation of 3.6 and 111 ng/L of NDMA, respectively, showing that this is indeed an environmentally relevant NDMA formation pathway. The proposed NDMA formation mechanism consists of different steps (i) the formation of 1,1-dimethylhydrazine (DMH) intermediate from the reaction of DMA with MCA followed by, (ii) the oxidation of DMH by MCA to form NDMA, and (iii) the reversible chlorine transfer

reaction between MCA and DMA which is parallel to (i). We can conclude that reactions involving MCA (as a disinfectant) are potentially important pathways for NDMA formation.

Chapter 6: Moringa oleifera seed (MOS) was used as a biosorbent for the removal of water treatment disinfection by-products (DBPs), haloethers (HEs), trihalomethanes (TMHs) and haloketones (HKs) from water samples. MOS has polar functional groups such as O-H, C=O, C-N and others which facilitate the extraction of these DBPs. Experiments were conducted in batch and fixed bed column modes. Using batch mode different parameters were optimized such as MOS dosage, sample pH, contact time and agitation speed. The effect of the thickness layer and flow rate were also studied using the fixed bed mode. Maximum adsorption occurs using the batch mode with removal efficiencies of 120.5 mg/g, 114 mg/g and 111.5 mg/g for HEs, THMs and HKs, respectively. Adsorption equilibrium followed Freundlich model and the kinetic data obeyed the pseudo-second-order model, revealing that the MOS had higher adsorption capacity than other reported sorbents. Shorter removal time with higher adsorption capacity of DBPs by MOS, suggest that this material was effective for water treatment, in dealing with the removal of the DBPs considered.

ملخص الرسالة

الاسم الكامل: عبد الناصر خالد الشرع

عنوان الرسالة: تطوير طرق تحليلية للقياس الكمي للمستويات القليلة للمركبات الناتجة عن تحلية المياه وذلك في عينات المياه و العينات البيولوجية

التخصص: الكيمياء التحليلية

تاريخ الدرجة العلمية: مايو 2016

تعتبر المملكة العربية السعودية من البلدان التي لا تمتلك موارد مائية كافية كباقي البلدان , ما يقارب 70% من مياه الشرب فيها يتم تأمينه من محطات التحلية (27 محطة تحلية بالمملكة). عملية التحلية هي الأكثر فاعلية لحل مشاكل نقص مياه الشرب. أكبر محطة تحلية مياه تم انشاؤها مؤخرا بمدينة الجبيل بالمنطقة الشرقية. تعتبر عملية الكلورة الطريقة الاكثر استخداما بمحطات التحلية. وتستخدم الكلورة للتقليل من الامراض الناتجة عن البكتريا مثل التفوئيد و الكوليرا و فيروس الكبد الوبائي. ولكن بنفس الوقت مادة الكلورين المضافة ممكن ان تتفاعل مع المركبات الطبيعية العضوية الموجودة بالمياه لتشكل مركبات جانبية ضارة جدا تدعى (Disinfection by-products) . التعرض بشكل كبير ولمدة طويلة لمثل هذه المركبات يزيد من احتمالية الاصابة بمرض السرطان وكذلك امراض جانبية اخرى. الابحاث الحالية اثبتت ان ليس فقط التعرض لهذه المربات عن طريق الفم يعتبر خطيرا وانما ايضا عن طريق الاستنشاق او حتى السباحة يمكن ان يؤدي الى بعض الاخطار. ومن الغريب انه لا يوجد معلومات كافية عن هذه المركبات بما يتعلق بالمملكة العربية السعودية. ولذلك يعتبر من المهم جدا وبشكل عاجل تطوير طرق تحليلية حديثة لتحديد هذه المركبات وتحليلها بشكل دوري بعينات مختلفة من المياه ومن العينات البيولوجية المتواجدة بالقرب من محطات التحلية.

الوحدة الثانية: تم تطوير طريقة حديثة لتحليل مركبات (THMs) و (HANs) و(HKs) في العينات البيولوجية باستخدام طرق الاستخلاص السائلة وبمساعدة المايكروف تسمى هذه الطريقة (MA-HS-LPME). يتم تعبئة غشاء بمحلول عضوي للاستخلاص ومن ثم وضعه بانبوب جهاز المايكروف على ارتفاع معين وبمساعدة حلقات لتثبيت الغشاء. يتم وضع العينة البيولوجية داخل الانبوب بالاضافة لمحرك مغناطيسي كما يتم اضافة حمض الازوت لتتم عملية هضم العينة البيولوجية بشكل كامل. بهذه الطريقة يتم استخلاص المركبات الطيارة بواسطة المحلول الموجود داخل الغشاء. ومن ثم حقن المحلول بجهاز الكروماتوغرافيا الغازية المتصلة بمطيافية الكتلة. تم دراسة كافة العوامل التي تؤثر على عملية الاستخلاص لزيادة الفعالية. بالنسبة لمركبات البروم كان المجال الخطي بين (0.3–100 ng/g) بينما المركبات الكلورية بين (0.5–100 ng/g). حدود

كشف هذه الطريقة تتراوح بين (0.051 to 0.110 ng/g). تم تحديد مركبات (HANs) و (THMs) و(HKs) في أنسجة الأسماك وعينات الطحالب الخضراء.

الوحدة الثالثة: تمثل مركبات الهالوايثر (HEs) فئة خاصة من المنتجات الثانوية التي تشكل أضرارا خطيرة للإنسان وأنها ربما تكون مسببة للسرطان. تم تطوير طريقة استخلاص حديثة تسمى (FA-EE-SPME) لتحديد 4-كلورو فينيل الايثير (CPPE) و 4 برومو فينيل الايثير (BPPE) في كميات كبيرة من عينات المياه. داخل منظومة الاستخراج، تعرض مختلف الألياف SPME التجاري في عينة 100 مل تتدفق بمعدل 50 مل بالدقيقة عن طريق وضع الغمر المباشر. العوامل الرئيسية التي تؤثر على كفاءة الاستخلاص مثل الوقت ، ومعدل تدفق المضخة، القوة الأيونية، تطبيق، عينة pHو SPME نوع من الألياف. بعد استخراج الألياف SPME يتم حقنها في جهاز كروماتوغرافية الغازية المتصلة بكاشف الكتلة (GC-MS). الطريقة المقترحة يجمع بين مزايا الجهد الكهربائي ونظام تدفق معا لتعزيز كفاءة استخراج SPME. أجري التحليل الكمي من خلال مجموعة تركيز ،5-100 ميكروغرام بالليتر وتم الحصول على نتائج جيدة مع حدود الكشف 0.05 و 0.07 ميكروغرام بالليتر، على التوالي، لCPPE وBPPE. كان الانحراف المعياري النسبي من المعايرة في حدود 1.1 و 3.6٪. تم اختبار تطبيق FA-EE-SPME لمختلف عينات مياه الشرب ومياه الصنبور التي تم جمعها من المنطقة الشرقية من المملكة العربية السعودية و مقارنة اداء الطريقة مع التقارير السابقة بهذا المجال.

الوحدة الرابعة: في هذه الدراسة، تم ايجاد طريقة استخلاص جديدة وفعالة للغاية وبسيطة لتحديد مركبات haloacetic acids (HAAs) في عينات المياه. تم استخدام ثلاثة أنواع مختلفة من هيدروكسيدات مزدوجة الطبقات (LDHs) واستخدامها في طريقة التشتت استخراج المرحلة الصلبة (DSPE). ويرجع ذلك إلى سلوك هذه المركبات LDHs في الوسط الحمضي (PH)، حيث انه لا توجد حاجة لتحليلها. ويتم حل LDHs ببساطة في حمض مباشرة بعد استخراجها و حقنها مباشرة بجهاز الكروماتوغرافية السائلة المتصلة بمطيافية الكتلة. تم دراسة العوامل المختلفة لزيادة كفاءة الاستخلاص لمركبات HAA مثل درجة الحرارة والوقت ودرجة الحموضة. تحت الظروف المثلى، كانت النتائج جيدة على نطاق التركيز ،0.5-100 ميكروغرام / لتر، وحدود الكشف في نطاق ،006-،0.5 ميكروغرام / لتر، مع انحرافات معيار النسبية بين 0.33 و 3.64٪. تم تطبيق الطريقة المقترحة لعينات مختلفة من المياه التي تم جمعها من محطة مياه الشرب.

الوحدة الخامسة: أجريت هذه الدراسة للتاكد في الفرضية القائلة بأن N-nitrosodimethylamine (NDMA)، واحدة من النتروزامين، يمكن أن تنتج بعد إضافة مطهر التي تشمل monochloramine (MCA) في عملية معالجة المياه. وأجريت

التجارب باستخدام ثنائي ميثيل أمين (DMA). تشكلت NDMA من التفاعل بين هذه المركبات إلى أنه ينبغي النظر في DBP المحتملين. وزاد تشكيل NDMA مع زيادة تركيز هذه المركبات وأظهر أقصى حد عندما اختلفت DMA بتركيزات MCA الثابتة. أدت إضافة 0.05 و 0.5 ملم من MCA لمياه الصرف الصحي المعالجة في درجة الحموضة 7.2 أيضا في تكوين 3.6 و 111 نانوغرام / لتر من NDMA، على التوالي، وتبين أن هذا هو في الواقع NDMA تشكيل مسار ذات الصلة بالبيئة. آلية تشكيل NDMA المقترحة تتكون من الخطوات المختلفة (أ) تشكيل 1،1-dimethylhydrazine (ب) أكسدة DMH لتشكيل NDMA، و (ج) نقل الكلور العكسي . يمكننا أن نستنتج أن وجود MCA (كمطهر) يحتمل أن يكون من الاسباب الهامة لتشكيل NDMA

الوحدة السادسة: في هذه الدراسة تم استخدم بودرة بذور المورينغا (MOS) باعتباره مادة طبيعية للامتزاز لإزالة مركبات معالجة المياه (DBPs)، haloethers (HEs)، trihalomethanes (THMs) وhaloketones (HKS) من عينات المياه. MOS تحتوي على مجموعات وظيفية القطبية مثل O-H، C = O، C-N وغيرها مما يسهل استخراج هذه المركبات DBPs. وأجريت التجارب بطريقتين اولا طريقة الدفعات والثانية طريقة العمود الثابت. وقد تم دراسة عوامل مختلفة مثل كمية الجرعة، الرقم الهيدروجيني، وقت الاتصال، وسرعة التهيج. تم دراسة تأثير سماكة الطبقة ومعدل التدفق أيضا باستخدام طريقة العمود الثابت. يحدث امتصاص الحد الأقصى باستخدام دفعة واسطة مع كفاءات إزالة 120.5 ملغم / غم، 114 ملغ / غ و 111.5 ملغم / غم HEs، THMs وHKS، على التوالي. و اكدت النتائج ان لهذه المادة قدرة امتصاص أعلى من مواد ماصة أخرى. حيث كان أقصر وقت إزالة مع قدرة امتصاص عالية من DBPs، نشير إلى أن هذه المواد كانت فعالة لمعالجة المياه، في التعامل مع إزالة DBPs.

CHAPTER 1

INTRODUCTION

1.1 OVERVIEW

The kingdom of Saudi Arabia has undergone tremendous changes over the past decades in relation to management of its water resources. Recently estimated that up to 11 million m^3 of desalinated water is produced daily in Saudi Arabia.

Disinfection of drinking water is one of the essential water treatment processes to inactivate microbial pathogens that saves millions of lives from infectious diseases such as cholera and typhoid [1]. Chlorination is the most common disinfectant used in current desalination systems, with chloramines and chlorine dioxide gaining more popularity for disinfection of desalinated water. Disinfection byproducts (DBPs) are unintentionally produced from the reactions of disinfectants with organic matter naturally present in the water [2]. Over 600 DBPs have been identified in drinking water treated with common disinfectants, usually strong oxidants, including chlorine, chlorine dioxide, chloramines, and ozone. Figure 1 shows chemical structure for some of DBPs.

Among DBPs identified in saline drinking waters, haloacetonitriles (HANs), haloacetic acids (HAAs), halonitromethanes (HNMs), nitrosodimethylamine (NDMA) and cyanogen bromide (CNBr) pose potential concerns, especially when desalinated waters are blended with organic-matter rich source waters.

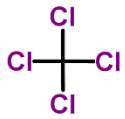

carbon tetrachloride

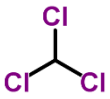

chloroform

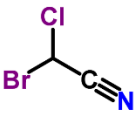

bromochloroacetonitrile

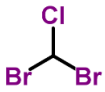

dibromochloromethane

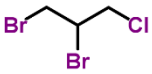

1,2-dibromo-3-chloropropane

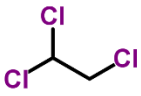

1,1,2-trichloroethane

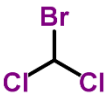

bromodichloromethane

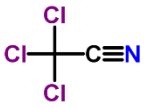

trichloroacetonitrile

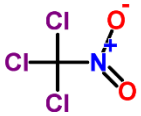

chloropicrin

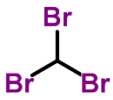

bromoform

tetrachloroethylene

Figure 1 Chemical structure of some DBPs

Many of the DBPs have been shown to cause cancer, and reproductive and developmental defects in laboratory animals [3]. They are harmful to humans and are suspected carcinogens even at low parts per billion (ppb) levels. The determination of various DBPs in drinking water generally requires of an appropriate extraction and isolation step by which analytes enrichment is achieved, before the actual analysis.

On the other hand, exposure to desalination discharges has been shown to lead to detectable marine ecological impacts which includes phytoplankton, invertebrate and fish. Massive losses of coral, plankton and fish in the Hurghada region of the Red Sea have been attributed to desalination discharges [4].

Many DBPs could also pose risks to aquatic ecosystems. In particular, phytoplankton and aquatic macrophytes appear to be particularly sensitive [5]. A review of available literature indicated that the most sensitive species for which data are available is the green alga *Scenedesmus subspicatus*, which showed a decrease in growth at concentration of monochloroacetic acid and monobromoacetic acid of 7 and 20 µg\L, respectively. Additional research is needed to assess the biotoxicity of other DBPs [5]

However, limited literature are reported on the impact assessment and bioaccumulation of disinfection by products in biota samples and no scientific data is available for eastern province where the world biggest water desalination plant is located.

The following reaction scheme (I) showing the chemistry of DBPs formation in water samples

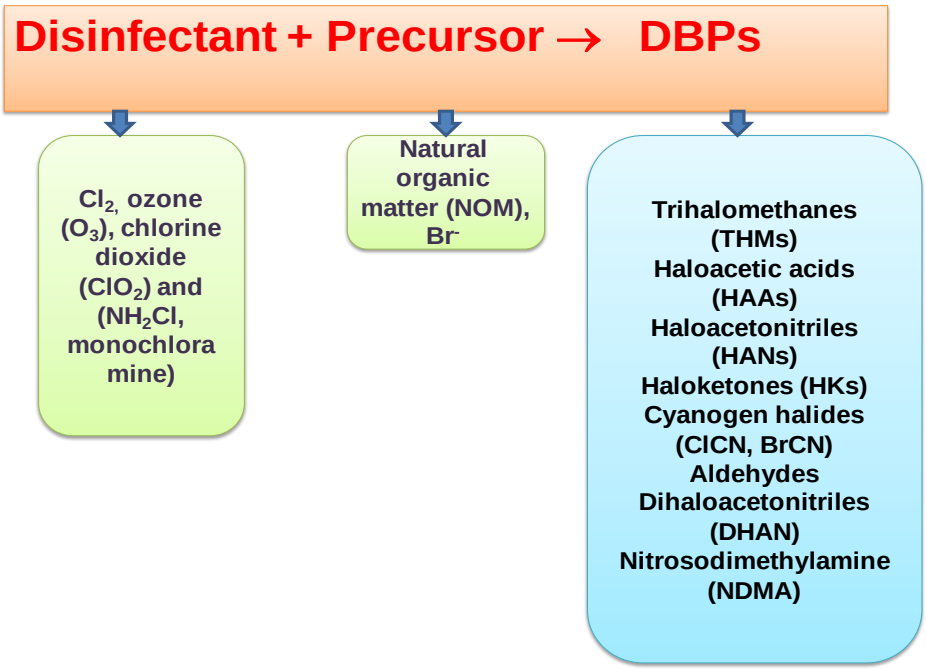

Water authorities and agencies in the world are currently reviewing the regulations for newly emerging DBPs and they could well be introduced soon. The existing regulations (for THMs and HAAs) have led many drinking water suppliers to change their disinfection practices over the last few decades. Furthermore, in order to ensure the best possible disinfection, many suppliers have introduced a multi-barrier concept in which most of the common disinfectants in use today (such as chlorine, ozone, chlorine dioxide, and chloramines) are combined within a single treatment plant. However, such combinations may cause the disinfectants to interact with dissolved organic matter to produce their own characteristic set of chemical DBPs in the water produced [6]. The levels of some emerging DBPs are actually increased when these alternative disinfection processes are used. Although 600 emerging DBPs have been reported in the literature [7], only 100 such DBPs have been studied due to lack of appropriate analytical methods for them [8].

Following reaction schematics (II) shows an example mechanism of DBP formation with chlorination of water (NOM, fulvic acids react with chlorine and produces THMs, HAA and HK) [9].

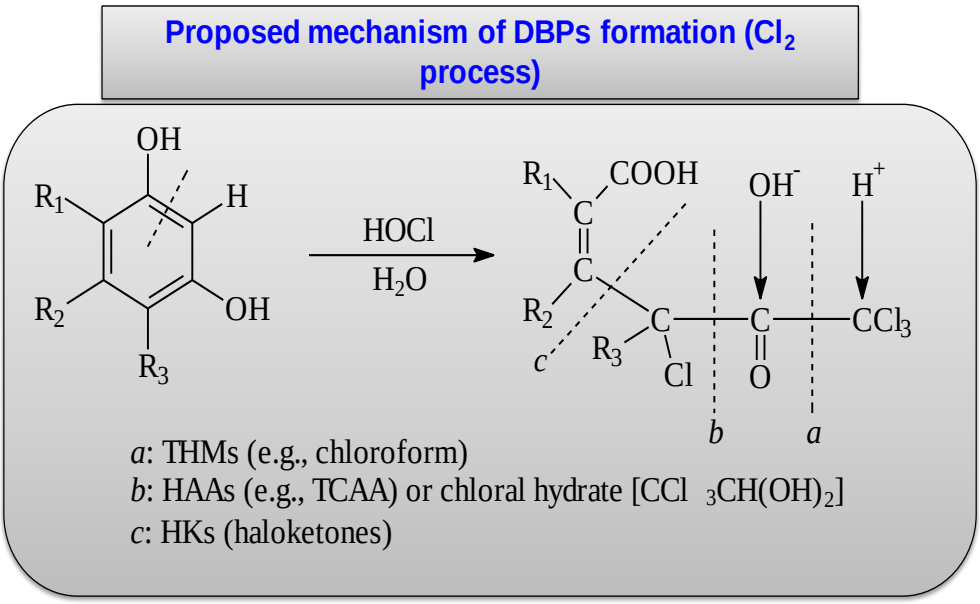

Due to the differences in the chemical structures, polarity, and volatility of DBPs the determination of trace concentration (e.g. ng/l) in drinking water is not a trivial matter.

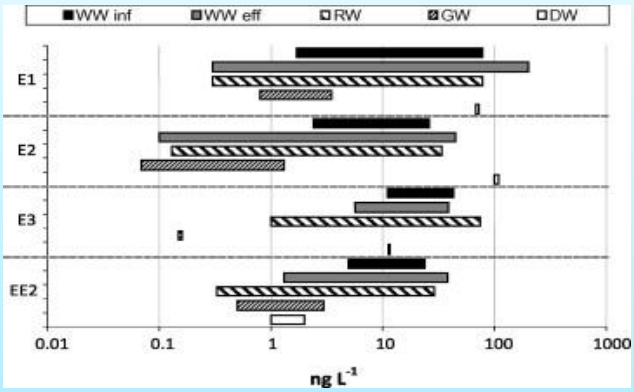

Occurrence of E1, E2, E3 and EE2 in environmental aqueous matrices. WWinf = wastewater influent; WWeff = wastewater effluent; RW = River water; GW = Ground water; DW = Drinking water (from ref-8)

Figure 2 Concentrations of DBPs in environmental waters

Figure 2 shows the concentrations of DBPs detected in various environmental waters [10-15]. Direct analysis of these DBPs (without preconcentration techniques) is not possible. There are four USEPA standard methods for determining DBPs concentrations in drinking water based on gas chromatography (GC) with an electron capture detector (ECD) [16-18]. GC with ECD and mass spectrometric (MS) [19-23]. Other alternatives include classical liquid-liquid extraction (LLE) [24-27], dispersive liquid-liquid microextraction (DLLME) using organic solvents [28, 29], vortex assisted liquid-liquid microextraction (VALLME) [30], single drop liquid phase microextraction (SDLPME) [31, 32] and hollow fiber liquid phase microextraction (HF-LPME) in two phase configurations [33, 34] methods required tedious and labor intensive derivatization procedures.

1.2 PROBLEM DEFINITION

Analysis of trace level of disinfection by-products (DBPs) from environmental water samples (ground water, seawater and drinking water) and biological samples (fish and green alge) is challenging; seawater and biological samples are classified as complex matrix samples. In the Conventional analytical, particularly sample preparation (extraction) techniques for water quality monitoring require large amounts of organic solvent and samples. In the case of routine sample analyses, a lot of samples need to be collected and transported to the laboratory for preconcentration of target analytes before analysis. With conventional procedures such as liquid-liquid extraction, handling of large numbers of samples, and in substantial quantities, is time-consuming and logistically challenging.

We have the vision to challenge present practices. Our goal is to develop new extraction methods for determination of DBPs in water and biological samples; these methods will include simple sample preparation process and fast detection of different groups of DBPs such as trihalomethanes (THMs), haloketones (HKs), haloacetic acids (HAAs) haloethers (HEs) and nitrogenous DPBs

that are found in water and biological samples. Because these analytes are chemically diverse, no single method would be suitable for their determination, and conventional methods are usually multi-step with high risk of analyte loss. Therefore, different simple and efficient methodologies that will suit each group of analytes will be developed in this research venture

1.3 AIMS AND OBJECTIVES

The following are the main objectives of this study:

1- To assess the potential formation of DBPs during seawater pretreatment, or in the treatment and distribution systems for desalinated water. Therefore, initial screening will be conducted to assess the quality of the water.
2- To develop simple analytical methods for trace level quantification of organic DBPs.
3- Many toxic organic DBPs have not been studied in the kingdom; this study will give clear information on the formation of these compounds in the desalination systems.
4- Biological samples will also be monitored to investigate the potential risks to aquatic ecosystems when brine reject is not diluted sufficiently in the receiving water.

For monitoring biological samples, efficient analytical methods are required, before application to real samples. However, this approach has to be tested for spiked samples initially.

A successful conclusion of the work will lead potentially to a new and more effective means of cleaning water of critical pollutants such as DBPs.

The following chart shows the approach for each target in each sample:

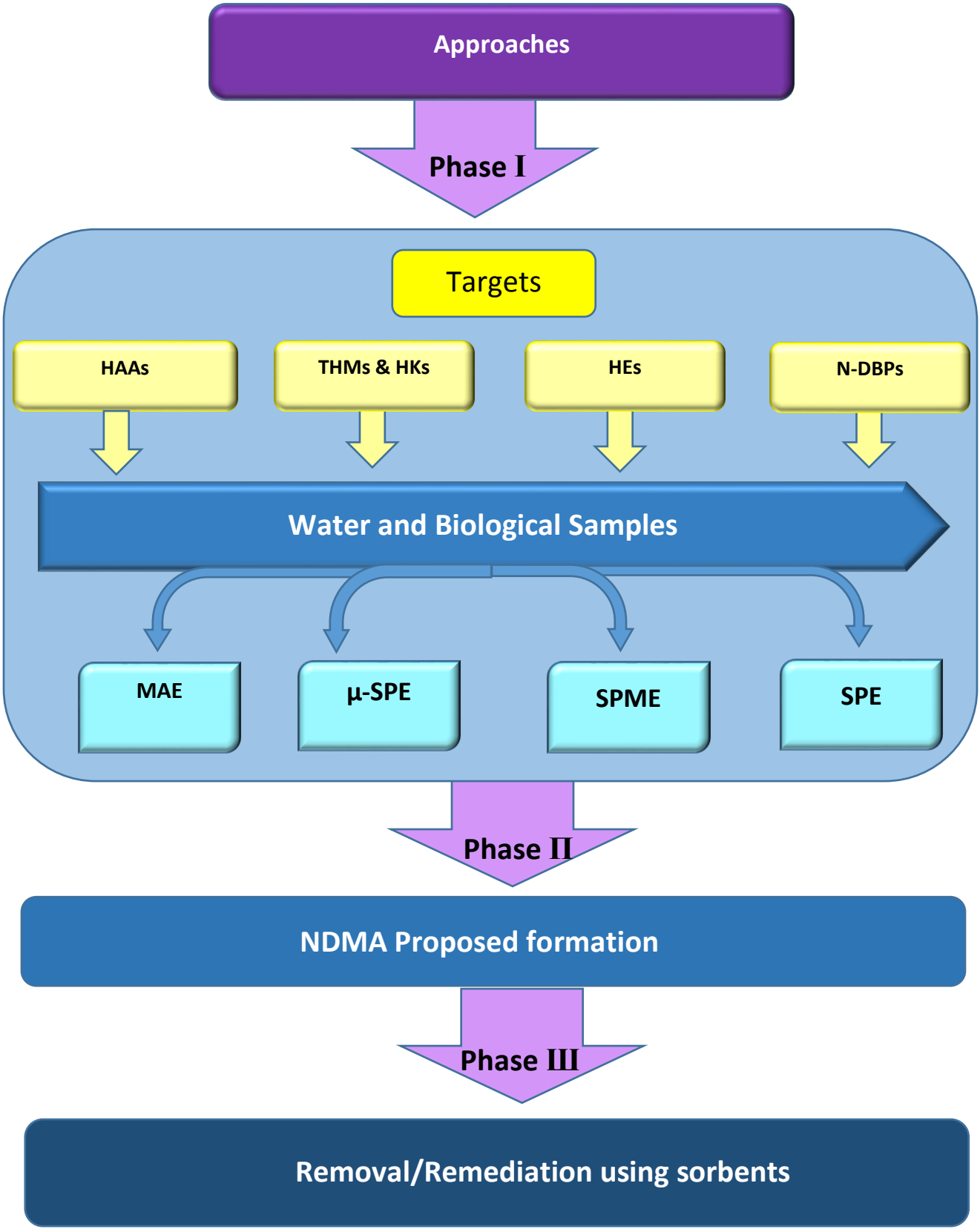
Approaches
Phase I
Targets
HAAs
THMs & HKs
HEs
N-DBPs
Water and Biological Samples
MAE
µ-SPE
SPME
SPE
Phase II
NDMA Proposed formation
Phase III
Removal/Remediation using sorbents

CHAPTER 2

DETERMINATION OF HALOACEDIC ACIDS IN WATER USING LAYERED DOUBLE HYDROXIDES AS SORBENT IN DISPERSIVE SOLID-PHASE EXTRACTION FOLLOWED BY LIQUID CHROMATOGRAPHY-TANDEM MASS SPECTROMETRIC ANALYSIS

2.1 LITERATURE REVIEW

Disinfection of drinking water is one of the essential water treatment processes to inactivate microbial pathogens, saving millions of human lives every year from infectious diseases such as typhoid and cholera [2]. Chlorination is the most common disinfectant used in current desalination systems, with chloramines and chlorine dioxide gaining more popularity for disinfection of desalinated water. Chlorination dramatically reduces the incidence of waterborne diseases, as well as gastrointestinal illness. However, chlorine can also react with natural materials in the raw water to form disinfection by-products (DBPs) that are hazardous to health [2]. Long term exposure to DBPs may potentially increase the risk of cancer [3], apart from causing other adverse health effects. Recently, researchers prove that not only is oral ingestion a route to human exposure to DBPs, but also inhalation, and dermal absorption during leisure activities or while bathing and swimming[35]. More than 500 DBPs have been detected in drinking water [36] treated with common disinfectants, such as chlorine, chloramines, chlorine dioxide, and ozone. Haloacetic acids (HAAs) are some of the identified DBPs in drinking water. The main types of HAAs are monochloroacetic acid (MCAA), monobromoacetic acid (MBAA), dichloroacetic acid (DCAA), dibromoacetic acid (DBAA) and trichloroacetic aicd (TCAA). The presence of such compounds in drinking water represents a potential concern, especially when desalinated waters are blended

with organic matter-rich source waters [37]. The determination of HAAs in drinking water generally requires of an appropriate extraction and isolation step by which analytes enrichment is achieved, before the actual analysis. Therefore, it is important to develop analytical methods and apply them to monitor regularly these DBPs in potable water samples in order to understand better the potential risks posed these contaminants.

Recently, layered double hydroxides (LDHs) have attracted much attention in different areas due to their interesting properties and special structures. LDHs are substances with two dimensional nanostructure layers, which consist of positive charged layers of metal hydroxides separated by charge balancing anions in addition to water molecules [38, 39]. The general formula of LDHs can be expressed by $[M^{2+}_{1-x}M^{3+}_{x}(OH)_2]^{x+}(A^{n-})_{x/n}\cdot mH2O$, where A^{n-} is the interlayer anion while M^{2+} and M^{3+} are divalent and trivalent metal cations, respectively [40].

Due to their advantages including good anion-exchange capacity, excellent specific surface area, acid–base buffering capacity and high porosity, LDHs can be considered as efficient sorbents for analyte enrichment [41]. LDHs have been employed for this purpose in a wide range of applications [42–44] especially in the environmental field [45–49]. The use of LDHs as solid-phase extraction (SPE) sorbents has been reported for different analytes, such as fluoride [41], dopamine [50] and polycyclic aromatic hydrocarbons [51]. One attractive feature of the application of LDHs as sorbents is that they can be dissolved under acidic condition; thus the analyte elution step which is customary in conventional SPE can be avoided completely[52].

The aim of the present work is to use LDHs to extract HAAs from water samples in dispersive SPE (DSPE) followed by liquid chromatography-tandem mass spectrometric (LC-MS/MS) analysis. HAAs have not previously extracted using these types of sorbents. Different DSPE

parameters were investigated, including extraction time, extraction temperature and the effect of pH. Comparison with conventional SPE was carried out. The procedure was applied to the analysis of real water samples.

2.2 EXPERIMENTAL

2.2.1 Materials and methods

2.2.1.1 Chemicals

A standard mixture of HAAs containing MBAA, MCAA, DBAA, DCAA and TCAA in methyl tert-butyl ether (MTBE) (2000 µg/mL of each compound) (Table 1) was purchased from Supelco (Bellafonte, PA, USA). Magnesium chloride ($MgCl_2.6H_2O$) (98%), aluminium chloride ($AlCl_3$) (99%), magnesium nitrate ($Mg(NO_3)_2 \cdot 6H_2O$) (98%), aluminium nitrate ($Al(NO_3)_3 \cdot 9H_2O$) (98%), formic acid and trifluoroacetic acid (TFA) (99%) were obtained from Alfa (Karlsruhe, Germany). Sodium carbonate and sodium hydrate were purchased from Merck Millipore (Darmstadt, Germany). LC-grade methanol was obtained from Tedia (Fairfield, OH, USA).

Table 1. Structures of the target analytes

Compound	Structure	Abbreviation	Elution order
Monochloroacetic acid	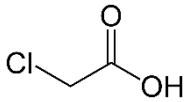	MCAA	1
Monobromoacetic acid	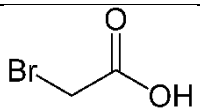	MBAA	2
Dichloroacetic acid	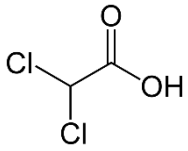	DCAA	3
Dibromoacetic acid	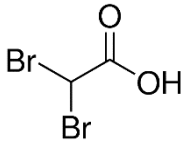	DBAA	4
Trichloroacetic acid	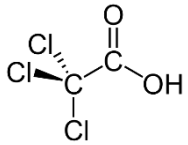	TCAA	5

2.2.1.2 Synthesis of Sorbents

The synthesis procedure of the three targeted types of LDHs was performed according to the method reported by Reichle [53]. As an example, to synthesize LDH-NO_3 15.25g $MgCl_2.6H_2O$ and 28.13 g $AlNO_3.9H_2O$ were dissolved in deionized water (100 mL) at 30°C under vigorous stirring. The solution pH was maintained at 11 by adding 3 mL of NaOH (0.1M). After 4 hours, the mixture was placed then in an autoclave and aged by hydrothermal treatment at 180°C for 36 h. Filtration for the obtained powder was carried out and then it dried at 70°C overnight.

2.2.1.3 Characterization

Physico-chemical characterization of sorbents to obtain information on surface chemistry, pore size, surface area, and elemental composition is essential since the adsorption is a surface phenomenon [54]. Different techniques were used in this study for characterization. Scanning electron microscopy (SEM) (Tescan, Brno, Czech Republic) was used for morphological analyses of the synthesized sorbents. X-ray diffractometry (XRD) (Rigaku MiniFlex, Tokyo, Japan) was used to study the crystalline phases in the LDHs. Fourier transform infrared (FT-IR) spectroscopy was used to identify the functional groups in the LDHs.

2.2.1.4 Extraction procedure

The following approach was applied during the experiments: A mixture of LDH (5 mg) and water sample (10 mL) was placed in a centrifuge tube. It was sonicated at ambient temperature (25 °C) for 7 min. Vortexing was applied to disperse the sorbent. The pH of the solution was adjusted to be between 4 and 12 by adding different volumes of NaOH (0.1M). At the same time, the temperatures of the solutions were varied using a water bath. Finally, centrifugation was applied to precipitate the sorbent in the mixture. The liquid was then decanted. One hundred microliters of

TFA (8%) was added to the sorbent to dissolve it, and 20 μL of the obtained solution which contain the target analytes was injected into the LC-MS/MS system for analysis. Figure 3 shows the schematic of the extraction procedure.

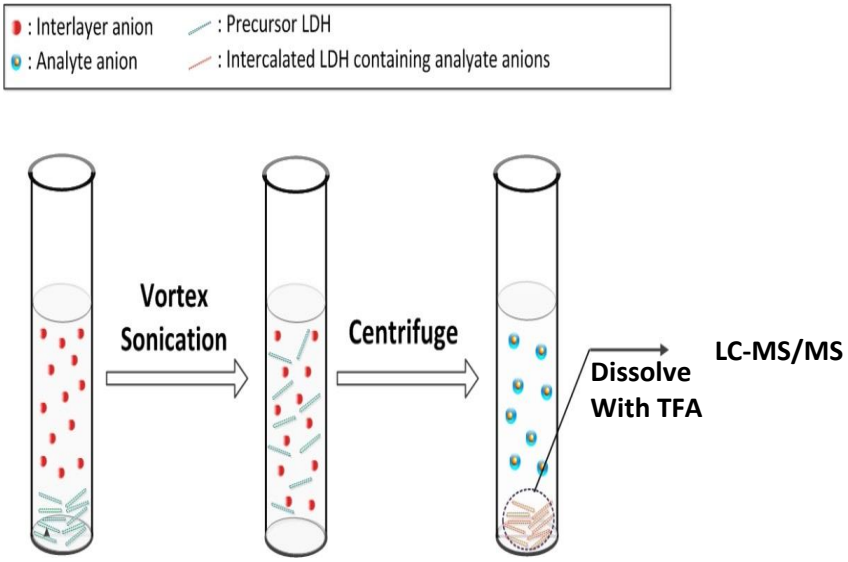

Figure 3: Schematic of DSPE procedure

2.2.1.5 Analytical and quantification method

HAA analysis was conducted using a Shimadzu Model 8050 LC-MS/MS instrument (Kyoto, Japan), equipped with a CTC Analytics auto sampler (Zwengen, Switzerland), Shimadzu LC-30 AD binary pumps, Shimadzu DGU-20A_{5R} degasser, and a Shimadzu CTO- 30A column oven. An IBD polar LC column was used for separation (3 µm particle size; 100 × 2.1 mm, Restek, Bellefonte, PA, USA).

The mobile phase consisted of solvent A (methanol) and solvent B (1% formic acid in deionized water). The gradient elution LC program was as follows: 95 % of A for 1 min, then amount of solvent B was increased gradually to 25 % in 3 min; finally return to the initial parameter for 5 min. The mobile phase constant flow rate was 0.3 mL/min. The oven temperature was 50 °C and the volume of the injected extract was 20 µL. The triple quadrupole MS detector was equipped with atmospheric pressure chemical ionization (APCI) and electrospray ionization (ESI) sources. To get the maximum intensity for the precursor ions, the interface conditions were optimized. Under these conditions, well separated HAAs peaks was observed within a short range of retention time. The analysis of HAAs was in negative ESI mode, and multiple reaction monitoring (MRM) was conducted to obtained product ions using a standard mixture of HAAs (1 mg/L) in methanol. For data processing, Lab Solutions software (Shimadzu) was used. Table 2 shows the MRM parameters applied.

Table 2: Experimental conditions of negative ion ESI-MS/MS.

Analyte	Molecular mass	Precursor ion	Product ion	Pause time[a] (ms)	Dwell time[b] (ms)	Q1 pre-rod voltage[c] (V)	Collision energy[d] (V)	Q3 pre-rod voltage[e] (V)
MCAA	94.49	93.10	92.20	2	100	15	35	20
			74.90					
MBAA	138.94	137.10	83.00	4	100	16	35	15
			78.80			17	14	29
DCAA	128.94	127.10	80.90	5	100	15	11	28
			79.00				17	26
DBAA	217.80	216.80	88.00	4	100	25	50	15
			78.90			26	28	29
TCAA	163.38	162.90	78.90	5	100	19	11	11
			71.70			18	35	28

[a] Time required for MS instrument to change and stabilize voltages for each MRM transition.
[b] Time that target ions spend in the collision cell.
[c] The voltage used to select the targeted precursor ion into the Q1 section.
[d] Energy used to fragment the precursor ions.
[e] The voltage used to select the targeted product ions into the Q3 section.

2.2.1.6 Calculation of enrichment factor

The enrichment factor (EF) was calculated as the ratio of the concentration of an analyte in the extract (C_{ext}) and the analyte's initial concentration in the standard solution (C_o).

$EF = C_{ext}/C_o$

Where C_{ext} was obtained using a calibration curve prepared by injections of HAAs standards directly in the extraction solvent.

2.3 RESULTS AND DISCUSSION

2.3.1 Characterization of LDHs

The LDHs were characterized using scanning electron microscopy (SEM), infrared spectroscopy (FT-IR), and by X-ray diffraction (XRD).The results confirmed the success of the synthetic process of the three sorbents. With every individual technique, the feature of our target synthesized LDH is expressed. Figure 4 presents FT-IR spectra for each kind of LDH. The arrows point to the main functional groups: at 3480 cm^{-1} the broad band corresponds to stretching vibration of interlayer water molecules and hydrogen bonding. The small peak appeared at 1640 cm^{-1} was assigned to the bending vibration of interlayer water molecules. Peak was observed around 1380 cm^{-1} due to CO_3^{2-} and NO_3^- stretching vibration. The stretching of metal-O_2-metal might be the responsible of those bands appeared between 500 and 800 cm^{-1}. The morphology of used LDHs were studied by SEM technique. SEM images of the sorbents (figure 5) reveals the crystalline structures for all types. As clearly seen in figure (5, a) for example, the small crystallites of LDH-NO_3 were thin platelets with thickness of about 20 nm and sizes ranging of 200 nm approximately

The X-ray diffraction spectrum patterns of the different kinds of LDHs (LDH-Cl, LDH-CO_3, LDH-NO_3) shown in figure 6 The intense and sharp diffraction peaks around 11°, 23°, 35°, 60°-62° related to the (003), (006), (009)+(012), (110), (113) planes of the LDHs crystal structure. All types of used LDHs showed pure and well-crystallized LDH phase. LDH-NO_3 had the strongest intensity in both planes (003) and (006) comparing with LDH-CO_3 and LDH-Cl. This result indicated that LDH-NO_3 had the best crystal structure in short range among the studied LDHs.

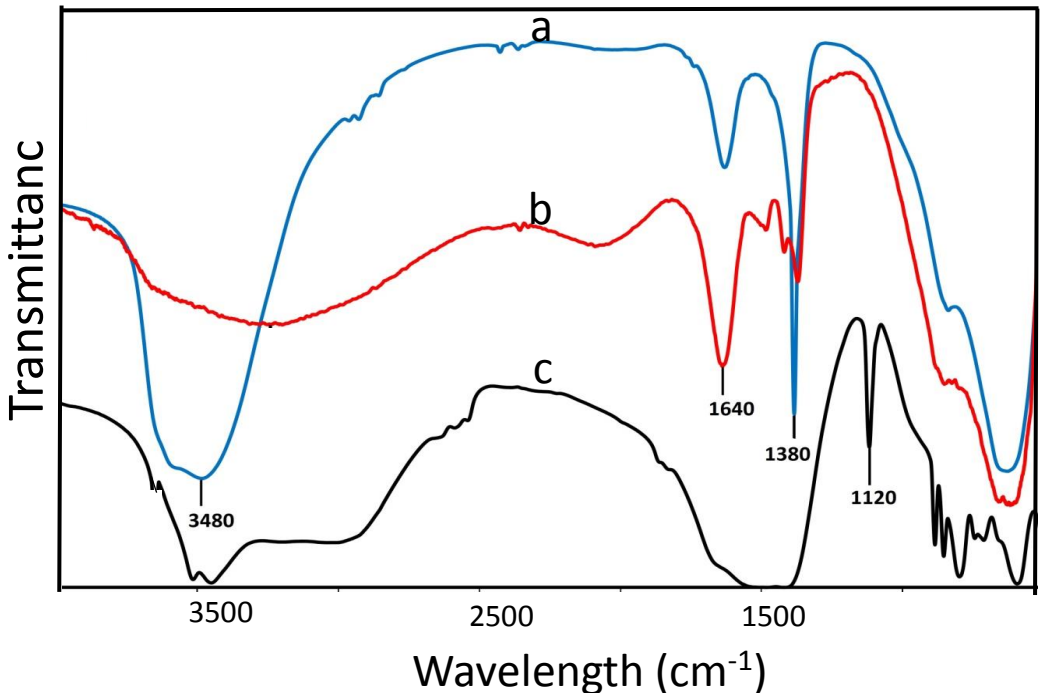

Figure 4. FT-IR spectra of (a) LDH-NO_3, (b) LDH-Cl, (c) LDH-CO_3

Figure 5. SEM images of (a) LDH-NO_3, (b) LDH-Cl, (c) LDH-CO_3.

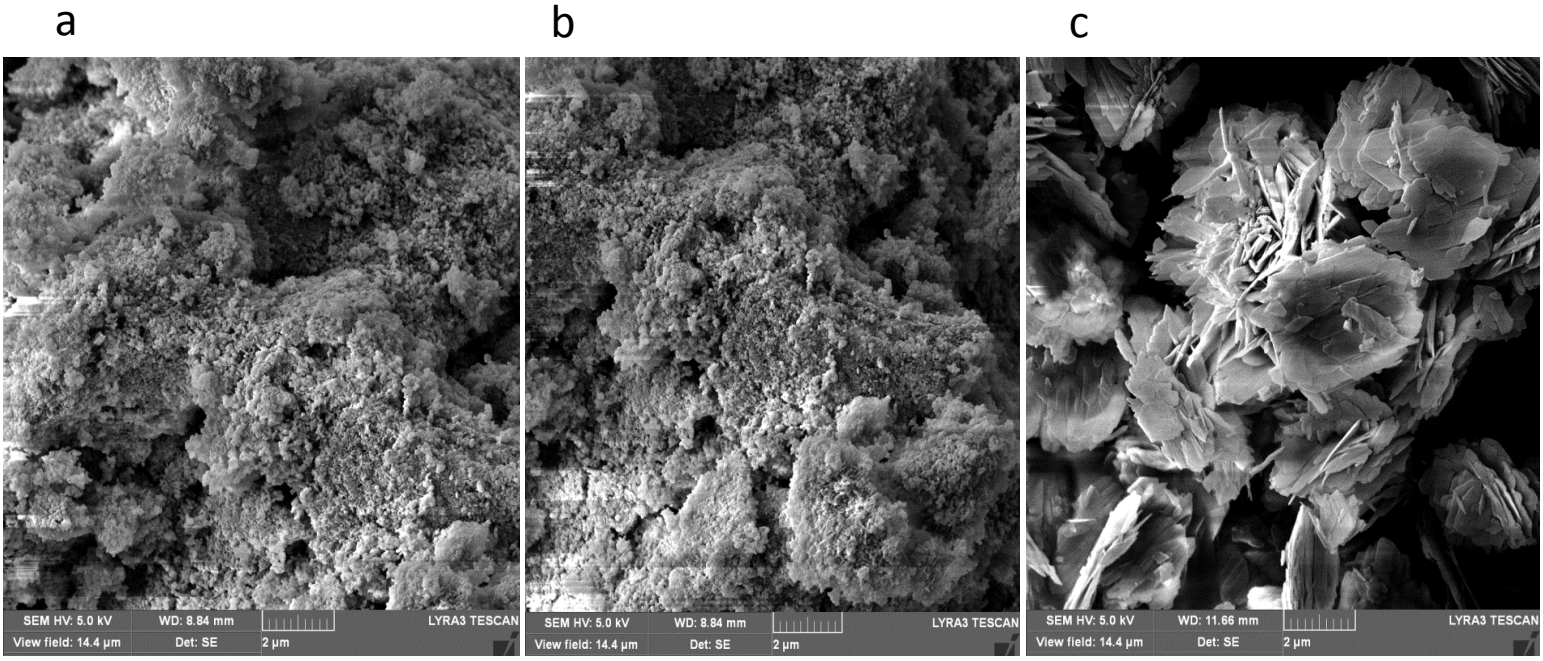

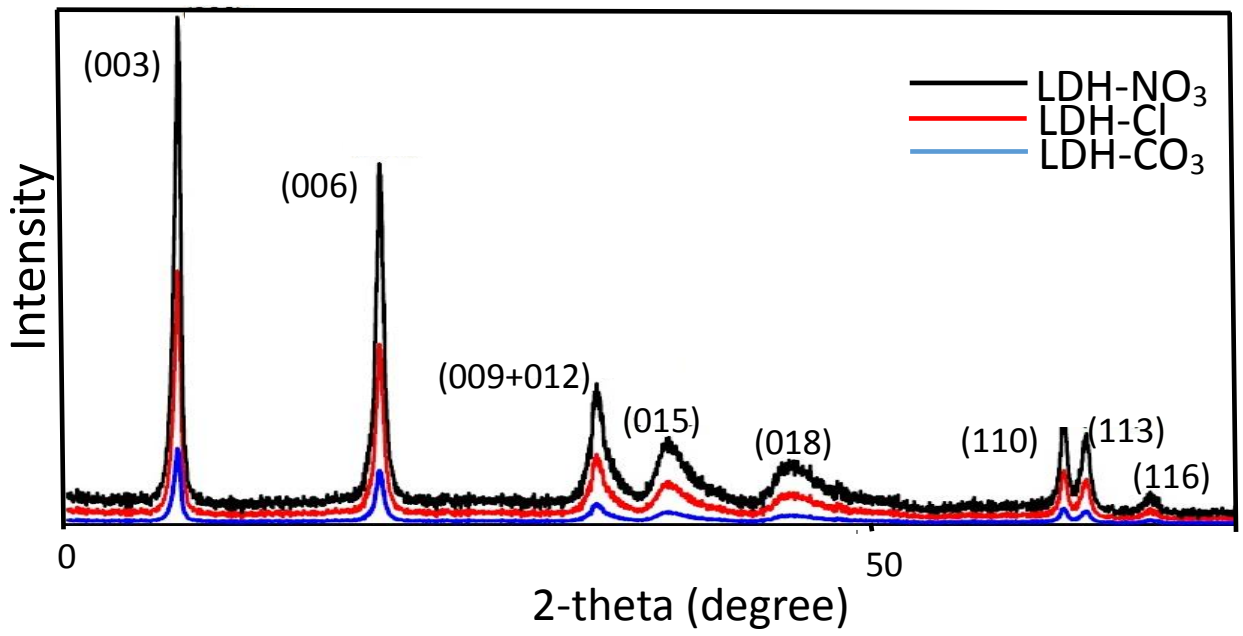

Figure 6. XRD patterns of the used LDHs (NO_3^-, Cl^-, CO_3^{2-}).

2.3.2 Optimization of DSPE

To obtain the most favorable EFs, various DSPE parameters that affect the extraction efficiency were optimized. These parameters were sorbent types, extraction temperature, time and sample solution pH.

2.3.2.1 Selection of sorbent

The effect of different LDH types was studied because the efficiency of the extraction was expected to be affected by the type of interlayer anions, since these possess different anion-exchange capabilities [55]. Figure 7 presents the results of using the three Mg-Al LDHs (with anions NO_3^-, Cl^-, and CO_3^{2-}). As can be clearly seen, higher EFs were obtained by using LDH-NO_3 as sorbent. The order of decreasing extraction efficiency was observed to be $NO_3^- > Cl^- > CO_3^{2-}$. This could be explained by the equilibrium constants of anion-exchange reported by Mitata [24]. LDH-NO_3 was therefore chosen as the sorbent for further extraction studies.

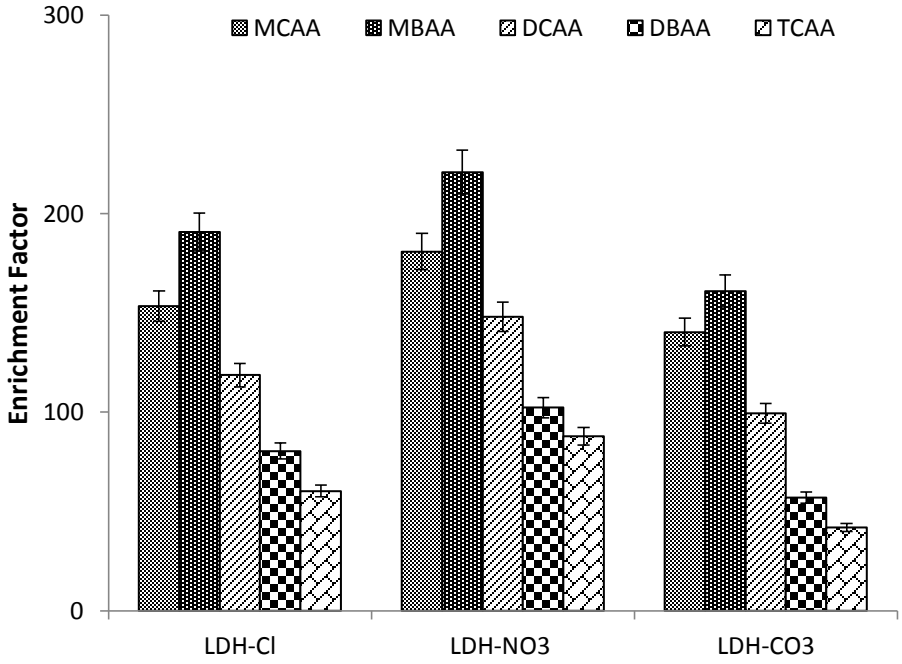

Figure 7: The extraction efficiency of LDHs for HAAs. (Extraction conditions: temperature 40 ^{o}C, extraction time 15 min and pH 6).

2.3.2.2 Effect of extraction temperature.

The effect of temperature on the extraction efficiency was investigated in the range between 30 and 80 °C. Figure 8 depicts that the EF was enhanced with increasing temperature until it reached the maximum value at 60 °C. As a general rule, a higher temperature increases diffusion coefficients, which encourage migration of the analytes towards the sorbent particles. As a result the analytes and sorbent connection will increase and a faster equilibrium will take place[56, 57]. On the other hand, the curves levelled off at 60 °C because adsorption is exothermic, and at this temperature the desorption process began to predominate [55].

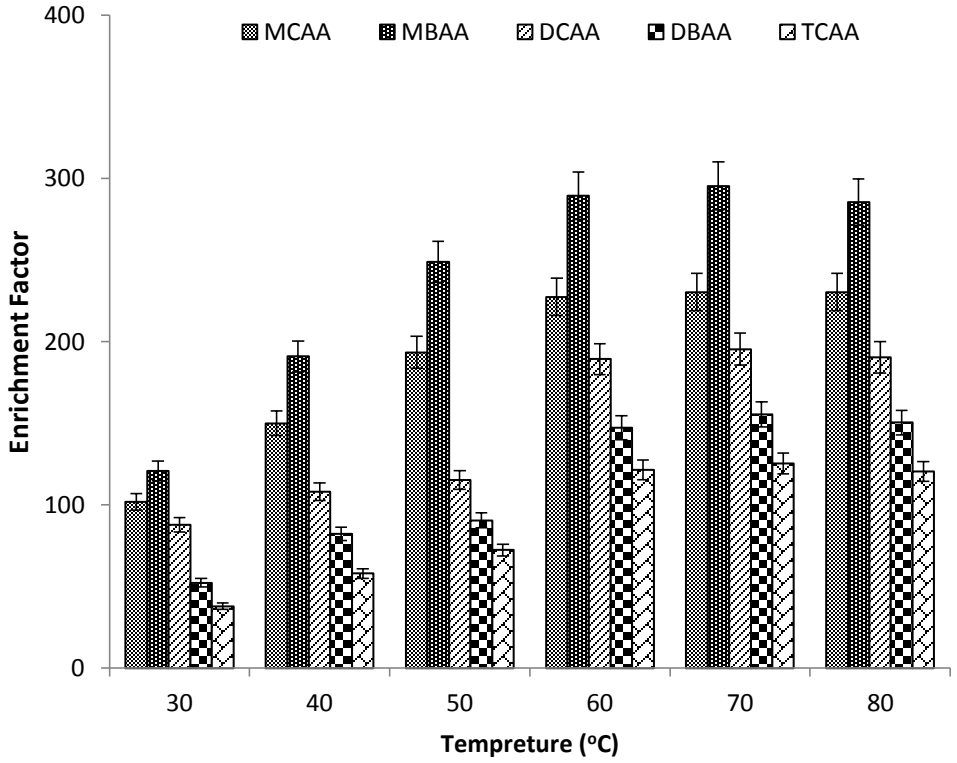

Figure 8: Effect of extraction temperature. (Extraction conditions: LDH-NO_3 as sorbent, other conditions as in Figure 2.

2.3.2.3 Effect of extraction time

The extraction time was varied in the range from 5 to 35 min to study its effect on the extraction process. As can be clearly seen (Figure 9) EFs for all analytes increased up until 25 min of extraction time, and then levelled off. These results can be explained by the fact that the extraction process reached an equilibrium at 25 min, and was not enhanced any further at 35 min.

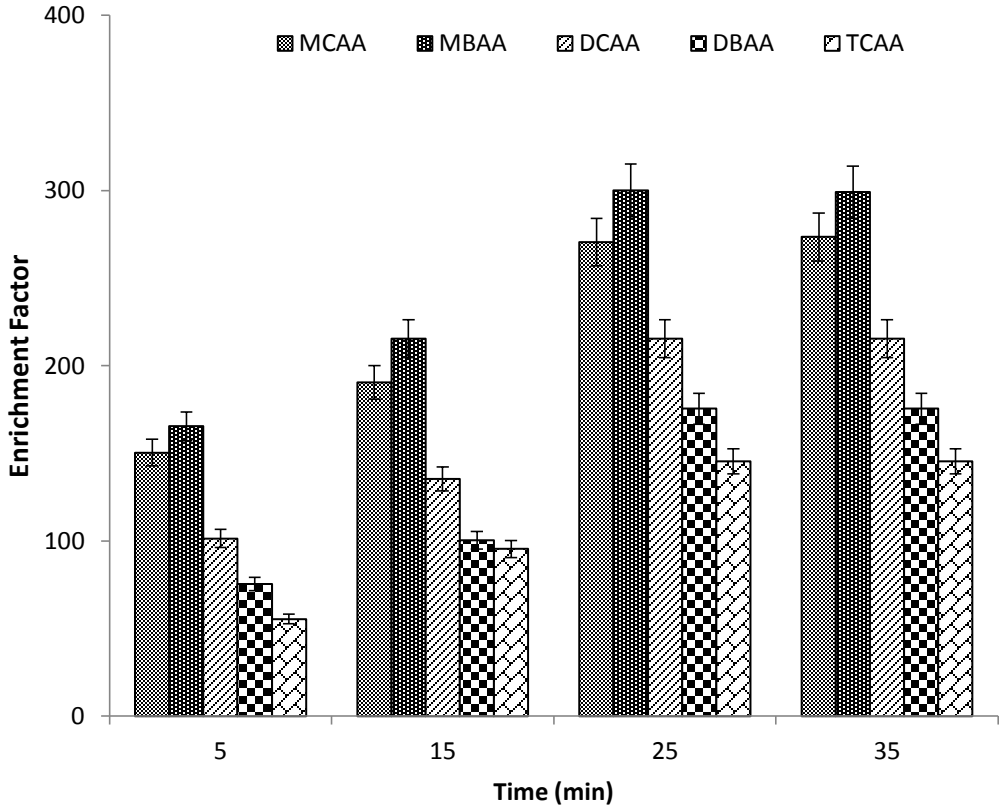

Figure 9: Effect of extraction time. (Extraction conditions: temperature 60 ºC, other conditions as in Figure 8).

2.3.2.4 Effect of pH

The pH influence on extraction recovery was studied in the range between 4 and 12. HNO_3 solution (0.1 M) was used to adjust the pH values in the acidic range (4 to 6) and NaOH solution (0.1 M) was used to adjust it in the basic range (8 to 12). Figure 10 shows that in acidic medium the EFs increased when the pH was reduced. This can be explained by two reasons: (1) the increased ionization of the analytes occurred at low pH; and (2) the strong acidic solution dissolved the LDH, releasing the analytes more efficiently. On the other hand, in basic media, the EFs of all analytes decreased due to the increasing concentration of OH^- ions [58]. This led to a decrease in surface positive charge, resulting in a reduction of the interaction between the analytes and the LDH [59]. In conclusion pH 6 was chosen as an optimum for further study.

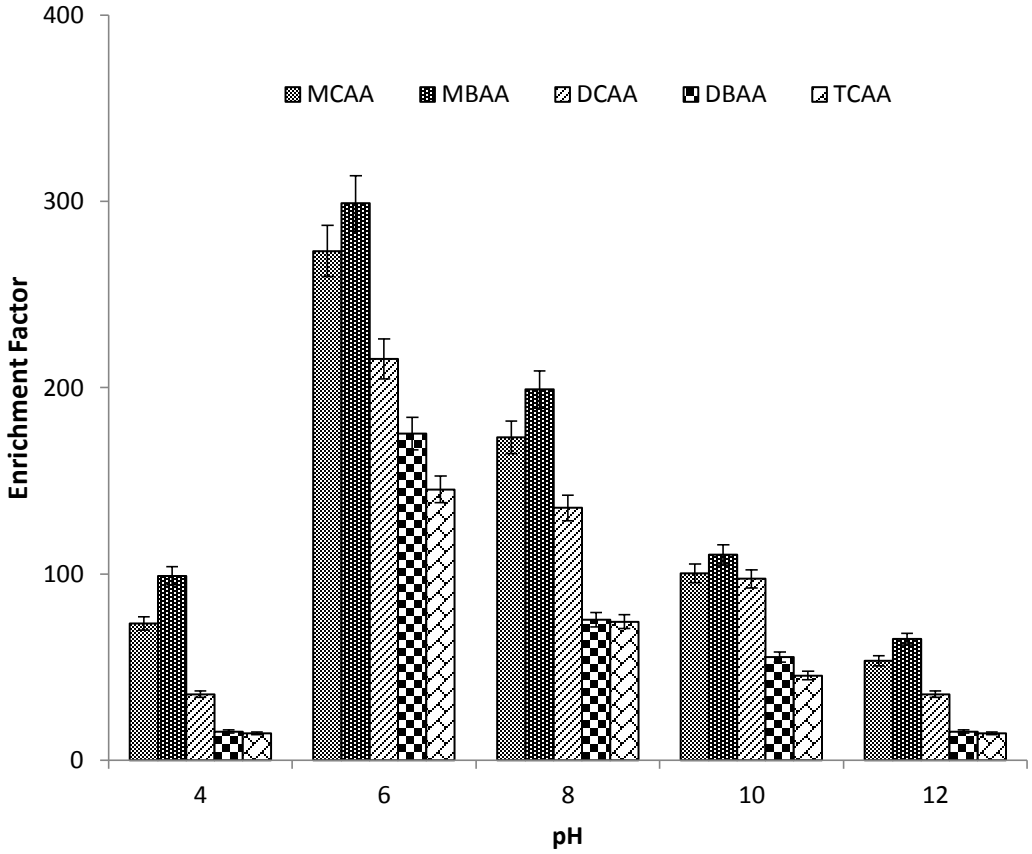

Figure 10: Effect of pH of sample solution. (Extraction conditions: time 25 min, other conditions as in Figure 9)

2.3.3 Method evaluation

The quantitative analysis of the HAAs using the proposed method was carried out by monitoring the peak areas at different concentration levels of the analytes (0.5, 1, 5, 10, 20, 40, 70, 100 µg/L). Quantitative parameters such as repeatability, linear range and limits of detection (LODs) were calculated under the optimized conditions and are summarized in Table 3. Good linearity of the calibration plots was observed over the concentration range of 0.5 to 100 µg/L, with coefficients of determination (R^2) $\geq$ 0.9884. Satisfactory reproducibility was observed (relative standard deviations (RSD) ranged between 0.33 and 3.64 % (n = 6). The LODs were calculated according to the guidelines of the American Chemical Society's Committee on Environmental Analytical Chemistry and IUPAC, from $S_{LOD} = S_{RB} + 3\sigma_{RB}$ where S_{LOD}, and S_{RB} are the signals at the LOD and of the reagent blank, respectively, while σ_{RB} is the standard deviation of the reagent blank. The method LODs ranged from 0.006 to 0.05 µg/L. The results confirmed that the proposed method was suitable for trace level analysis of HAAs in water samples. Table 4 gives a comparison between the proposed and other methods reported in the literature. The developed method showed promising results compared to those already reported.

Table 3. Performance of DSPE using LDH-NO_3 as sorbent, followed by LC-MS/MS.

Compound	R^2	Equation	%RSD (n = 6)	LOD (µg/L)
MCAA	0.9985	y = 14187x + 36.223	0.33	0.01
MBAA	0.9919	y = 12319x + 20.112	0.91	0.009
DCAA	0.9983	y = 110940x – 53.738	1.54	0.006
DBAA	0.9954	y = 62142x + 36.223	1.99	0.03
TCAA	0.9884	y= 1872.6x + 9965.5	3.64	0.05

Table 4: Comparison of DSPE-LC-MS/MS with other reported methods for the determination of HAAs in liquid samples

Analytical technique[a]	Derivatization time (min)	LODs µg/L	RSDs (%)	Ref.
LLE-GC-ECD (US EPA-552-1)	30	0.0074-0.14	7.0-59.0	[60]
LLE-GC-ECD (US EPA-552-3)	120	0.012-0.17	0.36-4.0	[61]
HS-HFLPME-GC-ECD	NA[b]	0.10-18.00	5.0-12.0	[62]
HS-SPME-GC-/ECD	5	0.01-0.40	6.3-10.9	[63]
SDME-GCMS	20	0.10-1.20	5.1-8.5	[64]
Evaporation-SPME-GC-MS	10	0.01-0.20	6.3-7.9	[65]
SLME-LC-UV	NA	0.02-2.69	1.5-10.8	[66]
LLE-ESI-MS	NA	0.13-0.60	NA	[67]
LLE-GC-MS/MS	180	0.025-1.00	0.9-19.9	[68]
UPLC-MS	NA	0.18-71.5	NA	[69]
µSPE-UPLC-UV	NA	0.001-0.092	0.03-7.40	[70]
DSPE-LC-MS/MS	NA	0.006-0.05	0.33-3.64	Present work

[a] LLE = liquid-liquid extraction; ECD = electron-capture detection; HS-HFLPME = headspace hollow fiber liquid-phase microextraction; SPME = solid-phase microextraction; SDME = single-drop microextraction; SLME = supported liquid microextraction; UV = ultraviolet detection; UPLC = ultra performance liquid chromatography; µ-SPE = micro-solid-phase extraction.

[b] NA = non-applicable

2.3.4 Conventional SPE versus DSPE

The comparison between the Table 5 present the comparison between the conventional SPE[41] and DSPE methods for the determination of HAAs in water samples. As clearly seen, the extraction using DSPE method gave better LODs than using conventional SPE also the linear ranges were wider. In addition to that, less solvent and sample volumes were consumed by using DSPE.

Table 5: Comparison of DSPE and conventional SPE

Method	Analyte	Linearity*	R^2	LODs (µg/L)
DSPE	MCAA	0.5-100	0.9985	0.01
	MBAA	0.3-100	0.9919	0.009
	DCAA	0.5-100	0.9983	0.006
	DBAA	0.3-100	0.9954	0.03
	TCAA	0.5-100	0.9884	0.05
Conventional-SPE	MCAA	0.5-50	0.995	0.91
	MBAA	0.5-50	0.997	0.89
	DCAA	0.3-50	0.991	0.88
	DBAA	0.2-30	0.989	1.10
	TCAA	0.2-30	0.988	1.15

* Linearity of DSPE unit is (µg/l) while linearity of conventional-SPE unit is (mg/l)

2.3.5 Application to the real water samples

Several reports have recently indicate the presence of HAAs in different water samples worldwide, such as surface waters [71], swimming pools [70] and drinking water [72]. To evaluate the applicability of DSPE-LC-MS/MS, different real water samples were tested. Five samples were collected and examined for HAA compounds from five different stages of a reverse-osmosis (RO) drinking water plant located in Jubail City, Saudi Arabia: (1) raw well water (feed water), (2) chlorinated feed water, (3) sand filter outlet water, (4) dechlorinated water, and (5) RO permeate water (final product). Table 4 illustrates the concentrations of the target analytes found in the tested samples. MBAA and DBAA were the compounds found most frequently and in the highest concentrations in the water samples (up to 87.9 μg/L for DBAA). By comparing the concentrations of detected HAAs in the stage 1 (feed water), and the final product of the treatment process, higher HAA concentrations were observed in the latter, indicating that such DBPs were formed during the treatment process mainly because of the chlorination step.

In addition, two more water samples, tap water collected from university campus and commercial drinking water collected from Al-khobar market, were analyzed. In both samples some HAAs were identified, as shown in Table 6 but at concentrations lower than the limits proposed by the United States Environmental Protection Agency (60 μg/l of total HAAs). Figure 11 shows LC-MS/MS traces of different water samples obtained from the RO drinking water plant, after extraction.

Table 6: Concentrations of HAAs (µg/L) found in different real water samples using DSPE-LC-MS/MS

Sample	MCAA	MBAA	DCAA	DBAA	TCAA
Tap water	7.6	8.8	6.3	13.9	1.0
Drinking water	ND[a]	3.1	ND	9.4	ND
Water samples from different stages of RO drinking water plant					
(1) Feed water	ND	3.4	ND	ND	ND
(2) Chlorinated feed water	25.2	64.3	45.4	87.9	ND
(3) Sand filter outlet	23.6	60.1	39.0	ND	ND
(4) Dechlorination	11.5	15.7	13.6	ND	ND
(5) Final product	ND	10.7	8.9	ND	ND

[a] ND = not detected

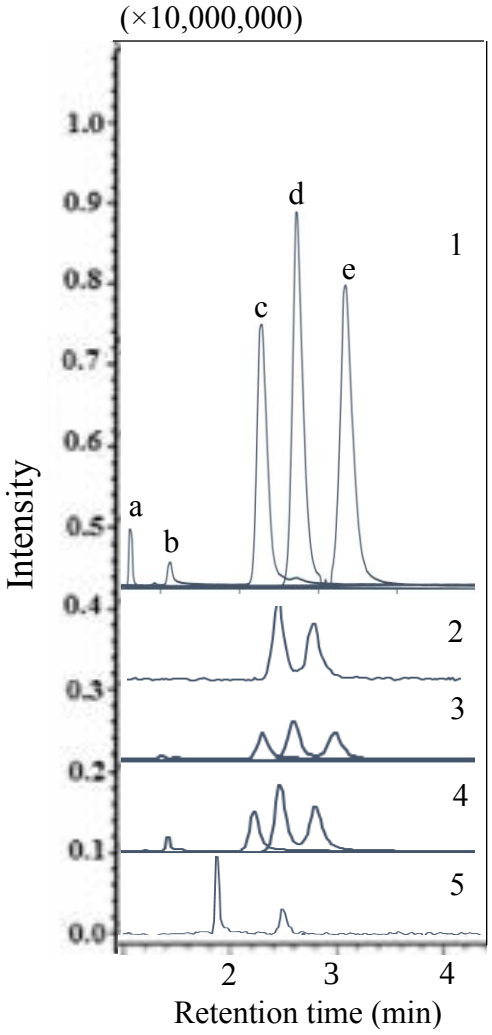

Figure 11: Chromatograms of HAAs extracted from different stages of RO drinking water plant, (1) 1 mg/L standard, (2) final product, (3) dechlorination, (4) sand filter outlet, (5) feed water. Peak identification: (a) TCAA, (b) DBAA, (c): DCAA, (d) MBAA, (e) MCAA.

2.4 CONCLUSION

In the proposed study, a dispersive-solid phase extraction method using different types of LDHs followed by LC-MS/MS analysis was established to determine HAAs in water samples. With LDH-NO_3 as sorbent, the procedure was efficient, sensitive, simple and relatively fast which did not need any derivatization. The developed method achieved better LODs compared with other those of other studies, good precision, linearity and repeatability. One of the most interesting features of using LDHs as a sorbent was that by controlling the solution pH, the dissolution of the sorbent immediately after extraction permitted the elimination of the analyte elution step normally needed in conventional sorbent-based extraction, thus shortening the experimental time. A disadvantage of such a sorbent is that it cannot be reused. However, since a very small amount is used each time this extraction approach is economical, apart from being conveniently.

CHAPTER 3

SINGLE-STEP MICROWAVE ASSISTED HEADSPACE LIQUID-PHASE MICROEXTRACTION OF DISINFECTION BY-PRODUCTS IN BIOLOGICAL SAMPLES

3.1 LITERATURE REVIEW

Arabian Gulf area has undergone tremendous changes over the past few decades in relation to management of water resources. According to recent estimations, daily production of desalinated water in gulf countries reaches up to 23 million cubic meter and only Saudi Arabia produces a lion share of it which is 11 million cubic meter [73]. The contaminants which are produced during the desalination have been extensively reported in the literature. Desalination contaminants have impacted the marine ecological environment and their detectable concentrations were found in phytoplankton, invertebrate and fish [73] and [74]. Massive losses of coral, plankton and fish in the Hurghada region of the Red Sea have also been attributed to desalination discharges [75, 76]. However, there exist only few reports on the impact assessment and bioaccumulation of disinfection by products (DBPs) in biota samples. Eastern province of Saudi Arabia where the world's largest water desalination plant is located has not been evaluated to assess the impact of DBPs on biota. In Saudi Arabia, drinking water supply is coming from desalination of seawater, after desalination, disinfection process has been used.

Disinfection is a process used in the water industry to destroy microorganisms and to produce safer drinking water. Chlorinated disinfection agents such as chlorine and chloramine are strong

oxidizing agents introduced into water and these disinfectants may react with naturally present organic matter, as well as iodide and bromide ions, to produce a range of DBPs. In fact, most of these DBPs are unintentionally produced from the reactions of disinfectants with the natural organic matter in the water [37]. Many of the DBPs have been shown to cause cancer, reproductive and developmental disorders in laboratory animals [3]. They are also harmful to humans and are suspected carcinogens even at parts per billion (ppb) concentration levels. Trihalomethanes (THMs), haloacetonitrile (HANs) and haloketones (HKs) are considered among the most prevalent DBPs [77, 78]. USEPA classified trichloromethane (TCM), bromodichloromethane (BDCM), tribromomethane (TBM), bromochloroacetonitrile (BCAN) and dibromoacetonitrile (DBAN) as carcinogens, while chlorodibromomethane (CDBM) was listed as a possible carcinogen [79]. Some toxicological effects of HKs are also reported, more prominently, chromosomal aberrations are associated with trichloropropanone (TCP) [80], and 1,1-dichloropropanone (DCP) has been reported to reduce cellular glutathione levels prior to cytotoxic effects [81]. Therefore, exposure to such compounds can lead to serious health implications.

The determination of various DBPs requires an efficient sample preparation method prior to chromatographic analyses. During the last two decades, different approaches of sample preparation have been reported for DBPs. Liquid–liquid extraction and solid phase extraction are commonly used conventional approaches [11, 13]. These methods have many shortcomings, including consumption of large volumes of hazardous solvents, time and labor extensive extractions which lead to low recoveries. Therefore, it is highly desirable to develop new extraction techniques for fast and accurate quantitation of trace level concentrations of DBPs in biological samples.

Microwave assisted extraction (MAE) has wide range of applications and it overcomes many of the above mentioned problems and is successfully applied to different biological samples such as

plant and fish [82-86]. Minimizing the degradation of volatile and semi-volatile compounds, shortening the extraction time, lowering hazardous solvent consumption, and simplicity of operation are major advantages of MAE [87-90]. Combination of headspace extraction with MAE is not common approach because to perform headspace extraction, instrumental modifications are required [91-92], which is by itself a tedious job.

In this work, for the first time, a single step microwave assisted headspace liquid-phase microextraction (MA-HS-LPME) was developed for determination of THMs, HANs and HKs in biota samples. In this method, a PTFE ring was placed inside the extraction vial to support the solvent containing porous membrane envelope, thus, no changes in the microwave instrument were required.

Table 7. Physical properties of target compounds [93-94].

Physical properties	**TCM**	**TBM**	**DBCM**	**BDCM**	**DCP**	**TCP**	**BCAN**	**DBAN**
Molecular weight (g/mol)	119.38	252.73	208.28	163.8	126.96	161.41	154.39	198.84
Solubility at 20-25 °C (g/L)	7.5	3.1	1.0	3.3	6.3	7.4	-	9.6
Boiling point °C	61.3	149.5	119	90.0	117.3	-	121.1	169
Vapor pressure at 20-25 °C (kPa)	21.28	0.75	2.0	6.67	-	-	-	3.01
Melting point °C	-63.2	8.3	-	-57.1	-	-	-	-
Density at 20 °C (g/cm)	1.484	2.90	2.38	1.98	1.291	-	1.932	2.296
log Kow[a]	1.97	2.38	2.08	1.88	0.20	1.12	-	0.47

a: Log octanol–water partition coefficient

3.2 EXPERIMENTAL

3.2.1 Material and methods

3.2.1.1 Chemicals and standards

A mixture of DBPs standard (figure 12) was obtained from Sigma–Aldrich (Bellefonte, PA, USA). This standard mixture contained THMs, HANs and HKs at 2000 ppm, which was prepared in methanol. Table 7 shows the physical properties of target compounds.

A 10 ppm stock solution was prepared in methanol. By appropriate dilution of the stock solution of DBPs in the same solvent, the working standard solutions were prepared on daily basis. Method optimization was carried out at concentration of 50 ng/g. Required solvents were obtained from Supelco (Bellefonte, PA, USA). Double deionized water was obtained from a Milli-Q system (Millipore, Bedford, MA, USA). HNO3 was obtained from Merck (Darmstadt, Germany). All glassware were washed with concentrated nitric acid and then rinsed with deionized water and acetone and then dried at 100 °C for 1 h in oven before use. A porous polypropylene membrane (2.5 cm × 2.5 cm with 0.03 mm wall thickness) was obtained from Membrena (Wuppertal, Germany).

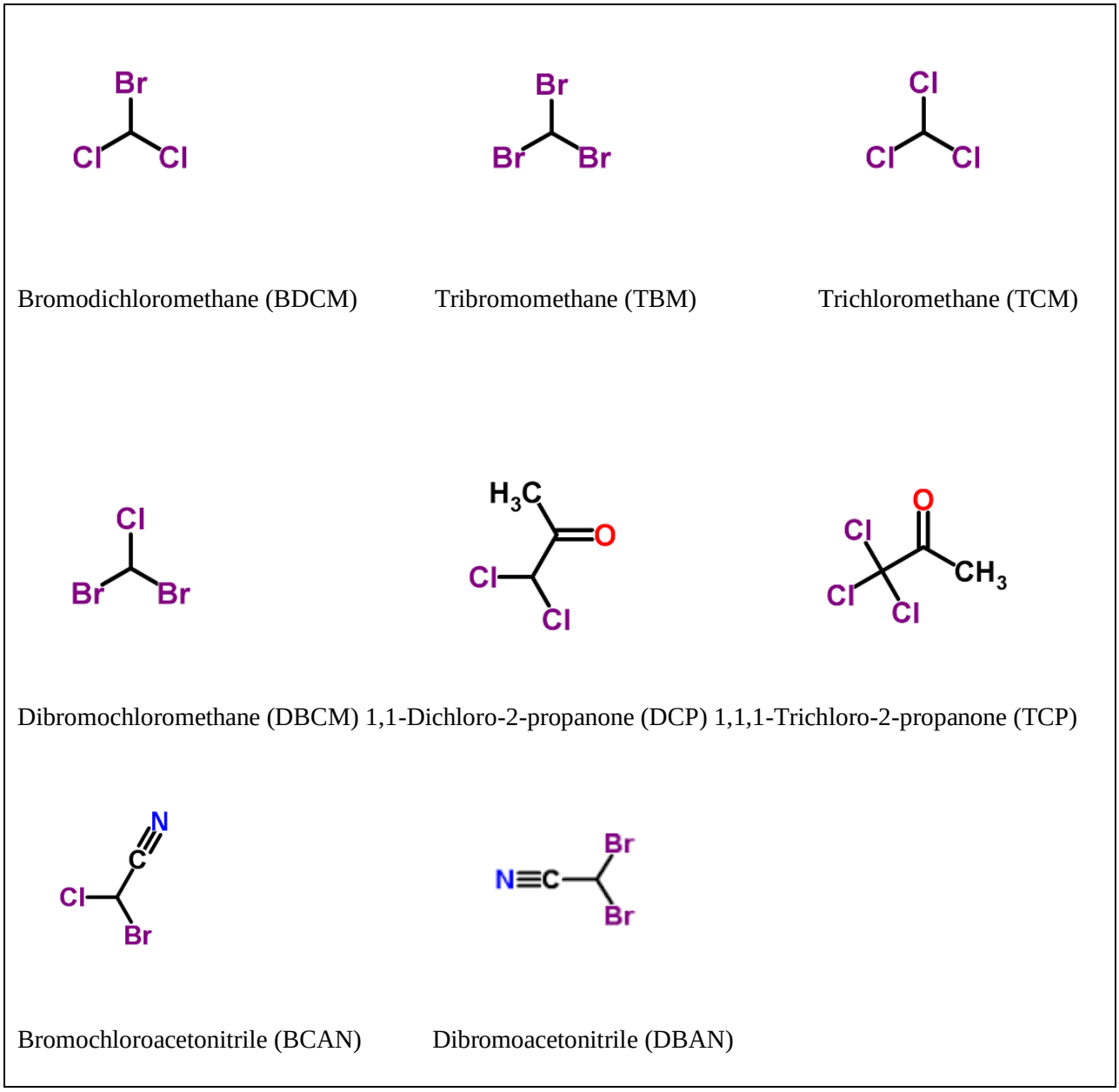

Figure 12. Chemical structures of the target compounds.

3.2.1.2 GC–MS analysis

Analyses were carried out using GC–MS (Shimadzu technologies, QP 2010 ultra system). HP-1 methyl siloxane column (Shimadzu Rxi-5Sil MS; 30.0 m × 0.25 mm × 0.25 μm thickness) was used. Carrier gas was helium with high purity (>99.999%) and a constant flow of 1.0 mL/min was used for analyzing samples. The following temperature program was used for the analyses: initial temperature of column was 40 °C and it was held for 5 min and then increased to 150 °C at 10 °C/min and held for 7 min. The total run time was 23 min. The injection port, ion source and interface temperatures were 200 °C, 220 °C, and 200 °C, respectively. For qualitative determinations, scan mode was operated from *m*/*z* 50 to 550 and for quantitative analysis selective ion monitoring mode was used.

Table 8: Gas chromatographic conditions for THMs, HANs and HKs determination

Instrument	Shimadzu technologies, QP 2010 ultra system
Column	Shimadzu Rxi-5Sil MS; 30.0 m × 0.25 mm × 0.25 μm thickness
He gas flow rate	1.0 mL/min
Injection mode	split
Oven temperature program	40 °C (5 min) Ramped at 10 °C/min to 150 °C and held for (7 min) The total run time (23 min)
Injection port temperature	200 °C
interface temperatures	200 °C
MS temperature	220 °C

3.2.2 Fish and green algae samples

Fresh fish samples (Striped Red Mullet) were obtained from fish markets in Dammam, Eastern province, Saudi Arabia. Fish samples were directly transferred to icebox (-4 °C) for temporary storage before reaching the laboratory where stored at -18 °C prior to analysis.

Green algae samples were collected from nearest desalination plant in Jabil, Eastern province, Saudi Arabia, and then used in the experiments after being air dried.

3.2.3 MA-HS-LPME procedure

MA-HS-LPME experiments were carried out using laboratory microwave extraction system with programmable temperature and pressure (Anton Paar, Graz, Austria). The microwave has enhanced safety features and suitable for the simultaneous extraction of 16 samples. The vessels volume is 100 mL and it can maintain high temperature and pressure (240 °C and 40 bars).

Aqueous solutions are highly suitable for microwave digestion of biological samples, additionally; tissues are easily digested by acidic or basic solutions [95]. 3 g of biological samples were transferred to the cleaned microwave vessels equipped with magnetic stirrer bars. 15 mL of 100 mM HNO_3 solution was added to each vessel. A porous polypropylene membrane bag was filled with 500 µL of an organic solvent and heat sealed. This bag was suspended to certain depth in the microwave vessel via a PTFE ring. The extraction solvent toluene is compatible with the porous membrane and it dilates the pores of the membrane which allows the permeation of analytes in gaseous form. Figure 13 shows a schematic for the setup used.

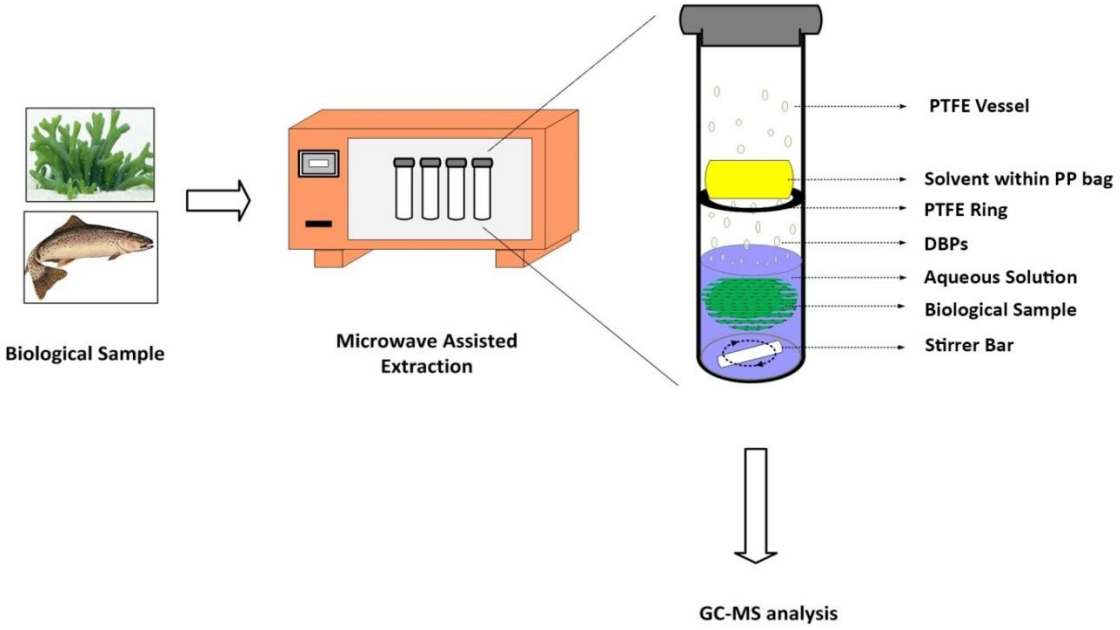

Figure 13 Schematic of extraction methods using MA-HS-LPME system.

This extraction system can be described as combination of two partitioning equilibria, digested sample versus headspace, and headspace versus organic phase (OP). Therefore,

$$C_0V_a=C_{a,eq}V_a + C_{hs,eq}V_{hs} + C_{op,eq}V_{op} \quad (3.1)$$

where C_0 is the original concentration of analytes in the aqueous sample. $C_{a,eq}$, $C_{hs,eq}$, and $C_{op,eq}$ are analytes concentrations in the aqueous sample, headspace, and OP, respectively. V_a, V_{hs}, and V_{op} are their corresponding volumes.

3.3 RESULTS AND DISCUSSION

MA-HS-LPME utilizes microwave energy for fast heating of the solutions by rotation of the molecules through migration of ions and dipoles [96]. The efficiency of the extraction method is controlled by different experimental parameters, such as type of extraction solvent, depth of the membrane envelope inside microwave vessel, extraction temperature, sample weight and extraction time.

3.3.1 Optimization of extraction parameters

Selection of solvent plays major role in MA-HS-LPME. Dielectric constant and the polarity of the solvent are important parameters to consider for selection of suitable solvent [83]. Toluene, isooctane, heptane and decane were selected as extraction solvents. Figure 14 shows that toluene gave higher recoveries compared to other solvents. That is due to two reasons: the polarity of toluene and its higher dielectric constant compared to other solvents which is in following order: heptane < isooctane < decane < toluene [97]. So toluene was selected as an optimum extraction solvent.

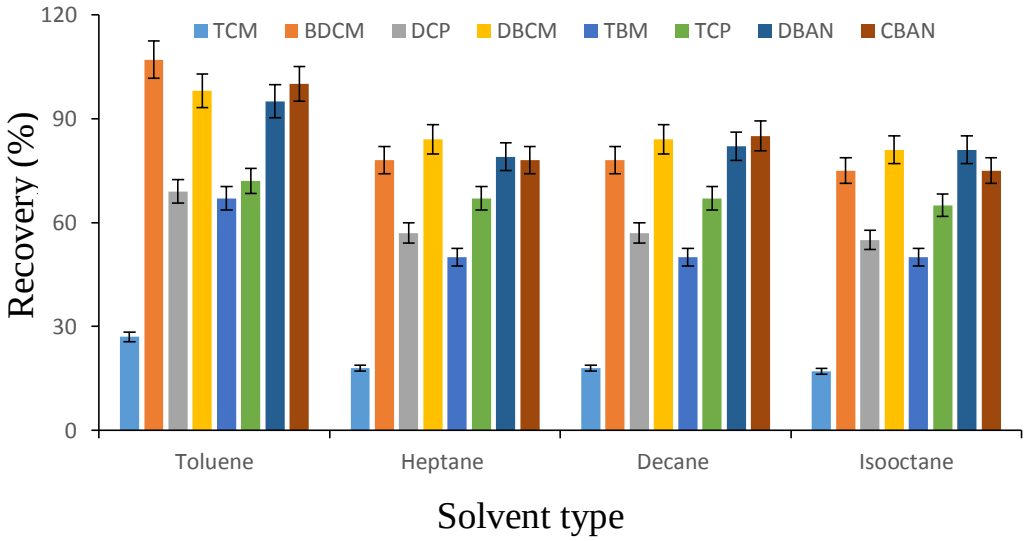

Figure 14 Effect of solvent type on the extraction of THMs, HANs and HKs by MA-HS-LPME

Depth of the solvent containing porous membrane was investigated in range of 1–7 cm on top of samples. (Figure 15) reflects the effect of membrane depth on the extraction efficiency of the target compounds. Relatively better extraction efficiency for all compounds was achieved at depth of 7 cm. Interaction of the vapors with liquid phase and disturbance created by stronger stirring at lower depths can reduce extraction efficiency of MA-HS-LPME. But as the vessel represents a closed system, homogenous vapor formation is expected at all depths, so no significant differences were seen in recovery of analytes.

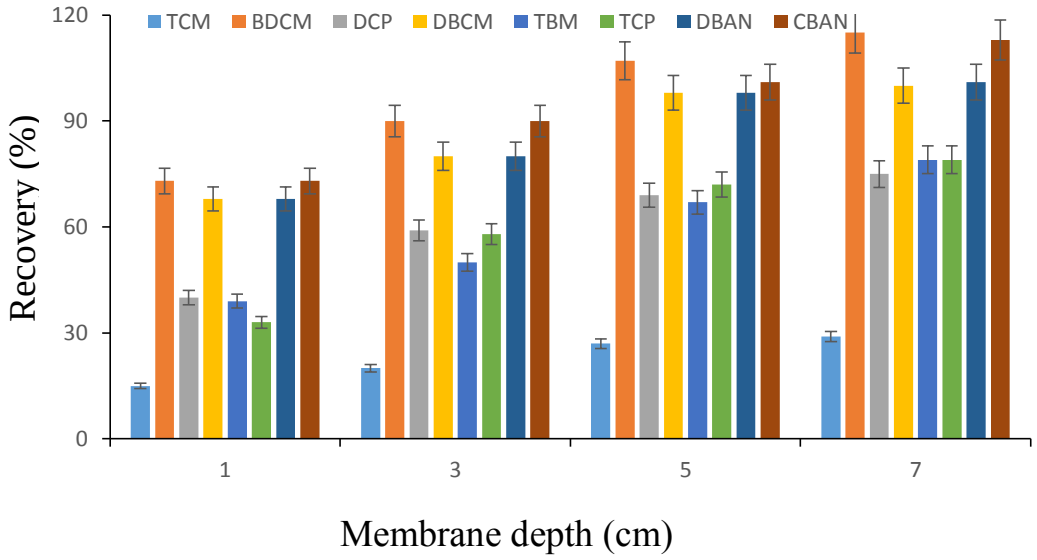

Figure 15 Effect of membrane depth on the extraction of THMs, HANs and HKs by MA-HS-LPME

The effect of the temperature on the extraction efficiency was evaluated between 40 and 100 °C. Figure 16 illustrates the recoveries of target analytes and extraction temperatures. Recoveries were increased up to 80 °C, and then levels off. Temperature below 80 °C was not enough to complete digestion of samples. By elevating the temperature, the extraction efficiency was improved. This increased extraction efficiency can be attributed to complete digestion of samples. However, at greater than 80 °C, loss of solvent was observed. Thus, 80 °C was selected as optimum temperature and used in further studies.

The effect of simultaneous extraction and digestion time was examined between 5 and 15 min. As it can be seen (Figure 17), recoveries increased up to 12 min and no further additional increments were observed after this time. This observation shows that 12 min is sufficient to completely digest the sample and vaporize the analytes.

After extraction time of 12 min, a constant amount of solvent (~187 μL) was lost from the membrane. The MA-HS-LPME is an equilibrium based extraction technique, the optimum conditions were maintained for the calibration and quantitation of real samples. Hence, the loss of the solvent does not affect the quantitation of the analtyes and the precision of the method.

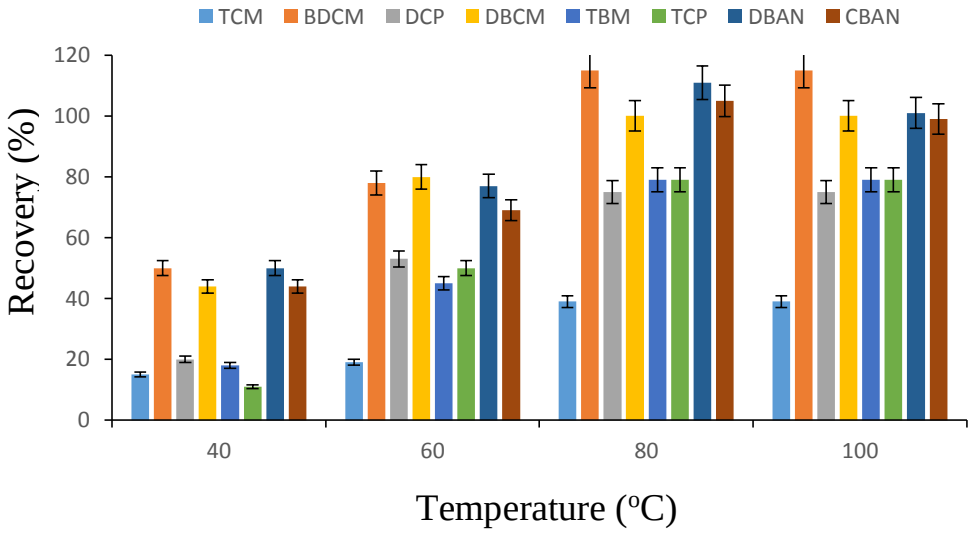

Figure 16 Effect of temperature on the extraction of THMs, HANs and HKs by MA-HS-LPME

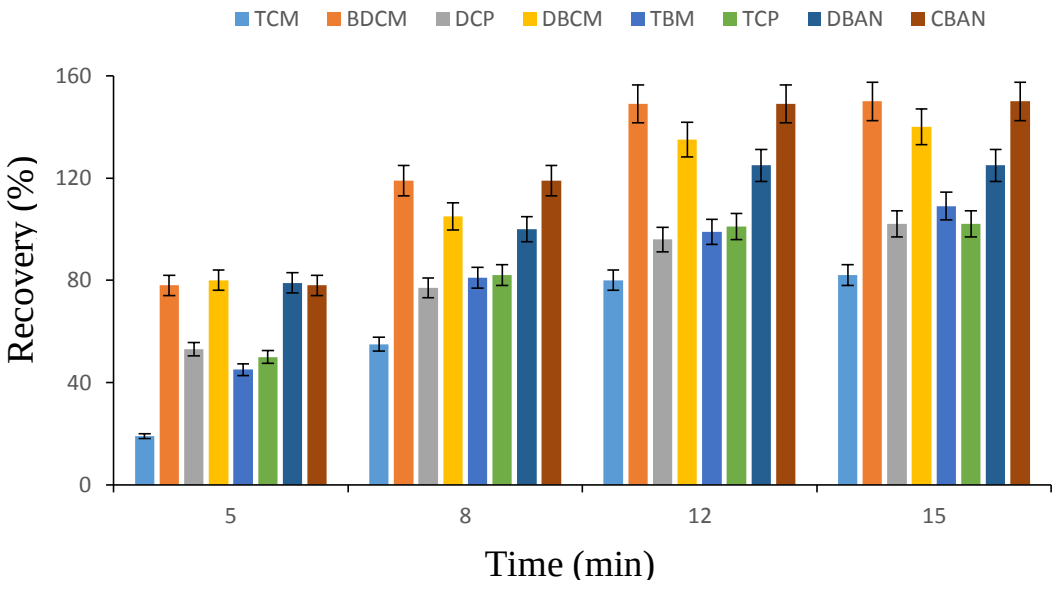

Figure 17 Effect of time on the extraction of THMs, HANs and HKs by MA-HS-LPME

Different sample size (1–5 g) was investigated to get optimum sample weight. Figure 18 shows the influence of sample weight on recoveries of analytes. As it can be clearly seen, the recovery increases upon increasing the sample weight. However, we did not attempt more than 5 g because it requires large volume of acid for digestion which increases sample digestion time.

In order to make a comparison, we applied headspace liquid-phase microextraction (HS-LPME) after the microwave digestion of biological samples. However, this separate digestion and extraction is time extensive. The extraction equilibrium was achieved in 30 min for this two-step HS-LPME and peak areas and recoveries were lower than our proposed single step MA-HS-LPME.

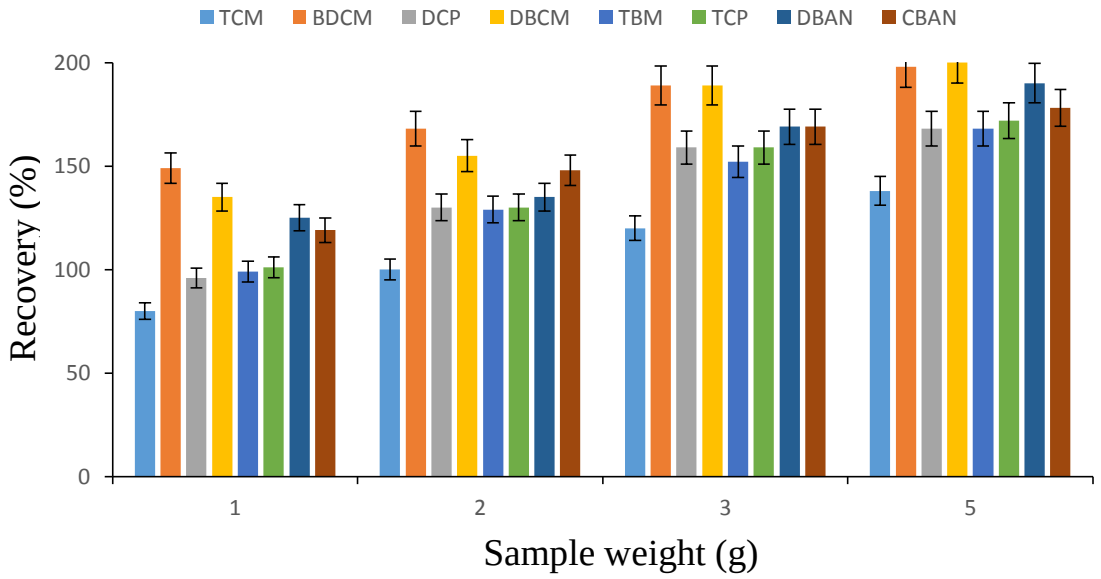

Figure 18 Effect of sample wieght on the extraction of THMs, HANs and HKs by MA-HS-LPME

3.3.2 Method validation and performance

In order to assess the matrix effect and to ensure more accuracy, matrix-matched calibration curves were used in this work by using matrix spiked with analyte standards. We used real tissues from a single fish for method development. Known concentration of analytes were spiked in the real fish tissues and the quantitation was performed using standard addition method. The regression equations were obtained by using 9 points standard concentrations (0.3, 0.5, 1, 5, 10, 20, 40, 70, 100 ng/g) as abscissa and the related peaks area as vertical axe. It is presented in Table 9 that the linearity in the concentration range of 0.3–100 ng/g was good for brominated targets while for the chlorinated ones was between 0.5 and 100 ng/g with determination coefficient (R^2) from 0.9836 to 0.9954. The sensitivity of the proposed method was determined by measuring the limits of quantification (LOQ) and the limits of detection (LOD) of tested DBPs for the biota samples, calculation done according to the guide lines of American Chemical Society's Committee on Environmental Analytical Chemistry and IUPAC, taken $S_{LOQ} = S_{RB} + 10\sigma_{RB}$ and $S_{LOD} = S_{RB} + 3\sigma_{RB}$ where S_{LOQ}, S_{LOD}, and S_{RB} are the signal at the limit of quantification, at the limit of detection, and of the reagent blank, respectively, while σ_{RB} is the reagent blank's standard deviation. The method LOQ was in the range from 0.175 to 0.351 ng/g while LODs of target analytes were ranged from 0.051 to 0.110 ng/g. The previous results for the proposed method confirm that it is suitable for the analysis of THMs, HANs and HKs trace level in biological samples.

Table 9. Feature of MA-HS-LPME method. Linear range, R^2, linear equations, LOQs, LODs, % RSDs.

No.	DBPs	linear equation	linear range (ng/g)	R^2	LODs (ng/g)	LOQs (ng/g)	%RSDs (n = 3)
1	TCM	y = 130.9x + 1476.1	0.5-100	0.9875	0.110	0.351	1.12
2	BDCM	y = 180.49x + 3737.5	0.3-100	0.9887	0.051	0.175	3.64
3	DCP	y = 59.129x + 404.19	0.5-100	0.9874	0.085	0.263	4.21
4	DBCM	y = 140.5x + 6713.6	0.3-100	0.9836	0.069	0.213	2.77
5	TBM	y = 1883.6x + 9939.4	0.3-100	0.9884	0.059	0.182	6.78
6	TCP	y = 151.69x + 994.31	0.5-100	0.9954	0.093	0.281	5.43
7	BCAN	y = 142.92x + 3976.5	0.3-100	0.9791	0.100	0.299	4.33
8	DBAN	y = 180.49x + 3737.5	0.3-100	0.9911	0.099	0.311	5.11

3.3.3 Real samples analysis

The developed MA-HS-LPME was applied for detection of THMs, HANs and HKs in different biological samples. Optimized conditions were used to quantitate DBPs in fish and green algae samples. The concentrations of target compounds that detected are shown in Table 10. The results indicate that contents of THMs, HANs and HKs in biota samples collected from different regions of Saudi Arabia were below than USEPA allowed limits [97]. As expected, fish scales have accumulated these compounds more than tissues because of direct and constant contact with the external contaminated environment [98, 99]. To assess the effect of matrix, real samples were spiked with 50 ng/g of target analytes, Figure 19 depicts the extraction recoveries which range from 90.5 to 102.5. Figure 20 presents the GC–MS chromatograms of unspiked and spiked fish scale sample which indicates that no sample matrix interference using this method.

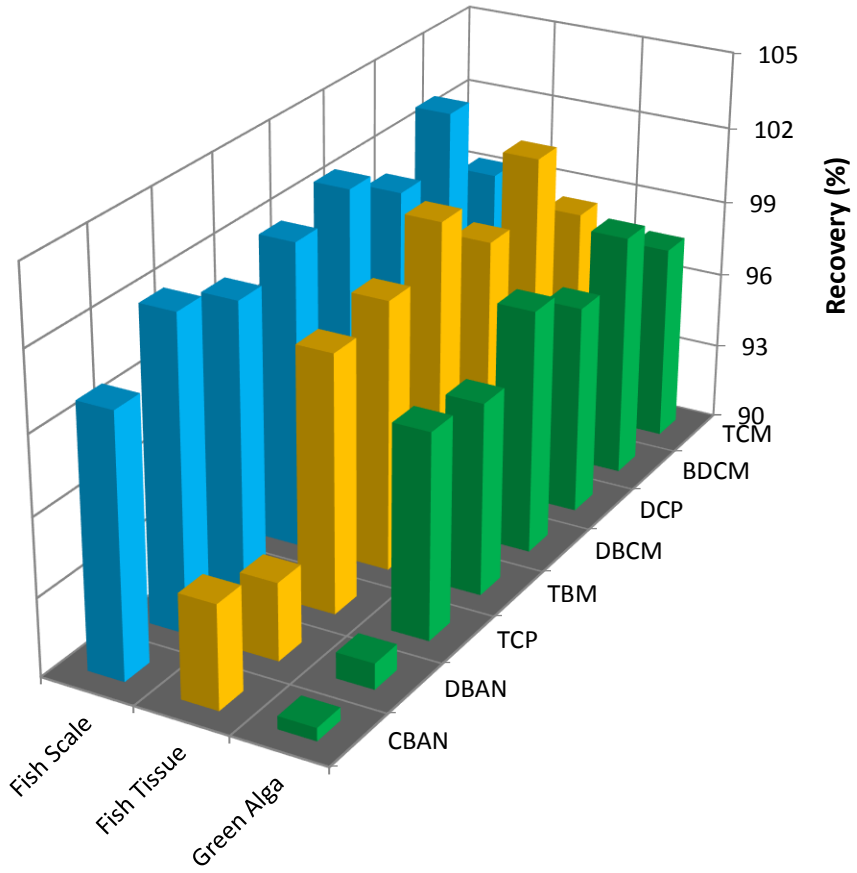

Figure 19 Extraction recovery of THMs, HANs and HKs from fish and green algae samples spiked by 50 ng/g using MA-HS-LPME.

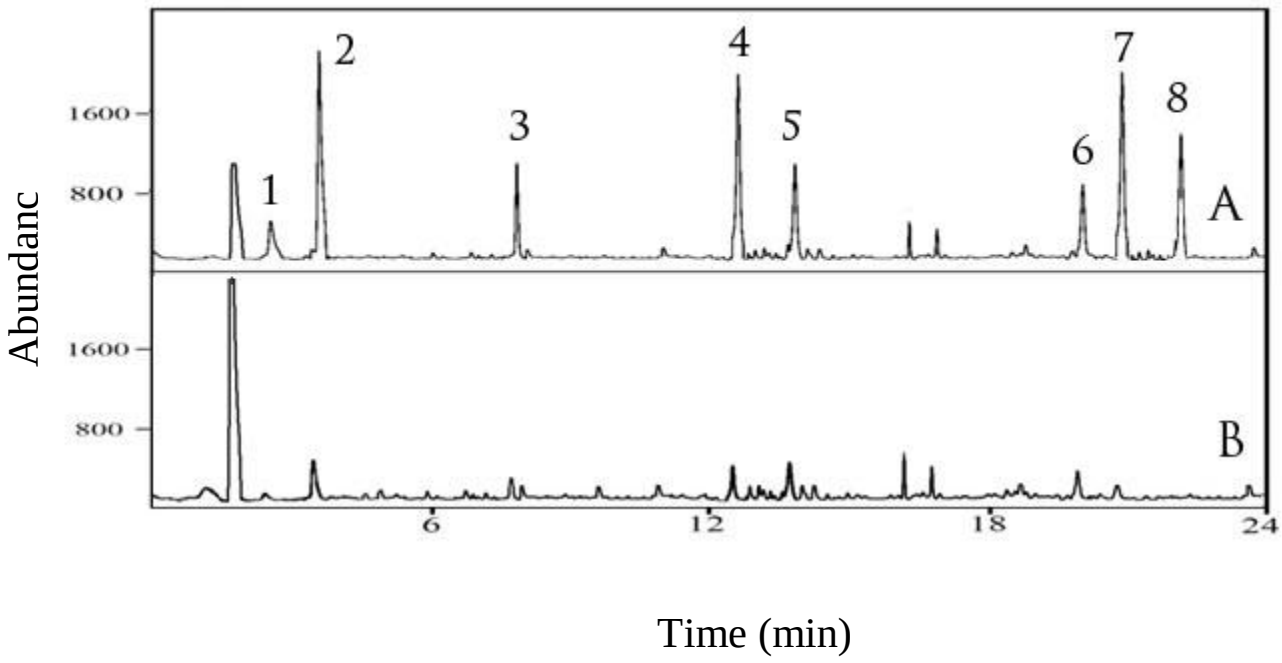

Figure 20 Chromatograms of THMs, HANs and HKs in fish scale sample extracted by MA-HS-LPME. A: spiked with 50 ng/g of DBPs, B: unspiked. Peak identification as in Table 9.

Table 10. Contents (ng/g) of the 8 analytes in the tested samples using MA-HS-LPME.

samples	TCM	BDCM	DCP	DBCM	TBM	TCP	BCAN	DBAN
Fish scale	3.0	5.2	3.1	5.2	4.9	3.5	0.5	ND
Fish tissue	1.9	3.9	2.0	3.5	3.9	2.1	ND	ND
Green algae	ND	2.9	ND	3.0	2.5	1.9	ND	ND

3.4 CONCLUSION

MA-HS-LPME, a novel and efficient extraction method was originally developed in this work. The feasibility of MA-HS-LPME was monitored by analyzing the trace level quantitation of THMs, HANs and HKs in fish and green algae with GC–MS. Sample cleanup, extraction and enrichment were done in one-step that makes the sample preparation much simpler and faster. MA-HS-LPME was an effective technique in reducing the sample preparation time and solvent consumption. MA-HS-LPME can be extended to other classes of organic pollutants in complex sample matrix

CHAPTER 4

FLOW-ASSISTED ELECTRO-ENHANCED SOLID-PHASE MICROEXTRACTION FOR THE DETERMINATION OF HALOETHERS IN WATER SAMPLES

4.1 LITIRATURE REVIEW

Haloethers (HEs) are chemical compounds which contain an ether moiety (R–O–R) and halogen atoms attached to the aryl or alkyl groups. HEs represent one important class of disinfection by-products (DBPs), which are unintentionally produced from the reactions of disinfectants with organic matter naturally present in the water [2]. They are harmful to humans and are suspected carcinogens even at low levels as parts per billion (ppb). In addition to that, HEs are widely used in industry [100- 102] as solvents for fiber processing, polymers, pesticides, medicine, and ion exchange resins and enter into aqueous environment. HEs can have great impact on the environment because of their persistent nature, carcinogenicity and toxicity [103- 106].

In 1979, five HEs were classified as priority pollutants by the United Sates Environmental Protection Agency (USEPA) and their maximum allowed contaminant level in water was proposed as 500 μg/L [107]. 4-chlorophenyl phenyl ether (CPPE) and 4-bromophenyl phenyl ether (BPPE) are among these HEs. USEPA methods 611 and 625 based on liquid–liquid extraction (LLE) technique were established to determine HEs from aqueous samples [103- 106]. However, this technique requires hazardous solvents, multi-step extractions, huge time consumption and there is a risk of losing HEs due to increased extraction and concentration steps [106, 108]. As a result, poor precision and low recoveries were reported [109].

Over the years, different analytical methods have been developed for the determination of HEs, such as liquid-phase microextraction (LPME) [110, 111], hollow fiber LPME (HF-LPME) [112-

114] and solid-phase microextraction (SPME) [103]. Among these methods, SPME is considered as solvent-free microextraction technique which integrates sampling, sample clean-up and pre-concentration into a single step [114, 115].

Although SPME offers single-step extraction procedure but the fibers used for SPME show low extraction capacity and thus cannot be a good choice for extraction from large volume samples. To improve the extraction capacity of SPME fibers, recently our group developed an electro-enhanced solid-phase microextraction (EE-SPME) [116]. Application of electrical potential to the SPME fiber enhances extraction of polar analytes via electrokinetic migration of charged analyte from samples toward the surface of the SPME fiber [116].

So far, most of the research has been carried out on static SPME methods for extraction of wide range of organic compounds. When compared to static mode, flow-assisted method showed considerable analyte enhancements. Therefore, the goal of the present study was to develop a method where electrical potential and flow can be combined together to enhance SPME extraction capacity from large volume of aqueous samples. Hence, we report flow-assisted electro-enhanced SPME (FA-EE-SPME) method for extraction of CPPE and BPPE from large volume of samples. Physical properties of target HEs are listed in Table 11.

Table 11. Physical properties of CPPE and BPPE

Physical properties	**CPPE**	**BPPE**
Chemical formula	$C_{12}H_9ClO$	$C_{12}H_9BrO$
Molecular weight (g/mol)	204.6	249.1
Solubility at 20-25 °C (mg/L)	1.43	0.82
Boiling point °C	161	305
Vapor pressure at 20-25 °C (mmHg)	0.0016	0.0005
Henry's law constant at 20 °C	0.012	0.009
Diffusion coefficient in air (cm^2 /s)	0.048	0.047
Diffusion coefficient in water (cm^2 /s)	6.18E-06	6. 27E-06

4.2 EXPERIMENTAL

4.2.1 Chemicals and Materials

A mixture of HEs standards was purchased from Supelco (Bellefonte, PA, USA). This mixture, containing CPPE and BPPE at 2000 µg/mL, was prepared in methanol. Working standard solutions were prepared on daily basis by appropriate dilution of stock solution of HEs using same solvent. Analytical grade solvents were obtained from Supelco. Double deionized water obtained from a Milli-Q system (Millipore, Bedford, MA, USA). Sodium hydroxide, sulfuric acid and sodium chloride were purchased (Merck, Darmstadt, Germany). All used glassware was washed with concentrated hydrochloric acid and rinsed with deionized water and acetone and then dried in an oven at 100 °C for 1 h. Three commercially available fibers polydimethylsiloxane (PDMS, 30-µm), carbowax/divinylbenzene (CW/DVB, 65-µm) and polyacrylate (PA, 85-µm) were purchased from Supelco (Supelco, Bellefonte, PA, USA) and used without any modifications for extraction of HEs. Platinum wire electrode (CHI115, CH Instruments Inc., USA) was used to complete the electrical circuit.

4.2.2 Water Samples

Different brands of drinking bottled water samples were purchased from local market in Khobar-Saudi Arabia. Samples of drinking water were also collected from KFUPM treatment plant. Tap water samples were collected from two different sources (main campus of KFUPM and Dammam housing) and tested without any further pre-treatment.

4.2.3 FA-EE-SPME

A 100 mL sample solution spiked with HEs was placed in a 125 mL flask which was connected by two PEEK tubes; the input tube passed through electrical pump to the extraction vial while the

output tube carried the solution back to the same flask. 20 mL modified auto-sampler extraction glass vial was connected to the tubes. SPME fiber and inert wire (platinum) were inserted in the sample solution. Both the Pt wire and SPME holder were connected via cable wires to the DC power supply. A negative voltage (−15 V) was applied to the needle of SPME holder and a positive (+15 V) potential was applied to the platinum electrode as shown in figure 21. A part of the needle of SPME holder was also immersed in the sample (to a depth of ca. 0.4 cm) to complete the circuit with the platinum wire. Now, it should be noted that SPME fiber from its outer side is connected with metallic needle of SPME holder. Metallic needle, which is a conductor, is directly in contact with SPME fiber which is also a conductive polymer. In this way, SPME fiber is negatively charged after application of potential and is capable of extracting positively charged analyte molecules at a faster rate than the conventional SPME fiber. Then, the sample was run at a flow rate of 50 mL/min for 10 min. After the extraction, the fiber was thermally desorbed in the GC–MS injection port at 280 °C for 3 min.

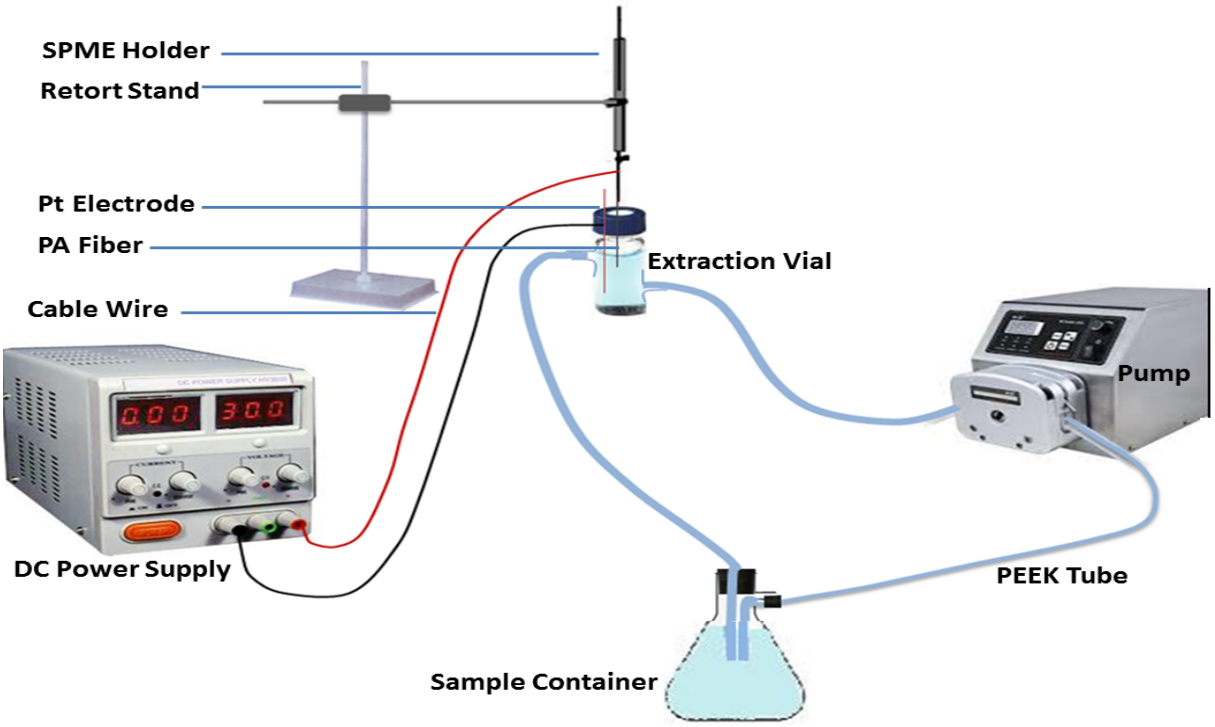

Figure 21 Schematic of FA-EE-SPME system

4.2.4 GC–MS Analysis

Analyses were carried out using a gas chromatograph (Agilent technologies, 6890N GC) coupled with a mass spectrometer (Agilent technologies, 5975B MSD). An HP-1 methyl siloxane column (Agilent 19091Z-213; 30 m × 320 µm I.D. × 1 µm thickness) was used. High purity helium (>99.999 %) was used as a carrier gas and the samples were analyzed in a constant flow at 1.2 mL/min. The fiber was thermally desorbed in the GC–MS injection port for 3 min at 280 °C. The temperature program used for the analyses was as follows: the initial temperature was 40 °C held 1 min which was then increased to 118 °C at 10 °C/min and held for 3 min, then to 190 °C at 15 °C/min and held for 7 min. The total run time was 21.6 min. The injection port, ion source and interface temperatures were 280, 230, and 250 °C, respectively. For qualitative determinations, the MSD was operated in full-scan mode from *m*/*z* 50 to 550 and selective ion monitoring mode was used for the quantification of the analytes.

Table 12: Gas chromatographic conditions for HEs determination

Instrument	Agilent technologies, 7890A GC coupled with Agilent technologies, 5975C MSD
Column	HP-5 used silica capillary column (Agilent 19091J-413; 30 m × 320 μm ID × 0.25 μm thickness)
He gas flow rate	1.2 mL/min
Injection mode	Split
Oven temperature program	40 °C (1 min) Ramped at 10 °C/min to 118 °C and held for (3 min) Then ramped at 15 °C/min to 190 °C and held for (7 min) The total run time (21.6 min)
Injection port temperature	280 °C
interface temperatures	250 °C
MS temperature	230 °C

4.3 RESULTS AND DISCUSSION

Different affecting parameters were optimized to enhance the extraction of target HEs from large volume of water samples. Detail of optimized parameters is given below.

4.3.1 Effect of Absorption Time of SPME

Effect of the absorption time profile using PDMS coated fibers was studied between 5 and 30 min extraction time. Figure 22 shows the percentage recovery of HEs and extraction time. Peaks were increased up to 10 min and then slightly decreased. Sampling agitation and stronger flow of water sample may increase the extraction profile quickly to reach equilibrium with the SPME fiber and then analytes may start desorbing slowly in the sample matrix. Thus, 10 min was selected as optimum value and used in further studies.

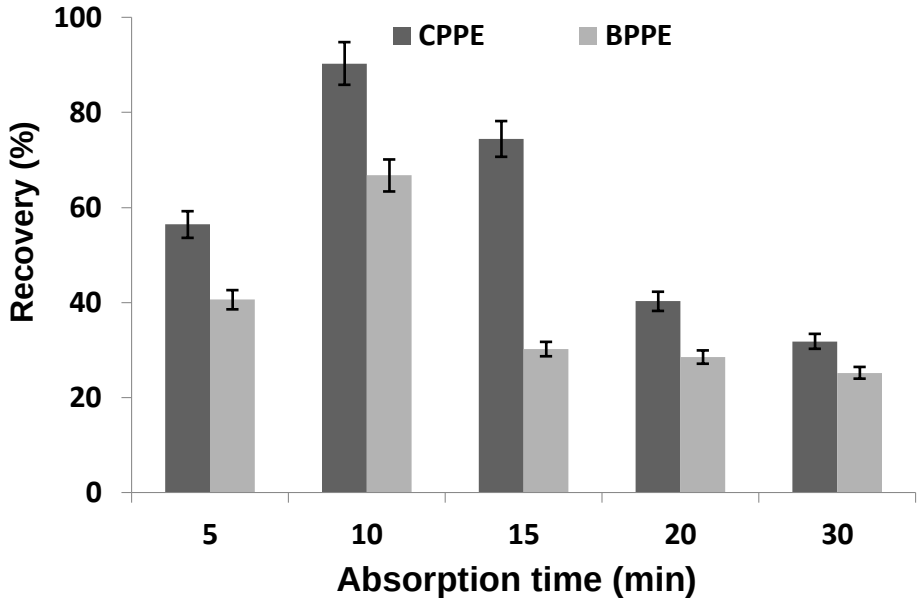

Figure 22. Effect of absorption time on extraction of CPPE and BPPE (PDMS coated fiber, 100 mL of sample spiked by 100 µg/L HEs, flow rate 50 mL/min, desorption time 3min, pH 5.7) Error bars show the standard deviation (n=3).

4.3.2 Effect of Pump Flow Rate

To investigate the effect of sample flow rate on the SPME extraction, samples were pumped using a peristaltic pump in the range between 0 and 80 mL/min. Figure 23 shows the influence of sample flow over static mode (0 flow rate). As we can see that the signal increased upon changing the flow rate till 50 mL/min and then started decreasing after that. Flow rate of 50 mL/min gave higher recoveries for both compounds compared to other flow rates. Concluding that the concentration of the adsorbed analyte at SPME surface decreased at the high pump flow rate due to strong vibration of SPME fiber and thus led to desorption of analytes back to the sample matrix.

The effect of flow was also tested by comparing the extraction efficiencies of EE-SPME and FA-EE-SPME. It can be seen that recoveries are threefold higher in case of FA-EE-SPME (Figure 24).

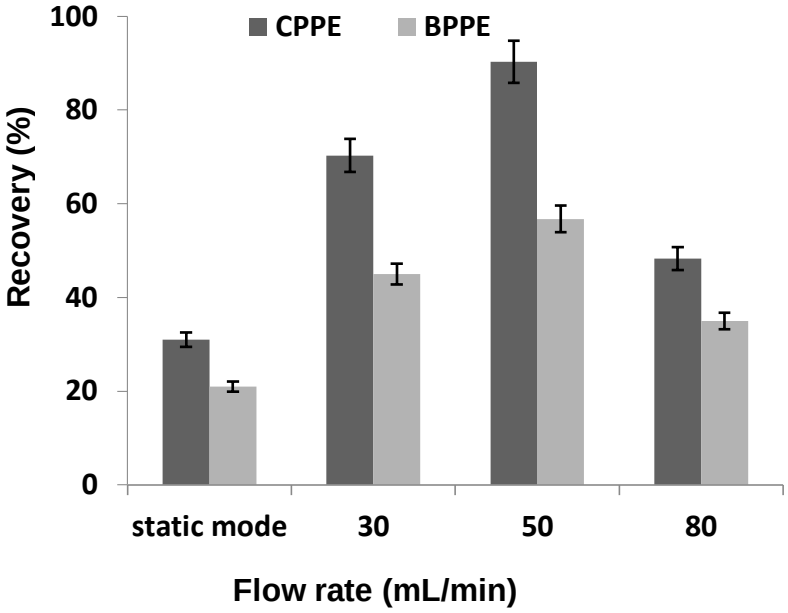

Figure 23. Effect of sample flow rate on extraction of CPPE and BPPE (10 min absorption time, other conditions as in figure 22)

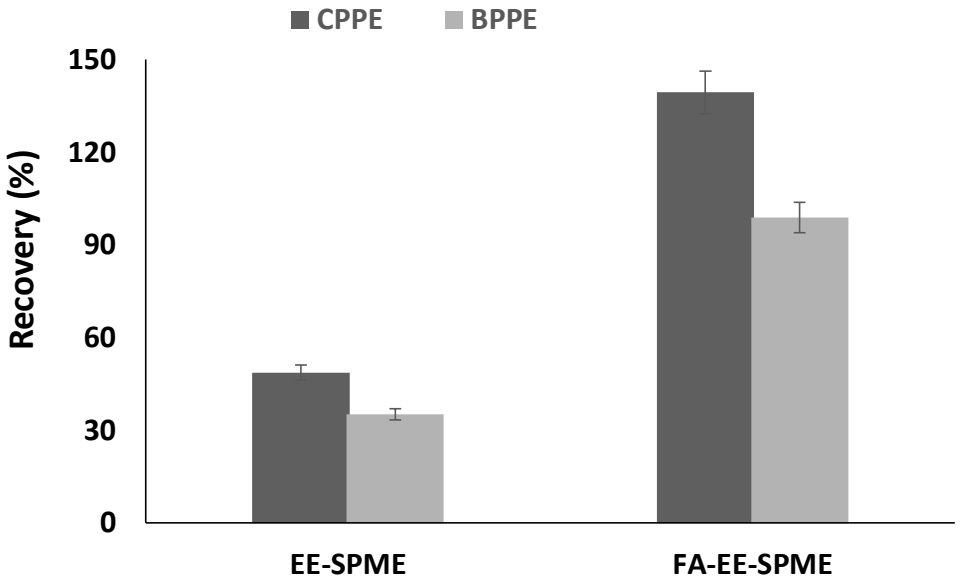

Figure 24. Comparison of EE-SPME and FA-EE-SPME (Optimum voltage -15 V, other conditions as in figure 23).

4.3.3 Effect of Ionic Strength

Figure 25 reflects the effect of ionic strength on the SPME extraction efficiency of HEs. NaCl concentration range (0–35) % (w/v) was used. As it can be seen, highest extraction efficiency for all HEs was at salt concentration 10 % (w/v). The response started decreasing for solution containing higher than 10 % (w/v) of salt. So 10 % (w/v) salt was chosen as an optimum parameter. We realize that the effect of NaCl on the extraction of HEs could be due to three factors. First one is that the salting-out effect, which decreases the solubility of the analytes, and thus increase the absorption [105, 114]. Secondly, dissolving salt in the solution may change the physical properties of the static aqueous layer on the fiber, and thereby reduce the rate of diffusion of the analyte through the static aqueous layer to the fiber [105]. Third cause is associated with the zwitterions of the resonance forms of the targets molecules. Such conduct enhances the solubility in water due to the increased contribution of zwitterion form to the resonance structure [104]. The mentioned factors together are responsible for the decreased peaks areas in solutions containing a high concentration of NaCl.

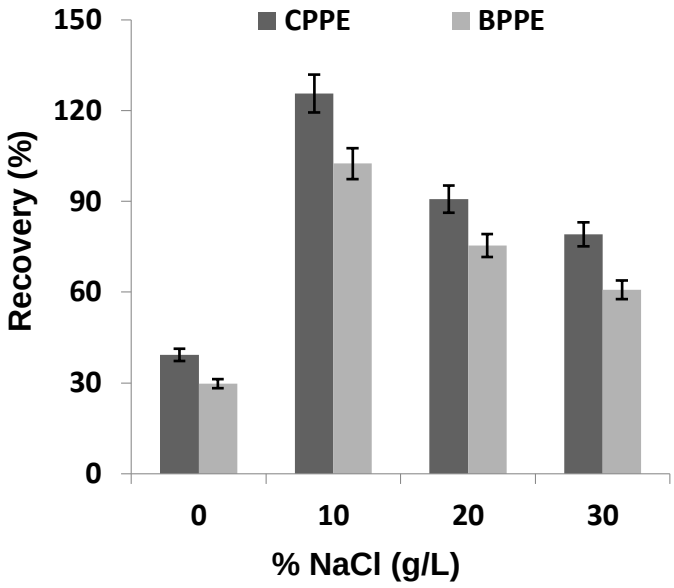

Figure 25. Effect of salt addition NaCl on extraction of CPPE and BPPE (Other conditions as in figure 24)

4.3.4 Sample pH

To find out the best detection medium pH, sample pH was examined in the range of 2–10, as shown in Figure 26. The best extraction efficiency was obtained at pH 2. At alkaline conditions, low efficiency was obtained; this could be due to hydrolysis of HEs. In acidic medium, the hydrogen ions may attach to the oxygen moiety of ether group and a positive charge might develop on the molecule. So this positively charged molecule may easily migrate towards the negatively charged SPME fiber. The applied potential enhances the migration of target analytes on the fiber surface. Without applying electrical potential, very slow extraction was observed. Therefore, pH 2 of sample solution was applied to all experiments as an optimum pH.

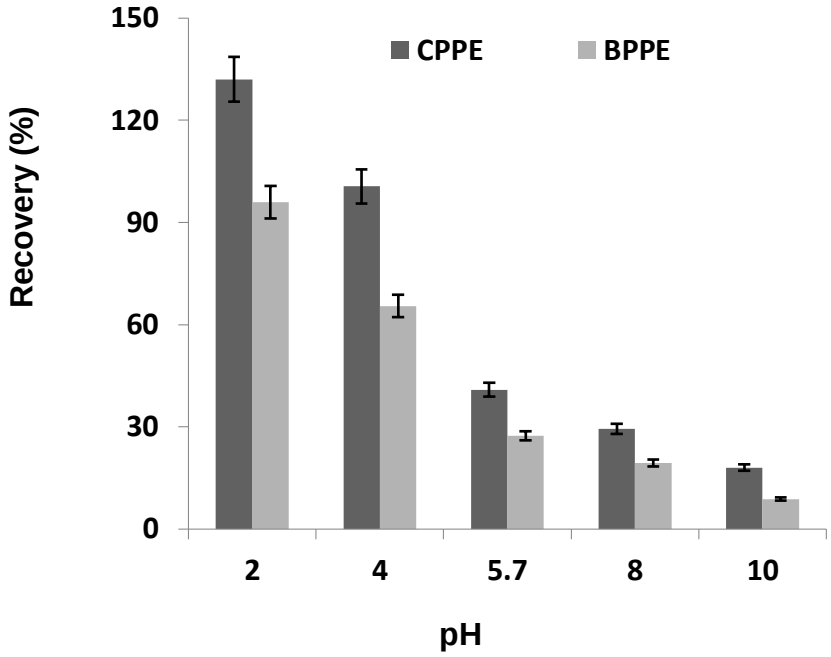

Figure 26. Effect of sample pH on extraction of CPPE and BPPE (% 10 NaCl, other conditions as in Figure 25)

4.3.5 Effect of Applied Voltage on SPME

A substantial enhancement of HEs response was observed with application of different values of electrical potential. Figure 27 displays the effect of different electrical potential on the extraction of HEs. Potential values from −20 to +5 V were applied for the SPME method. As expected, negative potential gives better result because the ionic form of CPPE and BPPE in the aqueous medium has positive charge. In electrical potential application mode, the tip of SPME holder was immersed in the sample solution together with the selected fiber. Thus, it led to completion of the electrical circuit between platinum wire electrode and the tip of the holder, as shown in Figure 18. Without applying potential, only small concentrations of target compounds were extracted and extraction process was relatively very slow (Figure 27). By applying potential, the extraction process was accelerated via electrokinetic migration because applying negative potentials made the fiber coating negatively charged and, therefore, this might enhance the extraction of positively charged molecules of target compounds via electrophoresis and complementary charge interaction [115]. At lower potential (−20 V), bubbles formation started on the SPME fiber which reduced the polymer coating active surface area. Thus, an optimum applied potential of −15 V was selected for further analysis.

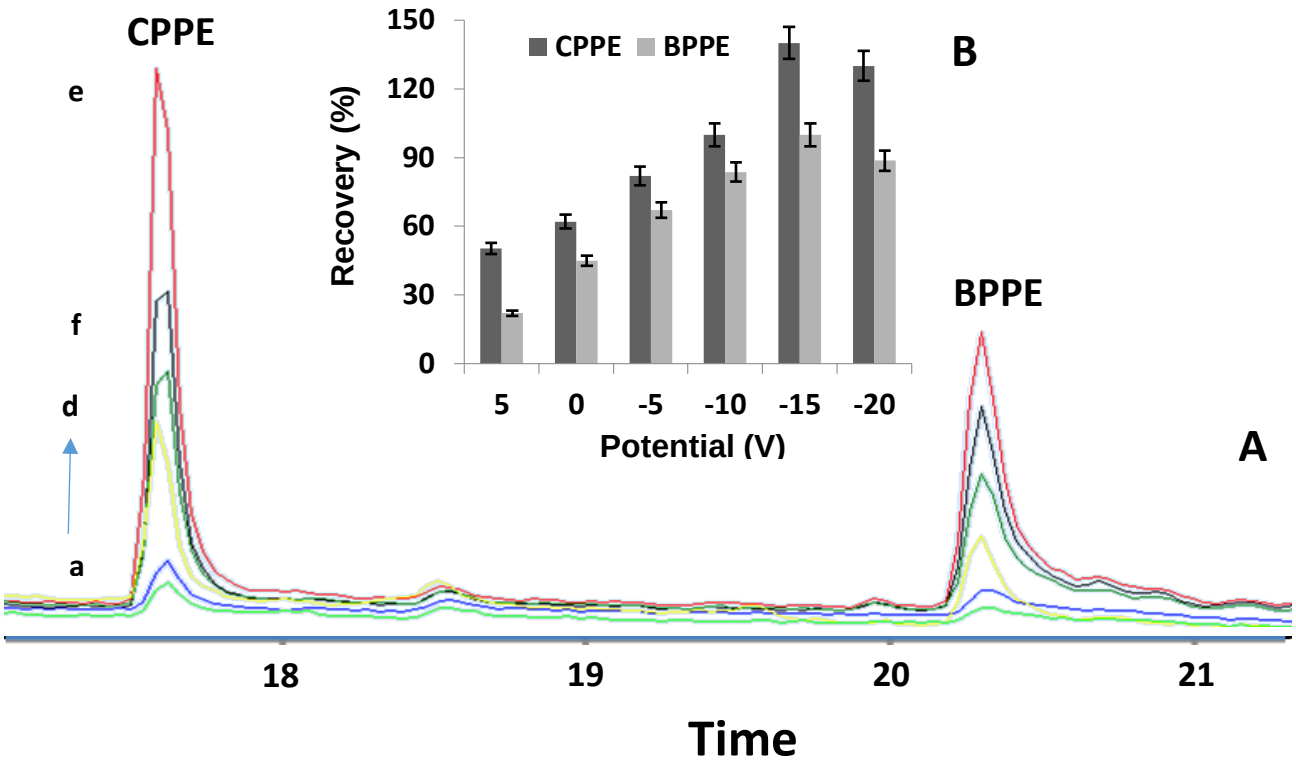

Figure 27. a Chromatograms of applying different potential on extraction of CPPE and BPPE, *a* +5.0 V, *b* 0.0 V, *c* −5.0 V, *d* −10.0 V, *e* −15.0 V, *f* −20.0 V. b *Inset* histogram of applied potential versus recoveries of target compounds (other conditions as in Figure 24)

4.3.6 Selection of SPME Fiber

To select the best SPME fiber, three commercially available fibers were tested to extract CPPE and BPPE. PDMS, CW/DVB and PA coated fibers were used without any modifications. The fibers were conditioned prior to use according to the instructions provided by the suppliers. Figure 28 shows the extraction performance of three tested fibers. PDMS gave the highest recovery for both analytes. This higher extraction efficiency could be due to the strong affinity of CPPE and BPPE to the PDMS fiber which is expected because of the high value of their octanol–water partition coefficients (log Kow) [CPPE (4.08) and BPPE (5.12)] [101]. In addition, PDMS has electrical conductivity which enhances the analyte extraction by applying potential in the flow mode. Hence, PDMS was selected as an optimum fiber for calibration and quantitation of real samples.

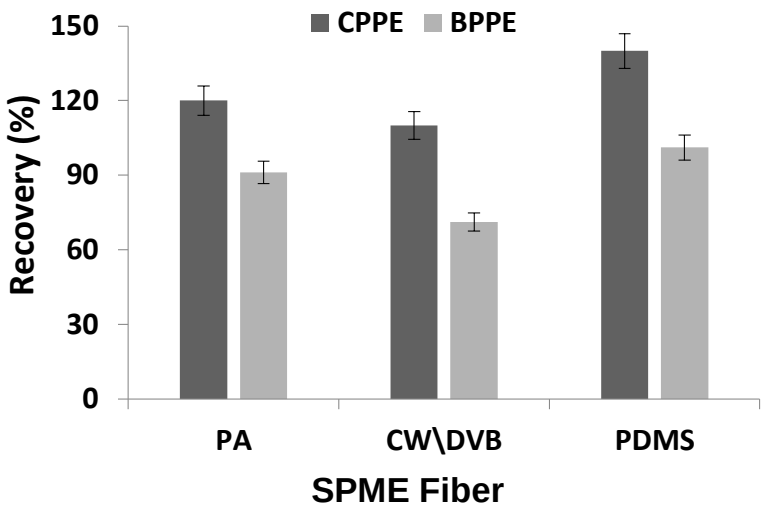

Figure 28. Selection of SPME fiber (100 mL of sample spiked by 100 µg/L HEs, absorption time 10 min, flow rate 50 mL/min, Applied potential -15.0 v, desorption time 3min, pH 2).

4.3.7 Analytical Performance of FA-EE-SPME Method

The quantitative behavior was assessed by monitoring the dependence of the CPPE and BPPE peak areas at a different concentration level of (0.5, 1, 5, 10, 20, 40, 70, 100 µg/L). Quantitative parameters (linear range, repeatability, and limits of detection) were calculated under the optimized conditions and summarized in Table 13. Excellent linearity was observed over the concentration range of 0.5–100 µg/L for CPPE and BPPE with coefficient of determination (R^2) ranging from 0.9954 to 0.9884. Satisfactory reproducibility of the relative standard deviations (RSD) was ranged between 1.1–3.6 % (n = 6). The sensitivity of the proposed method was determined by measuring the limits of quantification (LOQ) and the limits of detection (LOD) of tested HEs, calculation done according to the guidelines of the American Chemical Society's Committee on Environmental Analytical Chemistry and IUPAC, taken as:

$$S_{LOQ}=S_{RB}+10\sigma_{RB} \quad (4.1)$$

$$S_{LOD}=S_{RB}+3\sigma_{RB} \quad (4.2)$$

where S_{LOQ}, S_{LOD}, and S_{RB} are the signal at the limit of quantification, at the limit of detection, and of the reagent blank, respectively, while σ_{RB} is the reagent blank's standard deviation. The method LOQ was in the range from 0.16 to 0.21 µg/L while the LODs were ranged from 0.05 to 0.07 µg/L. The results confirmed that the proposed method is suitable for trace level analysis of HEs in water samples. Table 14 gives a comparison between the proposed method and methods reported in the literature. The developed method showed promising results compared to those already reported. The main advantages of our present flow-assisted electro-enhanced SPME technique over existing microextraction techniques lie in its simplicity, solvent-free preconcentration, single-step combination of electrical potential and flow system, which provide high precision and reasonably low detection limits.

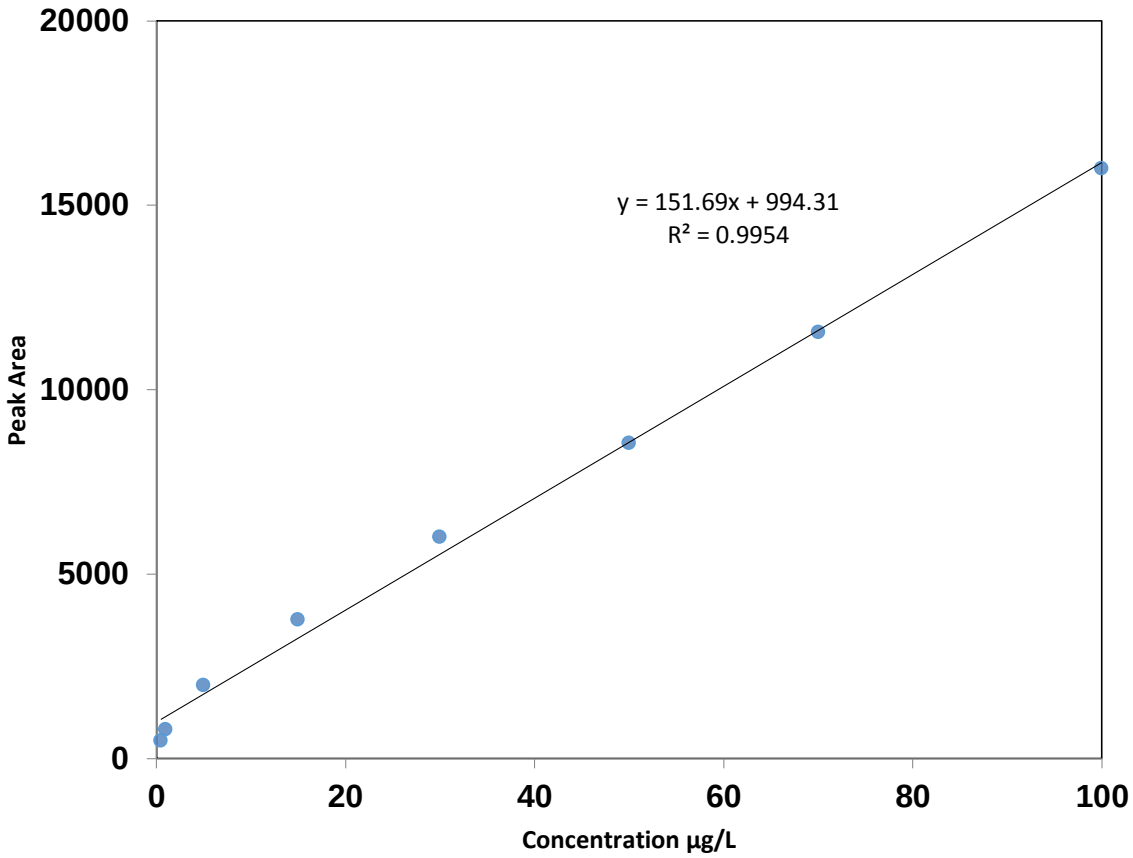

Figure 29 Calibration plot for CPPE at concentrations of 0.5-100 µg/L

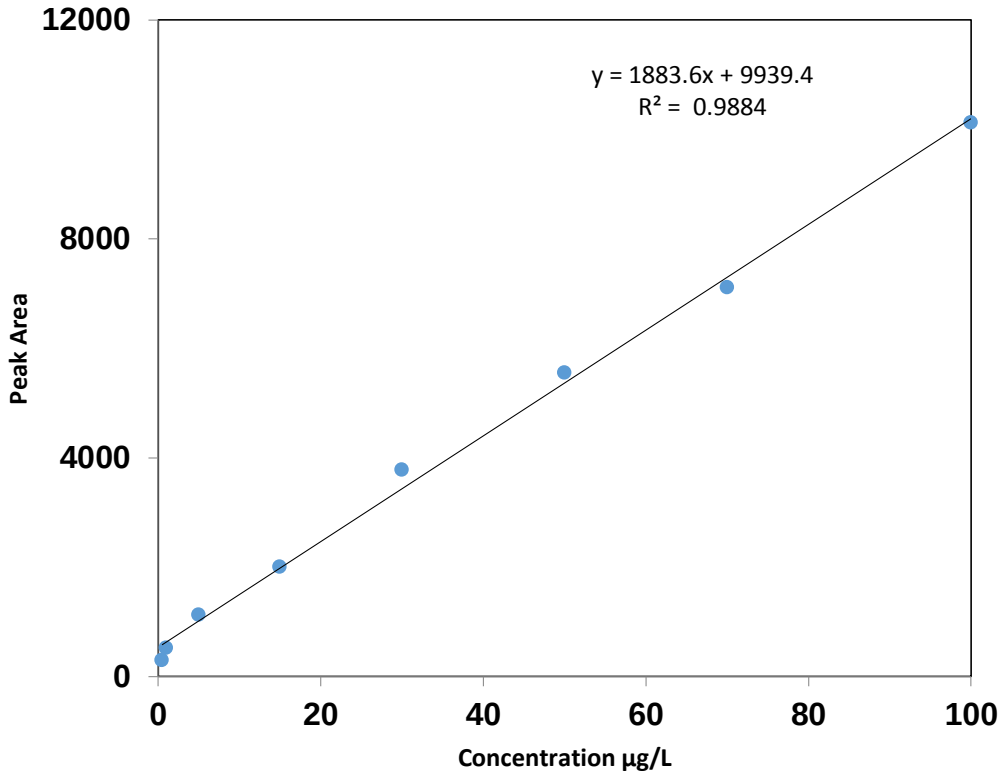

Figure 30 Calibration plot for BPPE at concentrations of 0.5-100 µg/L

Table 13. Features of FA-EE-SPME method. Linear range, coefficient of determination (R^2), linear equations, % RSDs, LOQs, LODs.

Compound	Linearity range (µg/L)	R^2	Equation	%RSDs (n = 6)	LOQs (µg/L)	LODs (µg/L)
CPPE	0.5 - 100	0.9954	y = 151.69x + 994.31	1.12	0.159	0.051
BPPE	0.5 - 100	0.9884	y= 1883.6x + 9939.4	3.64	0.211	0.069

Table 14. Comparison of the proposed method with those reported in literature.

Analytical technique	Extraction time	LODs µg/L CPPE BPPE	Ref-
SPME/ GC-FID[a]	40 (min)	0.04-0.06	104
HF[b]-LPME/GC-FID	30 (min)	0.55-0.66	111
HF-LPME/GC-ECD[c]	30 (min)	0.29-0.11	111
Method 611 of USEPA LLE	~ 2 (hrs)	3.9-2.3	107
FA-EE-SPME/GC-MS	10 (min)	0.051-0.069	Present work

a)Flame ionization detector b) Hollow fiber assisted liquid phase microextraction c) Electro capture detector.

4.3.8 Real Sample Analysis

The developed FA-EE-SPME was tested for the detection of HEs in different water samples. The optimized conditions were applied to drinking water and tap water samples. Large volume (100 mL) of water was used for the FA-EE-SPME extraction. The concentration of CPPE and BPPE detected by this method is shown in Table 15. To assess the matrix effect, real samples were spiked with 5 and 30 µg/L of target analytes and extraction recoveries were calculated in Table 15. Figure 31 Shows the GC–MS chromatograms of unspiked and spiked drinking water samples which clearly indicate that no sample matrix interferences are observed for this method.

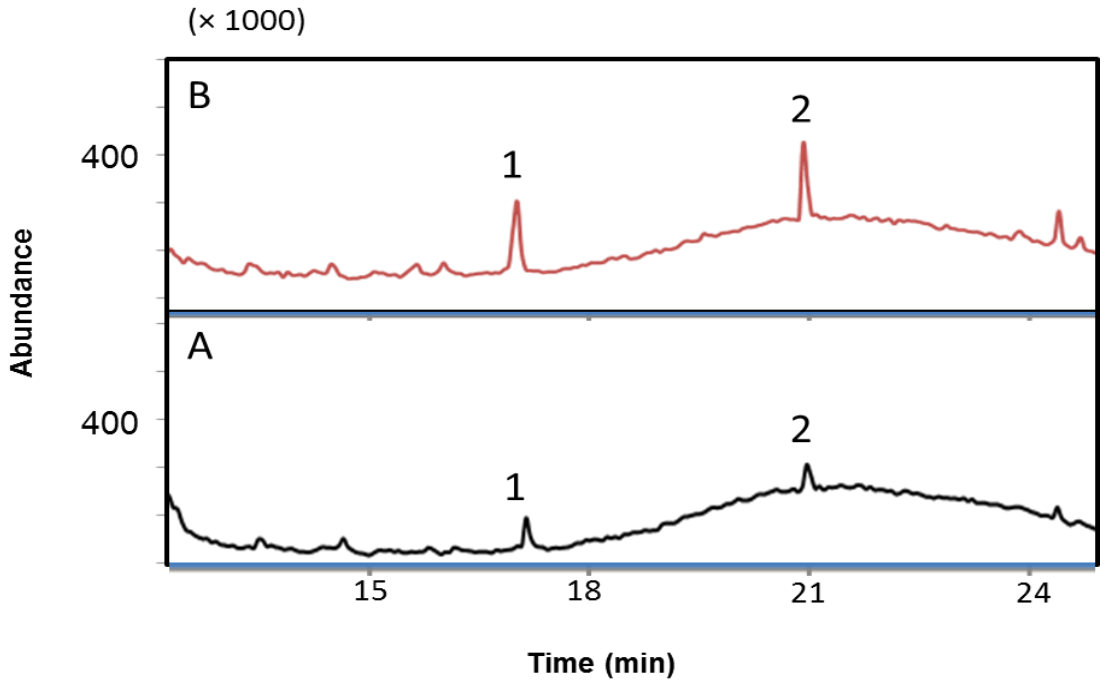

Figure 31. Chromatograms of (1) CPPE and (2) BPPE in drinking water samples. A: unspiked drinking water, B: drinking water spiked with 5 µg/L of HEs.

Table 15. Extraction recovery of CPPE and BPPE in unspiked and spiked (5 and 30 µg/L) water samples by FA-EE-SPME.

Cpds.	CPPE			BPPE		
	0 µg/L	5 µg/L	30 µg/L	0 µg/L	5 µg/L	30 µg/L
KFUPM Tap Water	4.1 ± 0.67	8.3 ± 0.25	33.2 ± 0.31	5.8 ± 0.45	9.8 ± 0.71	34.9 ± 0.65
Dammam Tap Water	5.1 ± 0.77	9.9 ± 0.27	34.2 ± 0.41	5.3 ± 0.36	10.0 ± 0.73	35.0 ± 0.46
KFUPM Drinking Water	4.0 ± 0.68	8.9 ± 0.58	33.1 ± 0.59	3.7 ± 0.45	7.8 ± 0.46	32.8 ± 0.77
Drinking Water (1)	3.9 ± 0.78	7.9 ± 0.48	32.1 ± 0.39	3.3 ± 0.55	7.8 ± 0.36	32.8 ± 0.27
Drinking Water (2)	3.1 ± 0.77	7.8 ± 0.35	32.8 ± 0.51	3.8 ± 0.55	8.4 ± 0.79	32.9 ± 0.69
Drinking Water (3)	2.5 ± 0.32	7.3 ± 0.12	32.1 ± 0.44	2.1 ± 0.65	7.0 ± 0.81	31.9 ± 0.42
Drinking Water (4)	3.8 ± 0.45	8.5 ± 0.39	33.0 ± 0.59	3.1 ± 0.11	8.0 ± 0.66	32.5 ± 0.35

4.4 CONCLUSION

In this work, we have demonstrated the use of flow-assisted electro- enhanced solid-phase microextraction (FA-EE-SPME) for the determination of CPPE and BPPE in water samples. Compared to reported methods, the FA-EE-SPME gave higher analyte enhancement for large volume samples. The developed extraction procedure provides a convenient and efficient method for assay at ultra-trace levels. Moreover, the proposed FA-EE-SPME is suitable for on-site applications

CHAPTER 5

STUDYING THE FORMATION MECHANISM OF *N*-NITROSODIMETHYLAMINE IN THE TREATED WATER

5.1 LITERATURE REVIEW

Nitrosamines, a group of nitrogenous disinfection by products (N-DBP), are chemical compounds which considered as carcinogenic, teratogenic and mutagenic [117, 118]. N-nitrosodimethylamine (NDMA) is the most commonly detected and reported nitrosamine in drinking water. United State Environmental Protection Agency (USEPA) has been classified NDMA as a probable human carcinogen [119]. Risk assessments from the USEPA identify 10^{-6} lifetime risk level of cancer from NDMA exposures as 0.7 ng/L [119]. Nitrosamines have been identified in different food staff, soils, wastewater and drinking water [120- 122]. It is generally thought that nitrosamine formation involves N-nitrosation, a reaction between nitrosatable amines and nitrite [123, 124]. Therefore, NDMA is likely to be found especially where both secondary amines and nitrite occur. Environmentally oriented NDMA occurrence and formation studies have been generally empirical in nature and have focused primarily on determining if nitrosamines may be formed in water. Ayanaba et al. [125] investigated the formation of NDMA in the lake water at neutral pH values when dosed with nitrite and dimethylamine (DMA) and trimethylamine (TMA). Other reports have demonstrated the influence of other precursors such as fulvic acid on nitrosamine formation with added nitrite [126, 121].

Recent studies show the presence of NDMA in highly purified wastewaters intended for recycle and also some treated drinking waters while absent in the influent streams [120]. Some current

reports indicate that NDMA commonly observed in treated water, which suggest that NDMA can be produced in the treatment and disinfection processes.

In the following study, investigation to the NDMA formation as N-DPB produced by addition of monochloramine (MCA) to the water samples having different amines in absence and presence of humic acid (natural organic matter) has been done. MCA is used as a disinfectant, which may also form in chlorinated water in the presence of ammonia. DMA has been chosen as a precursor because it exists in both surface and wastewater [127, 128]. A series of experiments were carried out to identify the formation of NDMA from the reaction between MCA and DMA. Finally a mechanism for NDMA formation has been proposed.

5.2 EXPERIMENTAL

5.2.1 Materials and methods

N-nitrosodimethylamine was purchase from Supelco (Bellefonte, PA, USA) (100 μg/mL in methanol). Humic acid, DMA, MCA and other tertiary amines were purchased from Sigma Aldrich, (TCI, Matrix Scientific, and Santa Cruz Biotechnology) and used without further purification. Tertiary aliphatic amines were chosen based on their chain length and functional groups attached to basic DMA structure. All other chemicals used in these experiments were analytical laboratory grade.

5.2.2 NDMA formation reactions

All experiments were conducted in 1 L sealed bottles at room temperature (25°C). Deionized water was used for reaction solutions preparation buffered with 1 mM bicarbonate, and adjusted to approximately pH 7.3 by acid addition. DMA was added from 0.01 to 0.2 mM at fixed MCA

concentration of 0.1 mM. On the other hand, MCA was added from 0.01 to 2.0 mM at fixed DMA concentration of 0.1 mM. The mixtures were reacted in the dark for (1 – 40) hours. Lastly, measured NDMA concentrations were used to calculate percent molar yield for each amine using Equation:

$$\text{NDMA Yield (\%)} = ([\text{NDMA}] / [\text{Amine}_0]) * 100 \quad (5.1)$$

5.2.3. NDMA analysis

Samples were passed through cartridges pre-packed with 2 g of coconut charcoal. Prior to sample extraction, cartridges were preconditioned with methanol and deionized water. Eluted samples were passed through cartridges pre-packed with 6 g of sodium sulfate and concentrated to 1 mL under high purity nitrogen gas. The extracts were analyzed using gas chromatography- mass spectrometric instrument (GC-MS). NDMA is quantified based on the mass detection of the characteristic molecular ion (m/z=74.048) of NDMA.

5.3 RESULTS AND DISCUSSION

5.3.1 NDMA formation studies

Effect of the reaction period was studied between (1 – 40) hours. Figure 32 shows that NDMA formation continued over 40 h period reaching 18 μg/L and the formation potential did not appear to be exhausted after 40 h.

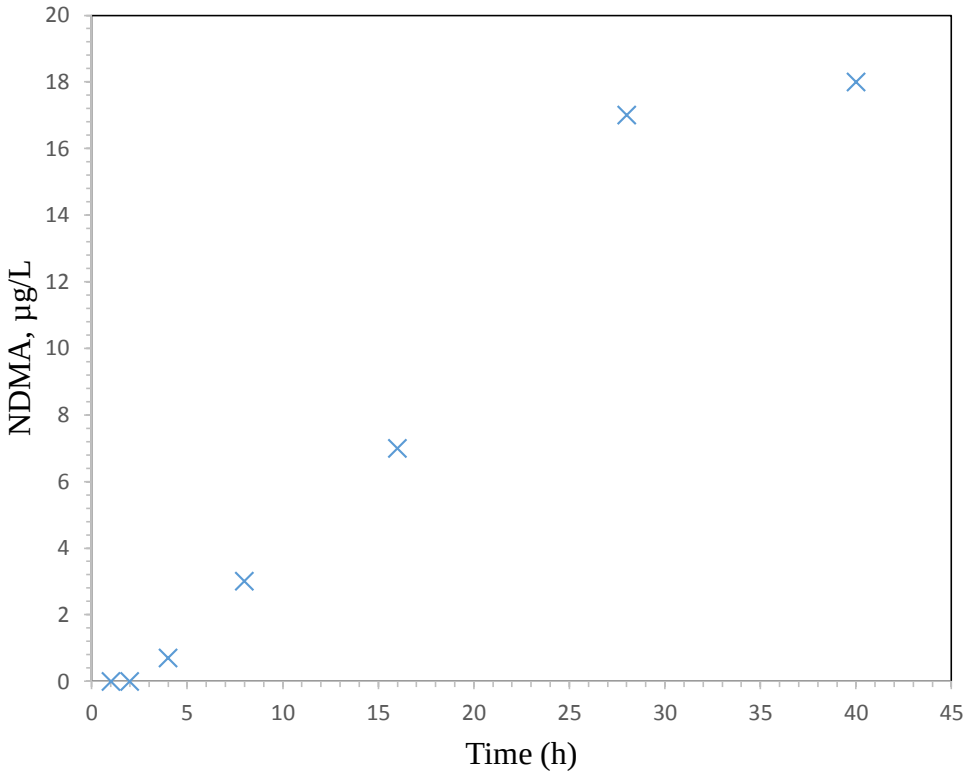

Figure 32. NDMA formation as a function of time. 0.1mM of DMA was reacted with 0.1mM of MCA. pH: 7.3. Solutions were kept in the dark, Temp: 25ºC.

NDMA formation was studied as a function of MCA concentration at a fixed DMA concentration of 0.1 mM (figure 33). NDMA formation increased with increasing MCA concentration from 0.01 to 2 mM. The formation appeared to reach an apparent plateau with addition of approximately 2 mM of MCA.

NDMA formation showed a maximum in yield when DMA was varied (0.01– 0.2 mM) at fixed MCA concentrations of 0.1mM (figure 34). The maximum occurred when the ratio of DMA to MCA was approximately 1.0 mM. The amount of NDMA produced rapidly decreased as the ratio of DMA to MCA was further increased beyond 1.0 mM.

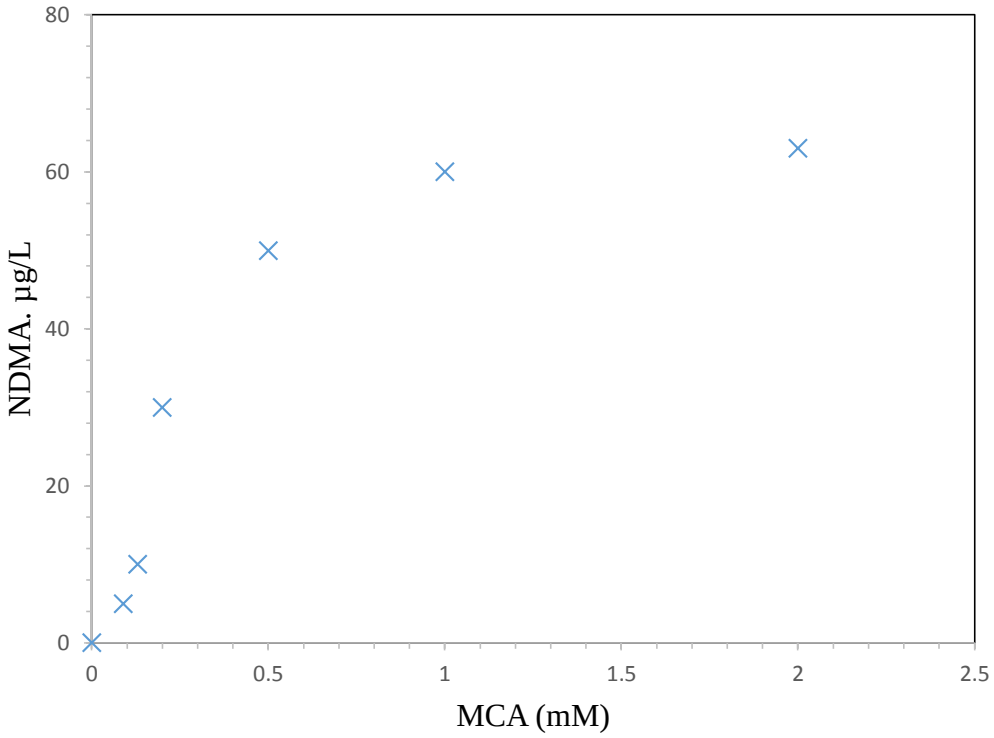

Figure 33. NDMA formation after 28 h as a function of MCA concentration. DMA concentration was fixed at 0.1mM. pH: 7.3. Solutions were kept in the dark, Temp: 25ºC.

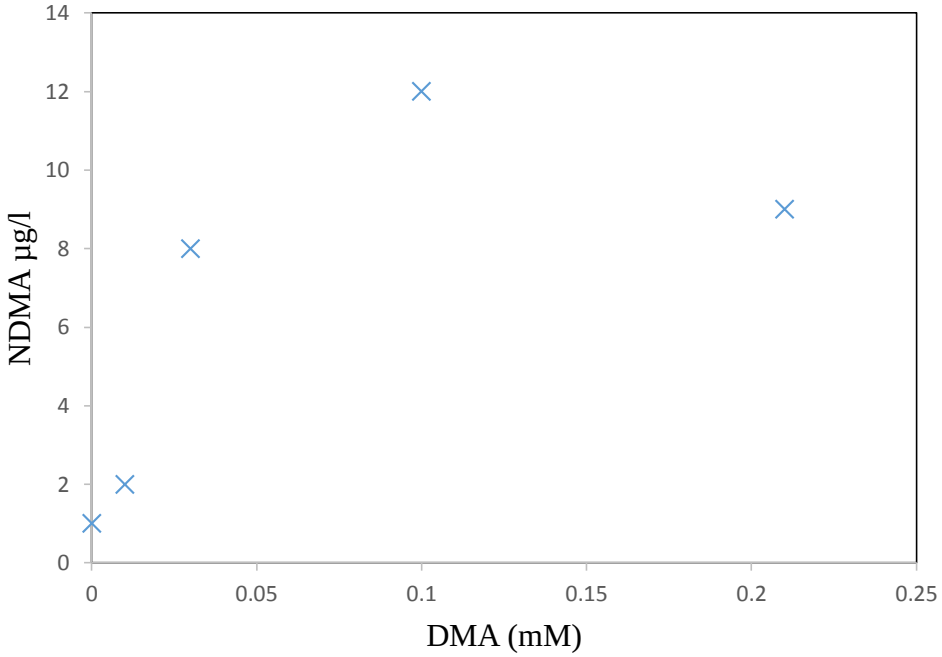

Figure 34. NDMA formation after 28 h as a function of DMA concentration. MCA concentration was fixed at 0.1mM. pH: 7.3. Solutions were kept in the dark, Temp: 25°C.

5.3.2 Effect of amine structure on NDMA formation:

The chain length of the alkyl group next to the nitrogen atom of DMA moiety did not significantly affect the NDMA yield. DMA and TMA exhibited about 3% of NDMA yields, and the yield decreased slightly as the number of carbon chain increases from -CH_3 (i.e., TMA) to -$CH_2CH_2CH_2CH_3$ (i.e., DMBA). These relatively low yields suggest that NDMA formation is not likely to be either enhanced or reduced by a long alkyl chain of tertiary amines.

However, higher NDMA yields were observed for both DMiPA (80.1%) and DMtBA (8.5%) which have branched alkyl groups (i.e., isopropyl and tertiary butyl) next to the nitrogen atom of DMA. Such high NDMA yields have not been previously reported for any aliphatic amine precursor. Assuming that the nucleophilic substitution between chloramine species and tertiary amine is the initial step of the NDMA formation, the stability of the leaving group may play a key role in the reactivity of precursor compounds. In other words, branched alkyl groups become carbocations such as $(CH_3)_2CH^+$ and $(CH_3)_3C^+$, which are more stable than unbranched ones such as CH_3^+ and $CH_3CH_2^+$ when the N-C bond is broken in aqueous solutions [129]. Thus, DMiPA and DMtBA, which have a good leaving group, formed more NDMA than DMA and TMA. Steric hindrance and hydration, because of a bulk tertiary butyl leaving group, may account for the lower NDMA formation from DMtBA (8.5%) than DMiPA (80.1%). The yield of NDMA from DMtBA was still significantly higher than those from unbranched aliphatic amines. Therefore, only aliphatic tertiary amines with branched alkyl groups attached to $N(CH_3)_2$ showed a high yield of NDMA, possibly due to the stability of their leaving groups (Table 16).

Figure 35. (a) shows that the mass spectra of NDMA produced from MCA and DMA was identical to that of commercially obtained NDMA (Figure 35. b). Both spectra show a parent molecular ion peak for NDMA at *m*/*z* ratio of 74. Note that the mass peak at *m*/*z* ratio of 42 is due to $CH_2=N=CH_2^+$ which is formed during the characteristic fragmentation of DMA [130]. Hence, we conclude that the formation of NDMA in this system is from the reaction of DMA and MCA. Surface and wastewaters may contain DMA or related compounds, and thus NDMA may also be formed by the reaction with MCA.

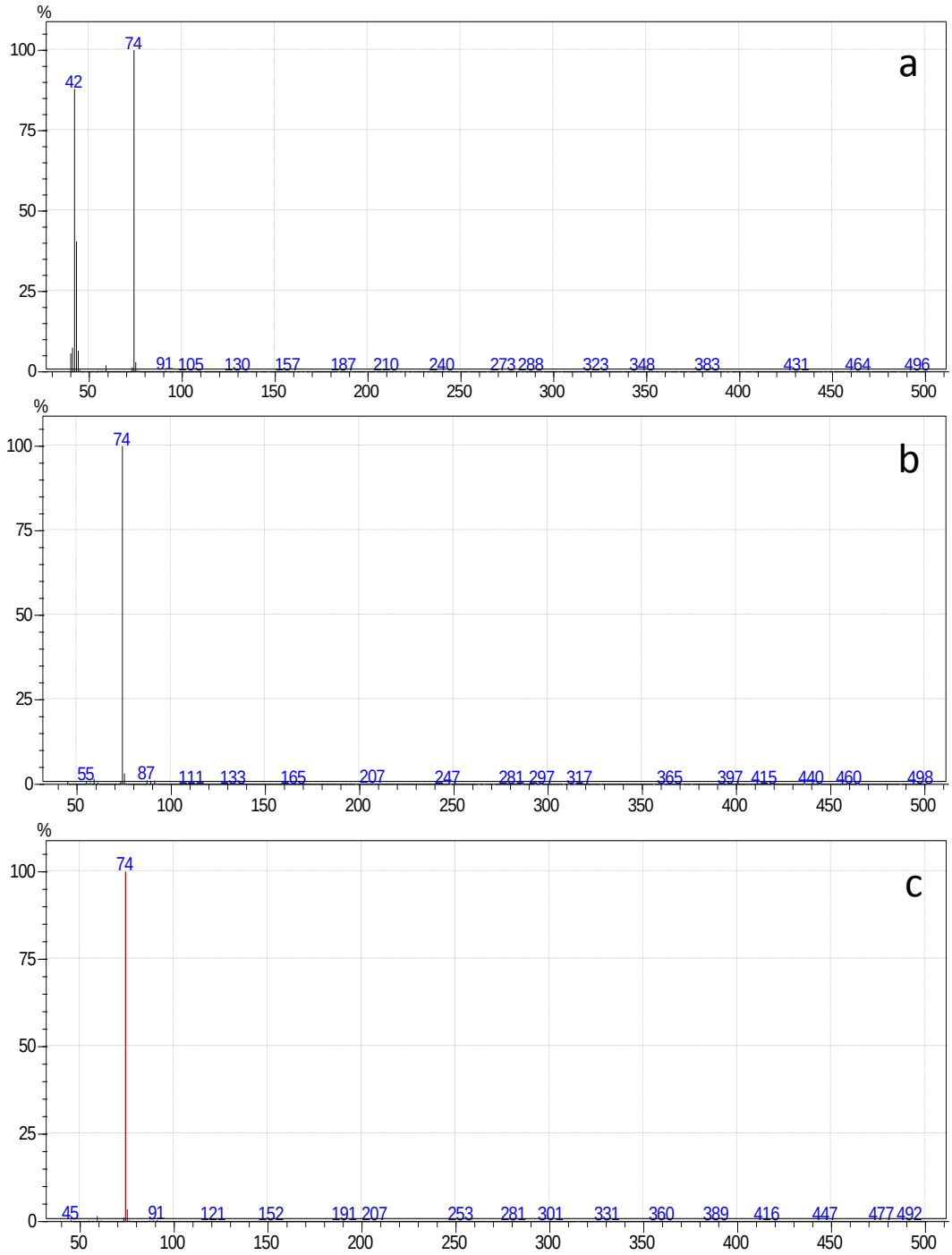

Figure 35 Mass spectra of NDMA from (a) commercial standard (b) the reaction of MCA and DMA (C) in presence of humic acid

5.3.4 The effect of humic acid on NDMA formation:

For a real application in water and wastewater treatment, it is important to understand the interactions of background matrix with NDMA precursors and their roles in NDMA formation. For this purpose humic acid was added to the deionized water samples having the selected precursors. The results indicate that the NDMA yields were higher in the presence of humic acid (91.7%) than in deionized water (80.1%). Therefore, the interactions between NDMA precursors and humic acid need to be considered as an important factor affecting NDMA formation in natural waters. Figure 35. (c) shows the mass spectra of NDMA formed in presesnce of humic acid.

5.3.5 Proposed reaction mechanism

In the present study, NDMA formation mechanism was proposed, which involves MCA that may occur in chloraminated water containing DMA or other potential precursors. This mechanism is not like other classical nitrosation, which used nitrite as a nitrosating agent [131, 132]. Figure 36 shows the schematic of the proposed key reactions.

$$NH_2Cl + (CH_3)_2NH \longrightarrow (CH_3)_2NNH_2 + H^+ + Cl^- \quad (5.2)$$

$$(CH_3)_2NNH_2 + 2NH_2Cl + H_2O \longrightarrow (CH_3)_2NNO + 2NH_4^+ + 2Cl^- \quad (5.3)$$

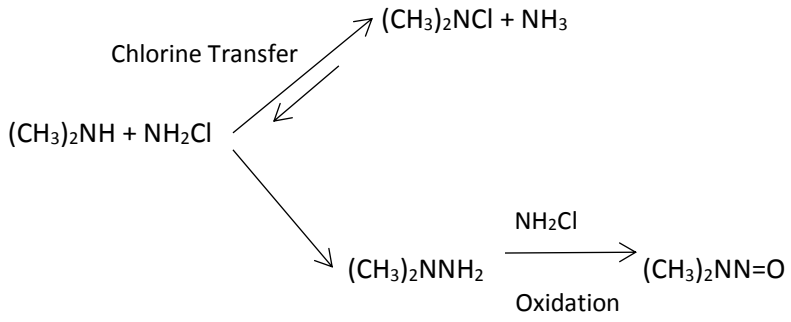

Figure 36 Proposed reaction scheme for NDMA formation from DMA and MCA

Table 16 Molar yields of NDMA from selected amine compounds

Compounds	Yield %
DMA	3.0
TMA	2.9
DMBA	2.5
DMiPA	81.1
DMtBA	8.5

The critical NDMA formation reactions consist of the following steps:

(i) The formation of 1,1-dimethylhydrazine (DMH) intermediate from the reaction of DMA with MCA followed by…

(ii) The oxidation of DMH by MCA (in presence of dissolved oxygen) to NDMA.

(iii) The reversible chlorine transfer reaction between MCA and DMA which is parallel with (i).

However, we suppose that DMH would be preferentially oxidized by MCA in presence of dissolved oxygen as shown in the reaction under these conditions.

In addition to the DMH formation, the reaction between MCA and DMA also leads to reversible chlorine transfer from MCA to DMA to form dimethylchloramine (DMCA) [132,133], as shown in reactions (5.2) and (5.3). The transfer of active chlorine between MCA and DMA can occur by direct chlorine transfer. Since direct chlorine transfer is subject to general acid catalysis especially in the near neutral and acidic pH range [134, 135], the rate of chlorine transfer reaction is expected to increases as pH decreases. In the suggested model, chlorine transfer via chloramine hydrolysis is not considered. However, the pathways involving chloramine hydrolysis may be important under other reaction conditions especially when free chlorine addition is practiced. A reaction of DMCA with ammonia producing DMH, although possible but not highly significant under these reaction conditions [136,137]. Otherwise, NDMA formation will not reach plateau and will continue increasing under these conditions where essentially all of the DMA is converted to DMCA.

5.4 CONCLUSION

N-nitrosodimethylamine can be directly formed by the reaction of monochloramine with dimethylamine. Given that *N*-nitrosodimethylamine should be considered as a potential nitrogenous disinfection by-product in drinking waters and wastewaters when contain dimethylamine or related compounds. This was demonstrated by observing *N*-nitrosodimethylamine formation from the addition of monochloramine to different amines in presence of humic acid. This reaction is therefore potentially important pathway for the formation of *N*-nitrosodimethylamine.

CHAPTER 6

REMOVAL OF HALOETHERS, TRIHALOMETHANES AND HALOKETONES FROM WATER USING *MORINGA OLIFERA* SEEDS

6.1 LITERATURE REVIEW

Disinfection is an essential water treatment procedure carried out to solve challenges relating to the production of drinking water, including the issue of water borne diseases. Since it first application in the 20th century, tremendous improvement in public health has been noted across the globe [138]. This can be attributed to the increase in the quality of water in public water systems. Notwithstanding, the formation of disinfection by-products (DBPs) from the use of chemical disinfectant to deal microbes in drinking water has also resulted in other public health concerns [2, 139].

Over 500 DBPs have been reported in drinking water treated with common disinfectants such as chlorine, chlorine dioxide, chloramine, ozone and their combinations [140]. DBPs are products of the reactions between disinfectants and organic matter/substances naturally present in the water [141]. While disinfectants have been known to be effective in killing pathogens, their strong oxidizing property enables them to oxidize organic matter and other anthropogenic contaminants present in water during the treatment process. Depending on the type of disinfectants used, DBPs formed during water treatment are broadly classified into trihalomethanes, haloacetic acids, haloacetonitrile, haloketones and inorganic compounds [141]. Trihalomethanes (THMs), haloethers (HEs) and haloketones (HKs) are particularly classified as hazardous compounds to

human health even at low parts per billion (ppb) levels by the United States Environmental Protection Agency (USEPA). Human exposure to DBPs is mainly by ingestion either through inhalation of volatile DBPs or dermal absorption. Different studies have associated bladder cancer risk [142] and reproductive and developmental defects in laboratory animals [4] with exposure to DBPs in water. The formation of DBPs in drinking water and its associated health effects has necessitated the exploration of less toxic, cost effective and environmentally benign technique for the removal of DBPs in water after the disinfection process.

Techniques that have so far been studied and applied in the removal of DBPs in water include electrochemical remediation [143], advanced oxidation [144], quartz sand filtration [145], membrane nanofiltration [146] and biological activated carbon filtration [147]. Varying extents of efficiency, cost effectiveness and ease of application of some of these approaches emphasize the need for developing alternative treatment methods.

The use of Moringa oleifera seed powder (MOS) as an adsorbent in water treatment process has been studied [148- 151]. However, these studies have been limited to the removal of metallic or inorganic contaminants [152- 155], as coagulants for total dissolved solids, or in the reduction of hardness and turbidity [156, 157]. Very little attention, however, has been given to its biosorption properties especially for the treatment of organic pollutants in water.

The application of MOS as an adsorbent in water treatment presents a cheap and environmentally benign approach to water treatment. Within the scope of our literature review, no research has been carried out on the removal of DBPs using MOS. As such, for the first time, this research work presents the use of MOS as a biosorbent for the removal of HEs, THMs and HKs from water

samples. Both batch and column adsorption experiments were conducted to investigate DBP removal using this approach.

6.2 EXPERIMENTAL

6.2.1 Chemicals and standards

DBP standards were obtained from Sigma-Aldrich (St. Louis, MO, USA). Standards containing mixtures of HEs (chlorophenyl phenyl ether (CPPE) and bromophenyl phenyl ether (BPPE)), THMs (trichloromethane (TCM), tribromomethane (TBM), dichlorobromomethane (DCBM) and dibromochloromethane DBCM)) and HKs (trichloropropanone (TCP) and 1,1- dichloropropanone (DCP)) at 2000 µg/mL, were prepared in methanol. Table 18 shows the physical properties of these compounds. Standard solutions were prepared daily by diluting stock solutions of DBP in the same solvent. All solvents used were obtained from Sigma-Aldrich. Doubly deionized water was prepared on a Milli-Q system, Millipore (Bedford, MA, USA). Nitric acid (HNO_3) and sodium hydroxide (NaOH) were obtained from Merck (Darmstadt, Germany). All glassware were washed with concentrated HNO_3, rinsed with deionized water and acetone and allowed to dry in an oven for an hour at 100 ºC. A polydimethylsiloxane (PDMS)-coated solid-phase microextraction (SPME) fiber (30-µm thickness coating) was purchased from Supelco (Bellefonte, PA, USA) and used without any modifications for extraction of DBPs before analysis by gas chromatography-mass spectrometry (GC-MS). Dried moringa olifera seeds were purchased from the local market (Alkhobar, Saudi Arabia) and ground to powder before use.

Table 17. Physical properties of target compounds [158- 161].

Physical properties	**TCM**	**TBM**	**DBCM**	**BDCM**	**DCP**	**TCP**	**CPPE**	**BPPE**
Molecular formula	$CHCl_3$	$CHBr_3$	$CHClBr_2$	$CHBrCl_2$	$C_3H_4Cl_2O$	$C_3H_3Cl_3O$	$C_{12}H_9ClO$	$C_{12}H_9BrO$
Molecular mass	119.38	252.73	208.28	163.8	126.96	161.41	204.6	249.1
Chemical family	THMs	THMs	THMs	THMs	HKs	HKs	HEs	HEs
Solubility at 20-25 °C (g/L)	7.5	3.1	1.0	3.3	6.3	7.4	1.43	0.82
Density at 20 °C (g/cm^3)	1.48	2.90	2.38	1.98	1.29	-	1.20	1.42
Log K_{ow}	1.97	2.38	2.08	1.88	0.20	1.12	4.08	5.24

6.2.2 Characterization

Physico-chemical characterization (pore size, surface chemistry, surface area, and elemental composition) of any adsorbent is essential since the adsorption process is a surface phenomenon [162]. Different techniques were used for characterization. Scanning electron microscopy (SEM) Tescan (Warrendale, PA, USA) was used for determining the morphology of MOS. X-ray diffraction (XRD) Rigaku, MiniFlex (Aubrey, TX, USA) was used to study the crystalline phases that exist in MOS. Perkin-Elmer 16F PC FT-IR spectroscopy, was used to identify the functional groups of MOS. Thermogravimetric analysis (TGA) and differential scanning calorimetry (DSC) analysis were done using SDT Analyzer Model Q600, TA instruments (New Castle, DE, USA) to characterize the stages of decomposition and thermal stability.

6.2.3 GC-MS analysis

DBPs were extracted from aqueous solutions (both batch and column system) using SPME. The PDMS-coated fiber was held directly in the solution (direct immersion mode) for extraction for 10 min, then removed and introduced in the GC port for 3 min for thermal desorption. A HP-1 methyl siloxane column (Rxi-5Sil MS; 30.0 m × 0.25 mm × 0.25 μm thickness) (Shimadzu, Kyoto, Japan) was used for DBP separation. Helium with high purity (>99.999%) was used as carrier gas at a constant flow at 1.0 mL/min. The analysis was conducted with the GC-MS set at the following temperature conditions: Initial temperature of 40 °C was held for 5 min and later increased to 118 °C at 10 °C/min, held for 3 min. The temperature was increased to 190° C at 15 °C/min and held for 5 min. The total run time was 23.6 min. The injection port, ion source and interface temperatures were set at 200 °C, 220 °C, and 200 °C, respectively. For qualitative determinations, the scan

mode was operated across a mass range of between m/z 50 to 550 and for quantitative analysis selective ion monitoring mode was used.

Table 18: Gas chromatographic conditions for THMs, HKs and HEs determination

Instrument	Agilent technologies, 7890A GC coupled with Agilent technologies, 5975C MSD
Column	A HP-1 methyl siloxane column (Rxi-5Sil MS; 30.0 m × 0.25 mm × 0.25 μm thickness)
He gas flow rate	1.0 mL/min
Injection mode	Split
Oven temperature program	40 °C (5 min) Ramped at 10 °C/min to 118 °C and held for (3 min) Ramped at 15 °C/min to 190° C and held for (5 min) The total run time was (23.6 min)
Injection port temperature	200 °C
interface temperatures	200 °C
MS temperature	220 °C

6.2.4 Adsorption tests

Adsorption experiments using batch mode were conducted as follows: 55 mg of MOS was added to 50 mL distilled water in an Erlenmeyer flask. Different parameters were considered in the adsorption study such as solution pH, contact time, agitation speed, and adsorbent dose. The pH of the solution was varied using 0.1M HNO_3 and 0.1M NaOH. Agitation of the flask was carried out using an orbital shaker. Finally, the residual concentration of DBPs in the solution was analyzed using SPME-GC-MS. The column experiment was conducted using a glass column of length 30 cm and 0.5 cm internal diameter in a fixed bed format. The column was filled with varying amounts of the MOS and capped both sides by glass wool to prevent movement of the adsorbent with the effluent. The sample solution (containing 15 mg/L of each analyte) was then uploaded to the column at 1.0 mL/min flow rate. The experiments were conducted at ambient temperature. Effluents were then collected and analyzed using SPME-GC-MS.

6.2.5 Data analysis

The percentage of DBPs removed from water samples was determined using Eq. (6.1):

$$\% \text{ Removal} = \frac{C0 - Ce}{C0} \times 100 \quad (6.1)$$

The adsorption capacities at equilibrium (qe, mg/g) and at time t (qt, mg/g) were computed using Eqs. (6.2) and (6.3):

$$qe = (C_0 - C_e) \times V/m \quad (6.2)$$

$$qt = (C_0 - C_t) \times V/m \quad (6.3)$$

where C_0 (mg/L) is the initial concentration, Ce and C_t (mg/L) are the concentrations at the equilibrium and at time (t) respectively, V (L) is the volume of the solution, and m (g) is the mass of the biosorbent used.

6.3 RESULTS AND DISCUSSION

6.3.1 Characterization of biosorbent material

Figure (37a) presents FT-IR spectra for MOS. The arrows point to the main functional groups: The broad band at 3,429.2 cm^{-1} corresponds to O-H stretching which exists in fatty acid and protein structures in MOS. Because of the high protein content in the seeds, amide groups appear within the same region as well. The stretching of C-H and CH_2 groups (symmetrical and asymmetrical) appear at 2,924 cm^{-1} and 2,853.6 cm^{-1} respectively. Those at 1,710.3 and 1,653.8 cm^{-1} are assigned to C=O bond stretching mode which represent protein and fatty acid structures. Peak observed around 1,543 cm^{-1} can be assigned to C-N stretching which confirms the protein structure in MOS. The FT-IR spectra of MOS after extraction (Figure 37b) shows appearance of new strong bands between 500 and 800 cm^{-1} which are attributed to the presence of halides (Cl, Br) since all the analytes contain chlorines and/or bromines.

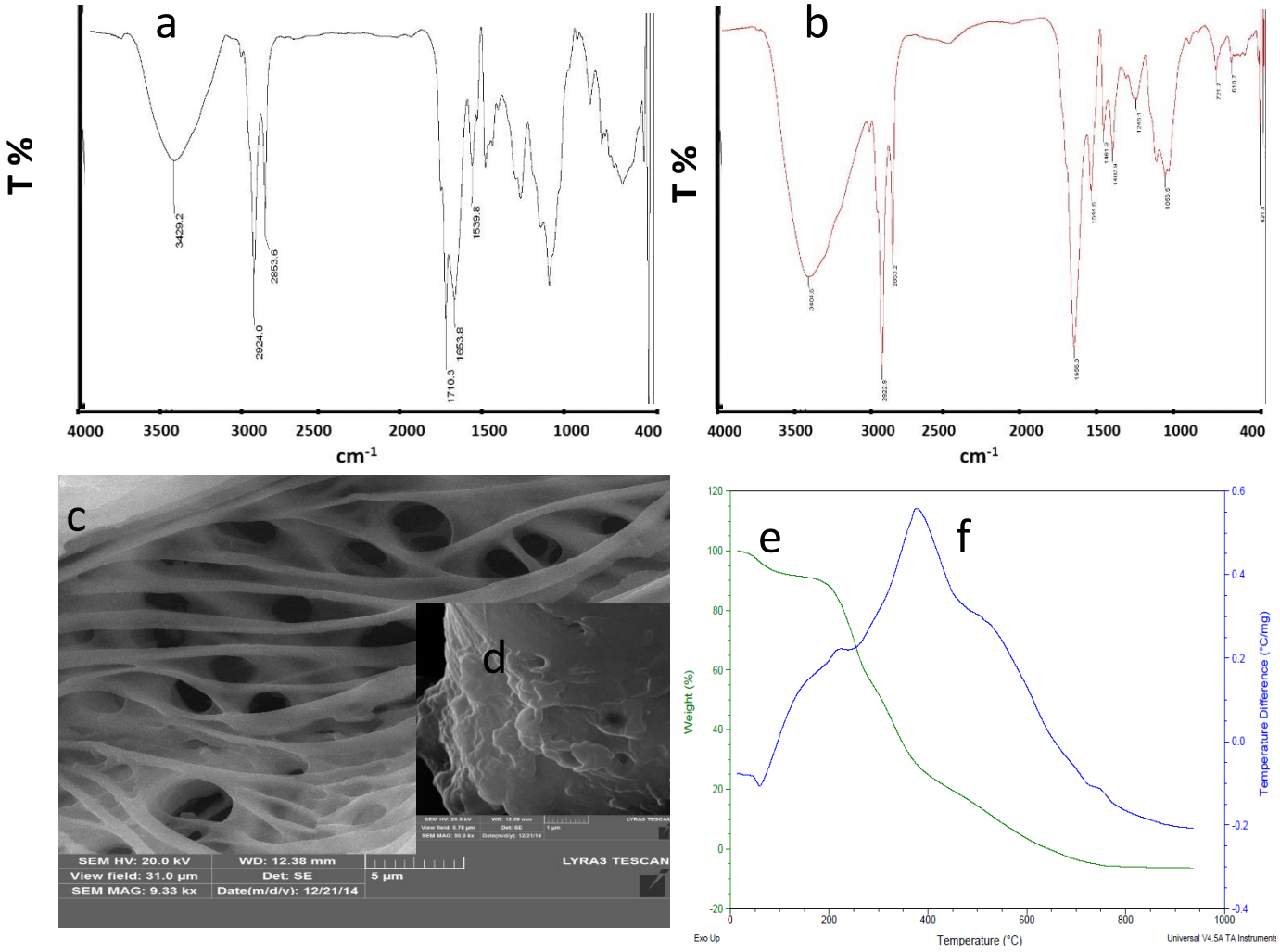

Figure 37. MOS characterization, FT-IR spectra before removal (a) after removal (b), SEM images at two different magnifications 5 µm (c) and 1 µm (d), TGA curve (e) and DSC curve (f).

The XRD spectrum patterns of MOS show broad peak poorly resolved which indicates the amorphous nature of the material (fig. not shown). The morphology of MOS was studied by SEM. The SEM image of the biosorbent (Figure 37 (c, d)) reveals the heterogeneous and porous structure of the MOS surface. This structure conceivably helps in the adsorption of the DBPs.

For studying the thermal stability and decomposition stages of MOS, TGA and DSC analyses were performed. Both techniques present the mass loss curve of the biosorbent material. The TGA curve (Figure 37e) indicates that the intermediates consist of a mixture of several components which confirms the heterogeneous structure for the material. The three main stages in the mass loss curve are:

1. From 30-128^{o}C: 8% of the mass loss is related to water desorption. This is comparable to the value reported by [28]. They reported an 8.9% mass loss.

2. From 128-268^{o}C: 32% of the mass loss is observed and may be attributed to the breakdown of organic matter and proteins present in the MOS.

3. From 268-541^{o}C: Greater decomposition of the seed constituents was observed. These may include fatty acids such as oleic acid.

At 950^{o}C, due to the presence of some inorganic oxides and ash, around 14.6% of total residue was observed [163]. These results were confirmed by the DSC analysis (Figure 37f). The above characterization reveals that MOS has the characteristics to retain and adsorb the target compounds, and hence can be used as a biosorbent.

6.3.2 Effect of adsorbent dose

The amount of MOS were varied to determine the effect of dosage on the removal of DBPs. Table 19 shows the adsorption capacity for HEs, THMs and HKs with varying doses of sorbent ranging from 0.1 to 2.0 g/L. The experiments were performed at fixed DBP concentration (15 mg/L), at ambient temperature and pH 6. The variation in biosorbent dose was observed to significantly affect the amount of DBPs adsorbed. The (q_e) increased rapidly as MOS dosage was increased from 0.1 to 1.1 g/L. Further increase after 1.1g/L resulted in very little increase in q_e. Hence, 1.1 g/L was chosen as the optimum dose. The initial increase in q_e can be attributed to the existence of a stronger interaction with sorbent functional groups and larger surface area. It can be deduced that with an increase in the MOS dose, a less than proportionate increase in adsorption was observed due to lower adsorptive capacity utilized by the adsorbent [164].

Table 19. Effect of dosage on the adsorption capacity of HEs, THMs and HKs on MOS (conditions: initial concentration 15 ppm; contact time 60 min; pH 6; agitation speed 120 rpm).

Adsorbent dose (g/L)	HEs qe (mg/g)	THMs qe (mg/g)	HKs qe (mg/g)
0.1	45.1	40.5	37.5
0.3	75.3	67.5	64.5
0.7	120.2	112.5	111.0
1.1	120.5	114.0	111.5
1.5	120.0	113.5	111.2
2.0	120.0	113.1	110.9

6.3.3 Effect of contact time

Figure 38 confirms that the contact time has significant impact on the removal of the contaminants. The rate of DBP removal was rapid initially; then it increased more slowly, and reached equilibrium at 50 min. Approximately 95% HEs, 91% THMs and 89% HKs were adsorbed after 50 min contact time, indicating the significant adsorptive ability of MOS.

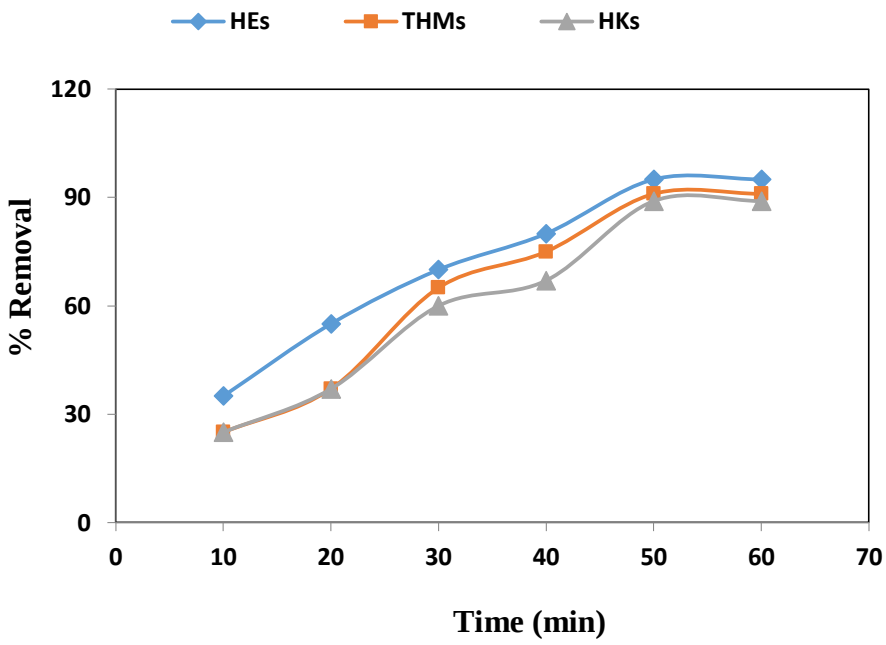

Figure 38. Effect of contact time on the amount of HEs, THMs and HKs adsorbed on MOS

6.3.4 Effect of pH

Studying the pH effect provides a better explanation of the adsorption process and the interaction between the target compounds and MOS. Jose et al and Makkar et al reported that MOS in an aqueous solution is a heterogeneous complex mixture that contains cationic polypeptides with different functional groups, specifically some amino acids [165, 166]. As is well known, amino acids are efficient phytochelators. The proteinacious amino acids have both positively and negatively charged ends, which depend on the pH. Therefore, manipulating the adsorption of anionic or cationic target species can be easily accomplished.

The removal mechanism by MOS of active target analytes has been explained as adsorption and charge neutralization [167- 169]. According to Okuda, for nonproteinic organic components, the coagulation mechanism is due to the enmeshment by a net-like structure, or sweep coagulation [170]. We can conclude that both mechanisms (adsorption and charge neutralization) may be taking place simultaneously due to the low molecular weight (<6.5 kDa) and high positive charge (pI above 9.6) of the biosorbent material [171]. The mentioned reasons are behind the appearance of the d graph shown in Figure 39.

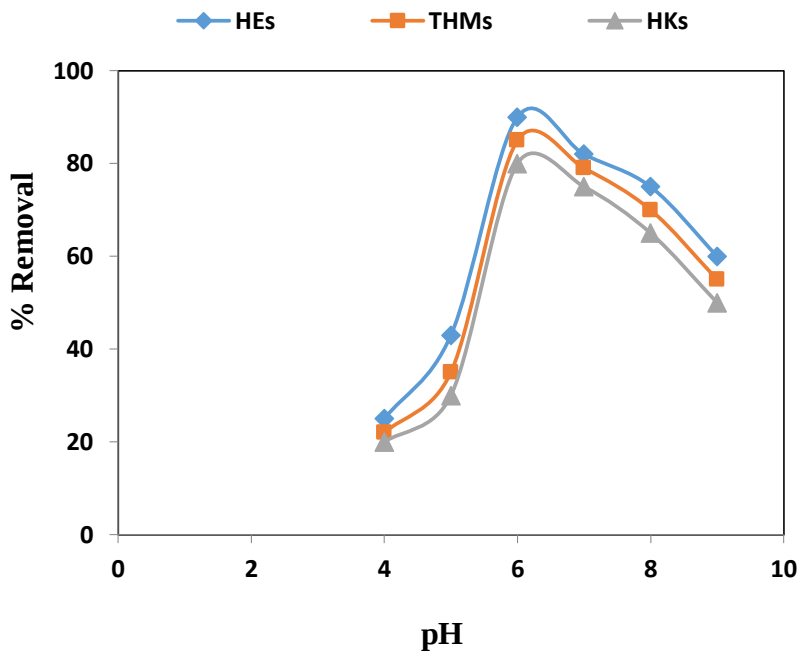

Figure 39. Effect of pH on the amount of HEs, THMs and HKs adsorbed on MOS

6.3.5 Effect of agitation speed

Agitation speed was varied from 0 to 120 revolutions per minute (rpm). Figure 40 depicts the adsorption of HEs, THMs and HKs by MOS based on agitation speed. The removal percentage was very low in static mode and increased gradually as the agitation speed was increased to 120 rpm. This behavior can be explained by the fact that an increase in the degree of mixing results in a decrease in the thickness of the boundary layer around the adsorbent particles.

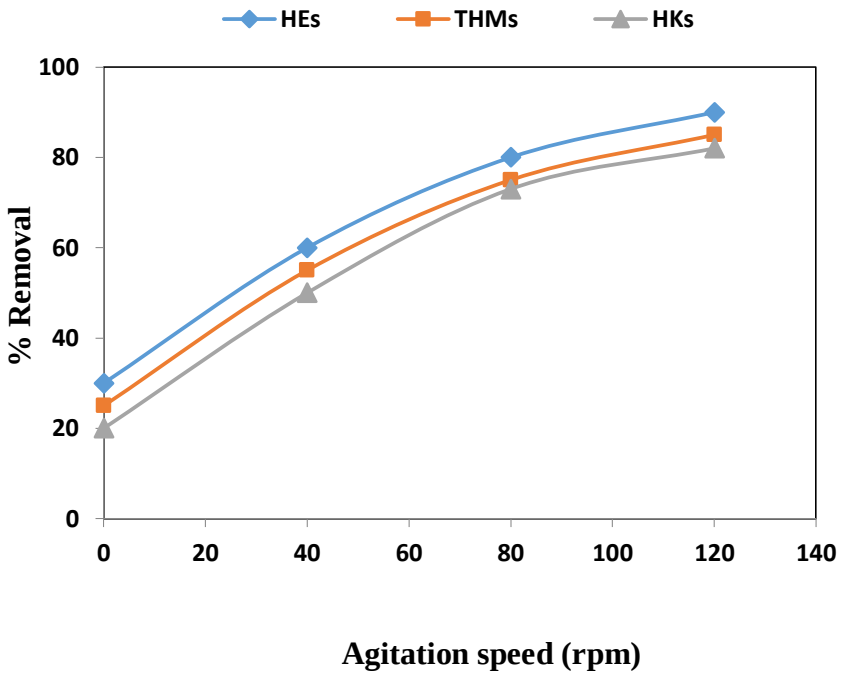

Figure 40. Effect of agitation speed on the amount of HEs, THMs and HKs adsorbed on MOS

6.3.6 Modeling of adsorption isotherms

Langmuir and Freundlich isotherm models were studied to explore the mechanism of the adsorption. The following Eq. (6.4) expresses the Langmuir isotherm:

$$C_e/q_e = C_e/Q_m + 1/Q_m b \quad (6.4)$$

where q_e and C_e are the concentrations of DBPs in MOS and solution, respectively, while Q_m and b are the Langmuir constants. The Langmuir model describes the monolayer adsorption mechanism process on completely homogeneous surfaces [172], the Freundlich model assumes the non-ideal adsorption taking place on a heterogeneous surface with multilayer adsorption process. Eqs. (6.5) and (6.6) express the Freundlich model:

$$q_e = k_f C_e^{1/n} \quad (6.5)$$

$$\log q_e = \log k_f + 1/n * \log C_e \quad (6.6)$$

where C_e and q_e the equilibrium concentrations of DBPs in the liquid and adsorbed phase, respectively, the Freundlich constants are k_f and n.

Langmuir constant values (Q_m and b) and Freundlich constant values (k_f and n), were obtained from their linear regression to find determine the most likely model. In addition to that, the regression coefficients (R^2) for all DBPs are listed in Table 20. Due to high value of (R^2) for all targeted DBPs, the Freundlich model seemed most appropriate to describe the adsorption phenomena. Related to ‘n’ values, MOS has maximum affinity for HEs.

Table 20. Langmuir and Freundlich isotherm model constants for DBPs adsorption.

DBPs	Log Kow	Langmuir isotherm			Freundlich isotherm		
		$Qm_{(mg/g)}$	b	R^2	K_f	n	R^2
HEs	4.08 - 5.24	142.76	1.89	0.972	112.11	9.25	0.997
THMs	1.88 - 2.38	95.87	1.95	0.978	105.45	6.00	0.998
HKs	0.2 - 1.12	65.21	2.45	0.964	100.00	4.67	0.996

From the different parameters studied above, it is observed that DBP adsorption onto the MOS followed the order: HEs > THMs > HKs. By comparing the log K_{ow} values of the studied DBPs: HEs > THMs > HKs, a clear relationship is thus noted between the two parameters. The log K_{ow} is defined as a measure of the hydrophobicity of an organic compound, so the greater the log K_{ow} value, the less water-soluble the compound is resulting in greater adsorption [173]. Thus HEs (CPPE - BPPE having a log K_{ow} values of between 4.08 and 5.24 respectively) were the most adsorbed DBPs while HKs (DCP – TCP) on the other hand show lowest log K_{ow} values of between 0.2 and 1.12 respectively, and were the least adsorbed.

6.3.7 Kinetics of the adsorption

A kinetic study was conducted to determine the adsorption rate as well as to provide valuable data to understand better the adsorption mechanism. Two kinetic models were employed to investigate the mechanisms of DBP adsorption (pseudo-first order and pseudo-second order). The pseudo-first order kinetics equation is presented as follows [174]:

$$\log (q_e - q_t) = \log q_e - \frac{k1t}{2.303} \quad (6.7)$$

From the equation, q_e and q_t are the adsorption capacities of DBPs (mg/g) at equilibrium and time t, respectively. k_1 is the rate constant of the first order (min^{-1}). A plot of t versus ln (q_e - q_t) is used to determine the values of k_1 and adsorption capacity (q_e). Table 21 presents the resulting values.

By comparing the calculated equilibrium adsorption capacities ($q_{e,\ cal}$) with the experimental ones ($q_{e,\ exp}$), it is observed that there is a significant difference between the

values. Also the obtained coefficients of determination (R^2) give poor linearity when the first model is applied. This means that the adsorption process does not follow the pseudo-first order model.

A pseudo-second order kinetic model may be applied as follows [175, 176]:

$$\frac{dqt}{dt} = k_2 (qe - qt)^2 \quad (6.8)$$

where k_2 is the pseudo-second order adsorption rate constant (g/mg.min), qt and qe are the adsorbed amounts of DBPs at time (t) and at equilibrium, respectively. The linear form of the pseudo-second order can be expressed as:

$$\frac{t}{qt} = \frac{1}{k2qe2} + \frac{t}{qe} \quad (6.9)$$

By plotting t/q_t against t, k_2 is obtained (Figure 41). The kinetic parameters are presented in Table 21. The initial adsorption rate is $h = k_2 q_e^2$ (mg/g.min). All compounds with different concentrations give $R^2 > 0.99$ which indicate that a pseudo-second order is the kinetic model for the adsorption process. The proximity of the values of the equilibrium adsorption capacity ($q_{e, cal}$) with the experimentally-determined ones ($q_{e, exp}$), also confirm this observation.

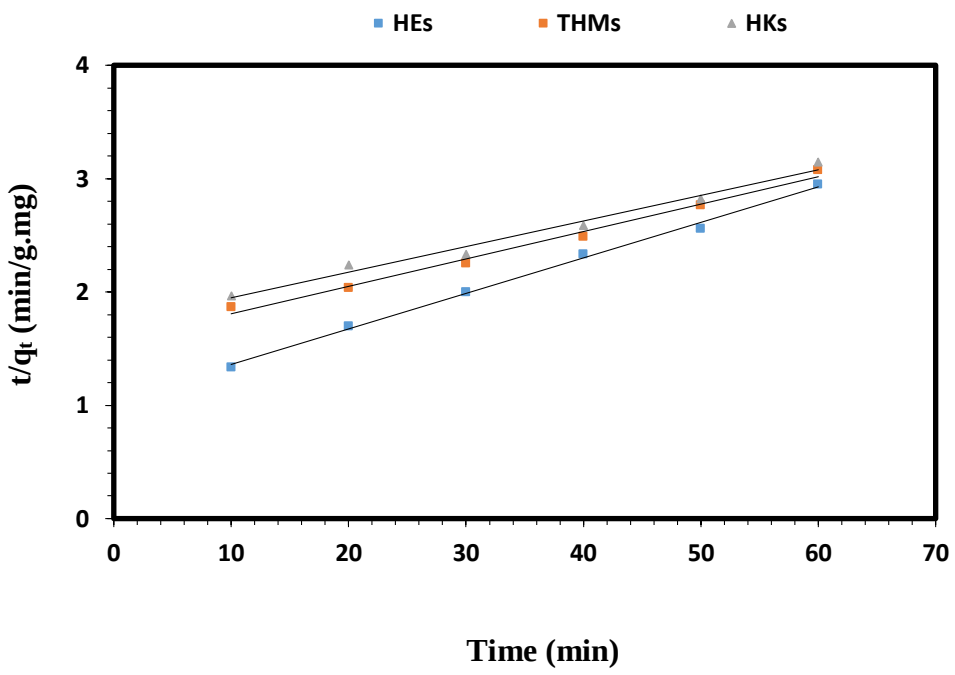

Figure 41 Pseudo-second order plot of DBPs on MOS at 15 mg/L initial concentrations of each compound

Table 21. Kinetic parameters for HEs, THMs and HKs on MOS.

Adsorbate	q_e (mg/g) (experimental)	C_0 (mg/L)	Pseudo-first order			Pseudo-second order		
			q_e (mg/g)	k_1 (min^{-1})	R^2	qe(mg/g)	k_2(g/mg.min)	R^2
HEs	120.5	15	133.5	0.1456	0.77	122.2	0.0743	0.995
	38.5	5	48.1	0.2178	0.812	38	0.0818	0.99
THMs	114	15	119.8	0.945	0.802	115.3	0.0781	0.998
	33.8	5	39.4	0.1644	0.897	32.9	0.0276	0.991
HKs	111.5	15	120.7	0.2365	0.842	110.9	0.0534	0.99
	30.3	5	37.3	0.0552	0.901	31.2	0.0321	0.996

6.3.8 Fixed bed adsorption studies

Column-packed experiments were applied using the results obtained from the batch mode study to remove the target compounds at fixed concentrations of 15 mg/L each Figure 42. illustrates the effect of different flow rates on the DBP removal process. The flow rate was studied within the range of between 0.5 and 4 mL/min to obtain the maximum removal of the target. It was observed that the percentage removal is inversely proportional to the flow rate. This is because the low flow rates conceivably allow greater contact between the contaminants and the adsorbent.

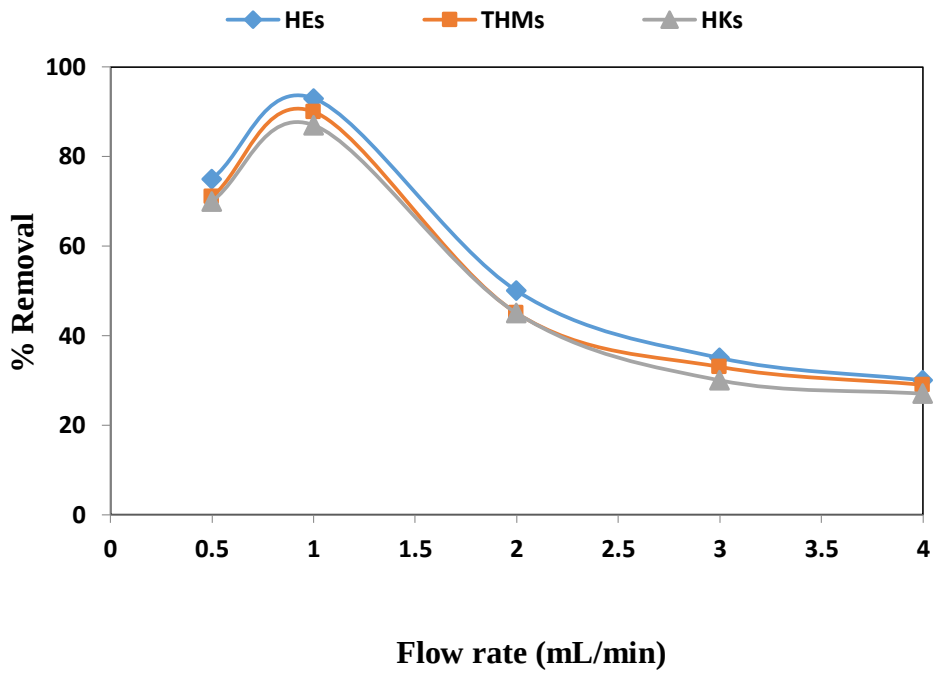

Figure 42 Effect of flow rate on the amount of HEs, THMs and HKs adsorbed on MOS

The removal of HEs, THMs and HKs by MOS was also studied by fixed bed adsorption. The thickness of the bed was varied while the flow rate was maintained at 1 mL/min. The maximum removal of DBPs were 95% for HEs, 90% for THMs and 86% for HKs. Also, increasing the layer thickness led to an enhancement of the removal percentages. This is due to two reasons: (i) An increase in the layer thickness leads to a corresponding increase in the interaction sites of the biosorbent. This provides more sites for adsorption; and (ii) The removal efficiency increases when more time is given for the adsorbate to diffuse into the adsorbent. Figure 43 depicts the effect that when the layer thickness of the adsorbent was increased from 2 mm to 10 mm, the DBP removal percentages increased from 35 to 95 %. Comparing the efficiency between batch and column modes, the former's adsorption capacity is higher than that in a fixed bed column method. This is due to interaction with relatively larger surface area and more active adsorptive sites on the composite during batch mode processing.

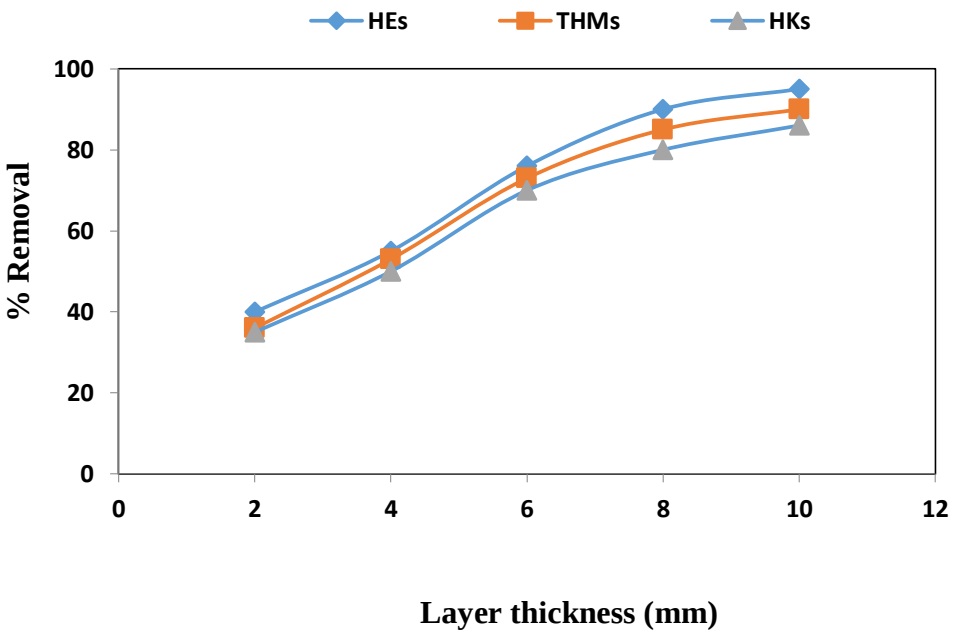

Figure 43 Effect of layer thickness on the amount of HEs, THMs and HKs adsorbed on MOS

Table 22 shows the comparison of DBP removal efficiency by MOS with other sorbents reported in the literature. These data clearly indicate that MOS can effect efficient removal of DBPs from water samples.

Table 22. Comparison of MOS with previously used sorbents for the removal of DBPs from aqueous effluents

Sorbent Material	Analyte	Efficiency	Reference
MOS	HEs, THMs, HKs	94.9%, 90.3%, 86%	Present study
QS[a]	HKs	12%	145
US[b] and QS	THMs	51%	145
NFM[c]	THMs	> 82%	146
BPAC[d]	THMs	> 54%	177
AOC[e]	THMs	91%	178

[a]quartz sand; [b]ultrasound; [c]nanofiltration membrane; [d]biological powder-activated carbon; [e]assimilable organic carbon

6.4 CONCLUSION

Moringa oleifera seeds were presented to be an efficient biosorbent material for the removal of different groups of disinfection by-products (DBPs) in water samples. The use of the material represents an ecofriendly and low cost approach to DBP removal. Using the batch mode and at initial concentrations of 15 mg/L, the biosorbent material offers high percentage removal of haloethers (HEs), trihalomethanes (THMs) and haloketones (HKs) (94.9%, 90.3% and 86%), respectively. The above mentioned values were confirmed with the removal of 90.1%, 85% and 82.3% of HEs, THMs and HKs via the column system. Characterization of MOS showed that functional groups as well as surface properties were responsible for its good adsorption capacity for organic pollutants. Kinetic studies showed that the adsorption mechanism followed a pseudo-second order model. We believe MOS could be used in compact columns in water filtration units for effective DBP removal.

7.0 GENERAL CONCLUSION

In this work, independent conventional, novel and efficient methods for trace level quantification of organic disinfection by-products (DBPs) such as haloethers (HEs), trihalomethanes (THMs), haloketones (HKs), haloacetonitriles (HANs) and haloacetic acids (HAAs) in water and biological samples, using Dispersive solid phase extraction (DSPE), microwave assisted extraction (MAE) and solid phase micro extraction (SPME) as the extraction techniques coupled with gas chromatography mass spectrometry (GC-MS) and liquid chromatography- tandem mass were developed and validated.

7.1 Haloacetic acids (HAAs)

i. layered double hydroxide were used in DSPE as a sorbent for extraction and determination of HAAs in desalinated water collected from reverse osmosis treatment plant as well as drinking water and tap water samples.

ii. Different factors controlling the extraction procedures were investigated. Results have shown that extraction time, pH and types of sorbent could also have significant effect on extraction enrichment factor.

iii. Comparison results have shown that this method could serve as a less costly and more viable alternative to other techniques that use large amount of organic solvents for the extraction.

iv. The method was successfully applied to the determination of HAAs different water samples with promising results.

7.2 Trihalomethanes, Haloketones and Haloacetonitrils (THMs, HKs and HANs)

i. In this investigation, we have developed a new simple and efficient method called single step microwave assisted liquid phase microextraction for determination disinfection by-products in biological samples .

ii. Various factors governing extraction have been studied. Results obtained indicate the optimized conditions as 12 min extraction time and toluene as organic solvent enhanced extraction recoveries.

iii. Detector response was found linear within the range of 0.3-100 μgL^{-1} of the analytes with brominated compounds while the linearity was between 0.5-100 μgL^{-1} for the chlorinated compounds with R^2 values that signify a very good correlation.

iv. These performances and all other appraisal indices such as LOD, relative recovery and %RSD indicate the suitable applicability of the present method in the analysis of biological samples.

7.3 Haloethers (HEs)

i. A flow assisted electroenhanced solid phase microextraction method (FA-EE-SPME) were developed for determination HEs in water samples.

ii. The extraction parameters were optimized such as: extraction time, flow rate, ionic strength, applied potential and pH.

iii. The FA-EE-SPME, displayed good linearity between a wide range of concentrations and is characterized by low LODs which would allow sensitive determinations of these analytes at their low concentrations in the water sample.

iv. The FA-EE-SPME method was shown to be efficient, simple and fast method and suitable for onsite application.

7.4 NDMA formation mechanism

i. In this part, we studied the formation mechanism of N-nitrosodimethelamine (NDMA) by reacting one of chloroamine as a disinfectant usually added in the water treatment process which is monochloroamine (MCA) and a potential precursor exist in surface and waste water which is dimethelamine (DMA).

ii. Different factors affecting this study had been investigated such as the reaction time and the DMA and MCA concentrations.

iii. The role of humic acid as one of natural organic matter (NOM) exist in the water had been studied.

iv. At the end a formation mechanism for NDMA had been proposed.

7.5 Removal of DBPs using Biosorbent

i. Moringa Olifera Seeds (MOS) powder were used for removal of THMs, HEs and HKs from water samples.

ii. Batch and column mode were applied in this part, with optimizing different parameters in every mode. Such as: pH, adsorbent dose, agitation speed layer thickness and flow rate.

iii. Isotherm study as well as kinetic study were investigated to give more details and to understand the mechanism of the adsorption process in comprehensive way.

iv. Using MOS as a biosorbent present an ecofriendly, efficient, simple and fast method for removal DBPs from water samples.

8.0 RECOMMENDATIONS AND FUTURE WORK

We have recommended many points for the future work to give a more comprehensive and deeper understanding about the disinfection by-products analysis and their formation mechanism during the water treatment process. In addition to that, taking in account the time for collection the samples and studying should be a very important factor. The following are the main recommended points:

- Studying the spatial and temporal evaluations of DBPs in KSA.
- Studying more groups of DBPs, both organic and inorganic types.
- More comprehensive studying for the formation mechanism should be deducted.

REFERENCES

[1] Centers for Disease Control and Prevention. Achievements in public health, 1900−1999: Changes in the Public Health System. MMWR; CDC: Atlanta, GA, vol.48, pp. 1141-1147, 1999.

[2] Richardson, S.D., Water analysis: emerging contaminants and current issues. Anal. Chem. Vol.81, pp.4645–4677, 2009

[3] Drinking Water Treatment, USEPA Document No. 810-F-99-013, Cincinnati, OH, 1999.

[4] Hanson, M., Solomon, K. R., Environmental Pollution, vol.130, pp.371-383, 2004.

[5] Kohn, R., Pattard, M., Water Research, vol.24, pp.31-38, 1990.

[6] USEPA, National primary drinking water regulations: stage 2 disinfectants and disinfection by products rule. Federal Register, vol.71, pp.387–493, 2006.

[7] Richardson, S.D., Drinking water disinfection-by products. Encyclopedia of Environmental Analysis and Remediation, vol.3 pp.1398–1421, 1998.

[8] Krasner, S.W., Weinberg, H.S., Richardson, S.D., Pastor, S.J., Chinn, R., Sclimenti, M.J., Onstad, G.D. and Thruston, A.D., Environmental Science and Technology, vol.40, no. 23, pp.7175–7185, 2006.

[9] Rook, J.J., Formation of haloforms during chlorination of natural waters: Water Treatment and Examination, vol.23, pp.234-243, 1974.

[10] Tan, B.L.L., Hawker, D.W., Muller, J.F., Leusch, F.D.L., Tremblay, L.A. and Chapman, H.F., Aust. Environ. Int., vol.33, pp.654–669, 2007.

[11] USEPA, Method 552.2: Environmental Monitoring and System Laboratory, Cincinnati, OH, 1995.

[12] USEPA, Method 552.1: Environmental Monitoring and System Laboratory, Cincinnati, OH, 1992.

[13]. USEPA, Method 552.3: Environmental Monitoring and System Laboratory, Cincinnati, OH, 2003.

[14] Edzwald, J.K, Becker, W.C and Wattier, K.L, J Am Water Works Assoc, vol.77, pp.122–132, 1985.

[15] Teo, C. C., Chong, W. P. K., Ho, Y. S., Metabolomics, vol.9, pp.1109–1128, 2013.

[16] Chiing-Chen, C., Ren-Jang, Chun, W., Chung-Shin, Y.L., J. Hazard. Mater, vol.172 pp.1021-1029, 2009.

[17] Jing-Shan, C., Shang- Da, H., Talanta, vol.71, pp.882-891, 2007.

[18] Montgomery, J.H., Welkom, L.M., Groundwater Chemical Desk Reference, Lewis Publishers, Chelsea, MI, 1990.

[19] Thomas, O.V., Stork, J.R., Lammert, S.L., J. Chromatogr. Sci. vol.18, pp.583-590, 1980.

[20] Sittig, M., Handbook of Toxic and Hazardous Chemicals and Carcinogens, third ed., Noyes Public, New Jersey, 1991.

[21] Sahng-Da, H., Chun Yi, T., Cheng-Shium, L., J. Chromatogr. A vol.769, pp.239-249, 1997.

[22] Fawell, J.K., Hunt, S., Environmental Toxicology: Organic Pollutants, Wiley, New York, 1988.

[23] Wennrich, L., Engewald, W., Poppb, P., lnrern J. Environ. Anal. Chem. Vol.73, pp.31-42, 1998.

[24] Wisconsin Department of Natural Resources Drinking Water & Groundwater Quality Standards/Advisory Levels, http://dnr.wi.gov/topic/drinkingwater/documents/haltable.pdf, Accessed on 12/08/2013.

[25] USEPA, Office of Water Regulations and Standards Criteria and Standards Division Washington DC 20460 440/5-80-050 October 1980.

[26] USEPA, National primary drinking water regulations: stage 2 disinfectants and disinfection by products rule. Federal Register, vol.71, pp.387–493, 2006.

[27] Levesquea, S., Rodriguezb, M. J., Serodesc, J., Beaulieua, C., Proulx, F., Water Research vol.40, pp.2921– 2930, 2006.

[28] Yanga, X., Shanga, C., Westerhoff, P., water research vol.41, pp.1193 – 1200, 2007.

[29] Scott, B. F., Spencer, C., Marvin, C. H., Mactavish, D. C. and Muir, D. C. G., Environ. Sci. Technol., 2002In press. Web Release Date: 30 Mar. 2002 (DOI: 10.1021/es011156h).

[30] Niu, Y., Zhang, J., Wu, Y., and Shao, B., J. Chromatogr. A, vol.1218, pp.5248–53, 2001.

[31] López-Darias, J., Germán-Hernández, M., Pino, V., and Afonso, A. M., Talanta, vol.80, pp.1611–1618, 2010.

[32] Yiantzi, E., Psillakis, E., Tyrovola, K., and Kalogerakis, N., Talanta, vol.80, pp.2057–2062, 2010.

[33] Liu, J., Chi, Y., Jiang, G., Tai, C., Peng, J., and Hu, J.T., J. Chromatogr. A, vol.1026, pp.143–147, 2004.

[34] Basheer, C. and Lee, H. K., J. Chromatogr. A, vol.1057, pp.163–169, 2004.

[35] Schmalz, C., Frimmel, F.H., Zwiener, C., Trichloramine in swimming pools formation and mass transfer. Water Res. Vol.45, pp.2681–2690, 2011

[36] US EPA, Federal Register, vol.71, pp.387–493, 2006

[37] Richardson, S. D.; Ternes, T. A. Water Analysis: Emerging Contaminants and Current Issues. Anal. Chem., vol.86, pp.2813–2820, 2014.

[38] Vreysen, S., Maes, A., Adsorption mechanism of humic and fulvic acid onto Mg/Al layered double hydroxides. Appl. Clay Sci. vol.38, pp.237–249, 2008.

[39] Zhan, Y., Zhu, Z., Lin, J., Qiu, Y., Zhao, J., Removal of humic acid from aqueous solution by cetylpyridinium bromide modified zeolite. J. Environ. Sci. (China) vol.22, pp.1327–34, 2010.

[40] Rives, V., Layered Double Hydroxides: Present and Future. Nova Publishers, 2001.

[41] Abdolmohammad-Zadeh, H., Rezvani, Z., Sadeghi, G.H., Zorufi, E., Layered double hydroxides: a novel nano-sorbent for solid-phase extraction. Anal. Chim. Acta vol.685, pp.212–219, 2011.

[42] Choy, J., Choi, S., Oh, J., Park, T.,. Clay minerals and layered double hydroxides for novel biological applications. Appl. Clay Sci. vol.36, pp.122–132, 2007

[43] Evans, D.G., Duan, X., Preparation of layered double hydroxides and their applications as additives in polymers, as precursors to magnetic materials and in biology and medicine. Chem. Commun. (Camb). pp.485–496, 2006

[44] Choy, J.-H., Kwak, S.-Y., Park, J.-S., Jeong, Y.-J., Cellular uptake behavior of [γ32P] labeled ATP–LDH nanohybrids. J. Mater. Chem. vol.11, pp.1671–1674, 2001

[45] Bruna, F., Pavlovic, I., Celis, R., Barriga, C., Cornejo, J., Ulibarri, M.A., Organohydrotalcites as novel supports for the slow release of the herbicide terbuthylazine. Appl. Clay Sci. vol.42, pp.194–200, 2008

[46] Bruna, F., Pavlovic, I., Barriga, C., Cornejo, J., Ulibarri, M., Adsorption of pesticides Carbetamide and Metamitron on organohydrotalcite. Appl. Clay Sci. vol.33, pp.116–124, 2006

[47] Serrano, J., Bertin, V., Bulbulian, S., 99 Mo Sorption by Thermally Treated Hydrotalcites. Langmuir vol.16, pp.3355–3360, 2000

[48] Pavlovic, I., Barriga, C., Hermosín, M.C., Cornejo, J., Ulibarri, M.A., Adsorption of acidic pesticides 2,4-D, Clopyralid and Picloram on calcined hydrotalcite. Appl. Clay Sci. vol.30, pp.125–133, 2005

[49] Extremera, R., Pavlovic, I., Pérez, M.R., Barriga, C., Removal of acid orange 10 by calcined Mg/Al layered double hydroxides from water and recovery of the adsorbed dye. Chem. Eng. J. vol.213, pp.392–400, 2012

[50] Abdolmohammad-Zadeh, H., Talleb, Z., Dispersive solid phase micro-extraction of dopamine from human serum using a nano-structured Ni-Al layered double hydroxide, and its direct determination by spectrofluorometry. Microchim. Acta vol.179, pp.25–32, 2012.

[51] Liu, Y.-L., Zhou, J.-B., Zhao, R.-S., Chen, X.-F., Using Zn/Al layered double hydroxide as a novel solid-phase extraction adsorbent to extract polycyclic aromatic hydrocarbons at trace levels in water samples prior to the determination of gas chromatography-mass spectrometry. Anal. Bioanal. Chem. vol.404, pp.1603–1610, 2012.

[52] Tang, S., Chia, G., Chang, Y., Lee, H., *Anal. Chem.* vol.86, pp.11070–11076, 2014.

[53] Reichle, W., Synthesis of anionic clay minerals (mixed metal hydroxides, hydrotalcite). Solid State Ionics vol.22, pp.135–141, 1986.

[54] Pal, S., Lee, K.-H., Kim, J.-U., Han, S.-H., Song, J.M., Adsorption of cyanuric acid on activated carbon from aqueous solution: effect of carbon surface modification and thermodynamic characteristics. J. Colloid Interface Sci. vol.303, pp.39–48, 2006.

[55] Parker, L.M., Milestone, N.B., Newman, R.H., The Use of Hydrotalcite as an Anion Absorbent. Ind. Eng. Chem. Res. vol.34, pp.1196–1202, 1995.

[56] Mitata, S., *Clays Clay Miner*., vol.31, pp.305−311, 1983.

[57] Louch, D., Motlagh, S., Pawliszyn, J., Dynamics of organic compound extraction from water using liquid-coated fused silica fibers. Anal. Chem. vol.64, pp.1187–1199, 1992.

[58] Ai, J., Solid Phase Microextraction for Quantitative Analysis in Nonequilibrium Situations. Anal. Chem. vol.69, pp.1230–1236, 1997

[59] Loos, R., Barceló, D., Determination of haloacetic acids in aqueous environments by solid-phase extraction followed by ion-pair liquid chromatography–electrospray ionization mass spectrometric detection. J. Chromatogr. A vol.938, pp.45–55, 2001.

[60] Hodgeson, J., Becker, D., US EPA Method 552.1, EPA/600/R-92/129 (Suppl. II), 1992.

[61] Munch, D., Domino, M., Pepich, B., Xie, Y., US EPA Method 552.3, 2003.

[62] Varanusupakul, P., Vora-Adisak, N., Pulpoka, B., In situ derivatization and hollow fiber membrane microextraction for gas chromatographic determination of haloacetic acids in water. Anal. Chim. Acta vol.598, pp.82–86, 2007

[63] Sarrion, M., Santos, F., Galceran, M., In situ derivatization/solid-phase microextraction for the determination of haloacetic acids in water. Anal. Chem. vol.72, pp.4865–4873, 2000.

[64] Siraji, M., Bidgoli, A., *J. Chromatogr. A*, vol.1216, pp.1059-1065, 2009.

[65] Sarrión, M.N., Santos, F.J., Galceran, M.T., Solid-phase microextraction coupled with gas chromatography-ion trap mass spectrometry for the analysis of haloacetic acids in water. J. Chromatogr. A vol.859, pp.159–171, 1999.

[66] Wang, X., Kou, D., Mitra, S., Continuous, on-line monitoring of haloacetic acids via membrane extraction. J. Chromatogr. A vol.1089, pp.39–44, 2005.

[67] Magnuson, M., Kelty, C., *Anal. Chem.*, vol.72, pp.2308-2315, 2000.

[68] Jia, M., Wu, W.W., Yost, R.A., Chadik, P.A., Stacpoole, P.W., Henderson, G.N., Simultaneous determination of trace levels of nine haloacetic acids in biological samples as their pentafluorobenzyl derivatives by gas chromatography/tandem mass spectrometry in electron capture negative ion chemical ionization mode. Anal. Chem. vol.75, pp.4065–4080, 2003.

[69] Chen, C.-Y., Chang, S.-N., Wang, G.-S., Determination of ten haloacetic acids in drinking water using high-performance and ultra-performance liquid chromatography-tandem mass spectrometry. J. Chromatogr. Sci. vol.47, pp.67–74, 2009.

[70] Nsubuga, H., Basheer, C., 2013. Determination of haloacetic acids in swimming pool waters by membrane-protected micro-solid phase extraction. J. Chromatogr. A 1315, 47–52. doi:10.1016/j.chroma.2013.09.050

[71] Berg, M., Müller, S.R., Mühlemann, J., Wiedmer, A., Schwarzenbach, R.P., Concentrations and Mass Fluxes of Chloroacetic Acids and Trifluoroacetic Acid in Rain and Natural Waters in Switzerland. Environ. Sci. Technol. vol.34, pp.2675–2683, 2000

[72] Benanou, D., Acobas, F., Sztajnbok, P., Analysis of haloacetic acids in water by a novel technique: simultaneous extraction– derivatization. Water Res. vol.32, pp.2798–2806, 1998.

[73] Roberts, D. A.; Johnston, E. L.; Knott, N. A. Impacts of Desalination Plant Discharges on the Marine Environment: A Critical Review of Published Studies. Water Res. Vol.44, pp.5117–5128, 2010.

[74] Lattemann, S.; Höpner, T. Environmental Impact and Impact Assessment of Seawater Desalination. Desalination, vol.220, pp.1–15, 2008.

[75] Hashim, A.; Hajjaj, M. Impact of Desalination Plants Fluid Effluents on the Integrity of Seawater, with the Arabian Gulf in Perspective. Desalination, vol.182, pp.373–393, 2005.

[76] Mabrook, B. Environmental Impact of Waste Brine Disposal of Desalination Plants, Red Sea, Egypt. Desalination, vol.97, pp.453–465, 1994.

[77] Levesque, S.; Rodriguez, M. J.; Serodes, J.; Beaulieu, C.; Proulx, F. Effects of Indoor Drinking Water Handling on Trihalomethanes and Haloacetic Acids. Water Res. Vol.40, pp.2921–2930, 2006.

[78] Yang, X.; Shang, C.; Westerhoff, P. Factors Affecting Formation of Haloacetonitriles, Haloketones, Chloropicrin and Cyanogen Halides during Chloramination. Water Res., vol.41, pp.1193–1200, 2007.

[79] Xu, X.; Mariano, T. M.; Laskin, J. D.; Weisel, C. P. Percutaneous Absorption of Trihalomethanes, Haloacetic Acids, and Haloketones. Toxicol. Appl. Pharmacol., vol.184, pp.19–26, 2002.

[80] Blazak, W. F.; Meier, J. R.; Stewart, B. E.; Blachman, D. C.; Deahl, J. T. Activity of 1,1,1- and 1,1,3-Trichloroacetones in a Chromosomal Aberration Assay in CHO Cells and the Micronucleus and Spermhead Abnormality Assays in Mice. Mutat. Res. Toxicol., vol.206, pp.431–438, 1988.

[81] Merrick, B. A.; Smallwood, C. L.; Meier, J. R.; McKean, D. L.; Kaylor, W. H.; Condie, L. W. Chemical Reactivity, Cytotoxicity, and Mutagenicity of Chloropropanones. Toxicol. Appl. Pharmacol., vol.91, pp.46–54, 1987.

[82] Niri, V. H.; Bragg, L.; Pawliszyn, J. Fast Analysis of Volatile Organic Compounds and Disinfection by-Products in Drinking Water Using Solid-Phase Microextraction-Gas Chromatography/time-of-Flight Mass Spectrometry. J. Chromatogr. A, vol.1201, pp.222–227, 2008.

[83] Wang, S.; Yang, L.; Zu, Y.; Zhao, C.; Sun, X.; Zhang, L.; Zhang, Z. Design and Performance Evaluation of Ionic-Liquids-Based Microwave-Assisted Environmentally

Friendly Extraction Technique for Camptothecin and 10-Hydroxycamptothecin from Samara of Camptotheca Acuminata. Ind. Eng. Chem. Res., vol.50, pp.13620–13627, 2011.

[84] Teo, C. C.; Chong, W. P. K.; Ho, Y. S. Development and Application of Microwave-Assisted Extraction Technique in Biological Sample Preparation for Small Molecule Analysis. Metabolomics, vol.9, pp.1109–1128, 2013.

[85] Wang, H.; Zhou, X.; Zhang, Y.; Chen, H.; Li, G.; Xu, Y.; Zhao, Q.; Song, W.; Jin, H.; Ding, L. Dynamic Microwave-Assisted Extraction Coupled with Salting-out Liquid-Liquid Extraction for Determination of Steroid Hormones in Fish Tissues. J. Agric. Food Chem., vol.60, pp.10343–10351, 2012.

[86] Ma, Y.; Cui, K.; Zeng, F.; Wen, J.; Liu, H.; Zhu, F.; Ouyang, G.; Luan, T.; Zeng, Z. Microwave-Assisted Extraction Combined with Gel Permeation Chromatography and Silica Gel Cleanup Followed by Gas Chromatography-Mass Spectrometry for the Determination of Organophosphorus Flame Retardants and Plasticizers in Biological Samples. Anal. Chim. Acta, vol.786, pp.47–53, 2013.

[87] Dong, S.; Huang, Y.; Zhang, R.; Wang, S.; Liu, Y. Four Different Methods Comparison for Extraction of Astaxanthin from Green Alga Haematococcus Pluvialis. ScientificWorld Journal., vol.02014, pp.1–7, 2014.

[88] Eskilsson, C. S.; Björklund, E. Analytical-Scale Microwave-Assisted Extraction. J. Chromatogr. A, vol.902, pp.227–250, 2000.

[89] Letellier, M.; Budzinski, H. Influence of Sediment Grain Size on the Efficiency of Focused Microwave Extraction of Polycyclic Aromatic Hydrocarbons. Analyst, vol.124, pp.5–14, 1999.

[90] Mandal, V.; Mandal, S. C. Design and Performance Evaluation of a Microwave Based Low Carbon Yielding Extraction Technique for Naturally Occurring Bioactive Triterpenoid: Oleanolic Acid. Biochem. Eng. J., vol.50, pp.63–70, 2010.

[91] Ma, W.; Lu, Y.; Hu, R.; Chen, J.; Zhang, Z.; Pan, Y. Application of Ionic Liquids Based Microwave-Assisted Extraction of Three Alkaloids N-Nornuciferine, O-Nornuciferine, and Nuciferine from Lotus Leaf. Talanta, vol.80, pp.1292–1297, 2010.

[92] Yeh, C.-H.; Tsai, W.-Y.; Chiang, H.-M.; Wu, C.-S.; Lee, Y.-I.; Lin, L.-Y.; Chen, H.-C. Headspace Solid-Phase Microextraction Analysis of Volatile Components in Phalaenopsis Nobby's Pacific Sunset. Molecules, vol.19, pp.14080–14093, 2014.

[93] http://www.guidechem.com/reference/dic-4656.html#id_-1077596984.

[94] http://www.who.int/water_sanitation_health/dwq/chemicals/en/trihalomethanes.

[95] Chan, C.-H.; Yusoff, R.; Ngoh, G.-C.; Kung, F. W.-L. Microwave-Assisted Extractions of Active Ingredients from Plants. J. Chromatogr. A, vol.1218, pp.6213–6225, 2011.

[96] http://macro.lsu.edu/HowTo/solvents/Dielectric%20Constant%20.htm.

[97] EPA Advice Note on Disinfection By-Products in Drinking Water, Advice Note No. 4. Version 2.

[98] King, R.P. and Jonathan, G.E. Aquatic environment perturbations and monitoring: African experience, USA, 166, 2003.

[99] Johal, M.S. and Dua, A. Sem study of the scales of freshwater snakehead Channa punctatus (Bloch.) upon exposure to endosulfan. Bull.Environ.Contam.Toxicol., vol.52, pp.718-721, 1994.

[100] Chiing. C. C., Ren. J. W., Chun, Y., Chung. S. L., Bis (2-chloroethoxy) methane degradation by TiO2 photocatalysis: parameter and reaction pathway investigations. J. Hazard. Mater vol.172, pp.1021-1029, 2009.

[101] Montgomery and Welkom 1990. Montgomery, J.H., Welkom, L.M., Groundwater Chemical Desk Reference, Lewis Publishers, Chelsea, MI. 1990

[102] Thomas, O.V., Stork, J.R., Lammert, S.L., The chromatographic and GC/MS analysis of organic priority pollutants in water. J. Chromatogr. Sci. vol.18, pp.583-594, 1980.

[103] Sittig, M., Handbook of Toxic and Hazardous Chemicals and Carcinogens, third ed., Noyes Public, New Jersey. 1991

[104] Sahng, D. H., Yi, T. C., Cheng. S. L., Determination of haloethers in water by solid -phase microextraction. J. Chromatogr. A vol.769, pp.239-247, 1997.

[105] Fawell, J.K., Hunt, S., Environmental Toxicology: Organic Pollutants, Wiley, New York, 1988

[106] Wennrich, L., Engewald, W., Poppb, P., Determination of chloroethers in aqueous samples using solid-phase microextraction. Acta Hydrochim. Hydrobiol. Vol.25, pp,329-336, 1997.

[107] USEPA. United States Environmental Protection Agency, Office of Water Regulations and Standards Criteria and Standards Division Washington DC 20460 440/5-80-050 October 1980

[108] Chladek E, Marano J, Chromatogr. Sci, vol.22, pp.313-321, 1984

[109] He, Y., Lee, H.K., Liquid-Phase Microextraction in a Single Drop of Organic Solvent by Using a Conventional Microsyringe. Anal. Chem. Vol.69, pp.4634-4642, 1997.

[110] Wang, Y., Kwok, Y.C., He, Y., Lee, H.K., Application of dynamic liquid-phase microextraction to the analysis of chlorobenzenes in water by using a conventional microsyringe. Anal. Chem. Vol.70, pp.4610-4619, 1998.

[111] Chiang, S., Huang, D., Determination of haloethers in water with dynamic hollow fiber liquid-phase microextraction using GC-FID and GC-ECD. Talanta vol.71, pp.882–886, 2007

[112] Shen, G., Lee, H.K., Hollow fiber-protected liquid-phase microextraction of triazine herbicides. Anal. Chem. Vol.74, pp.648-655, 2002.

[113] Zhao, L., Lee, H.K., Liquid-phase microextraction combined with hollow fiber as a sample preparation technique prior to gas chromatography/mass spectrometry. Anal. Chem. Vol.74, pp.2486-2495, 2002.

[114] Ouyang, G., Vuckovic, D., Pawliszyn, J., Nondestructive Sampling of Living Systems Using in Vivo Solid-Phase Microextraction. Chem. Rev., vol.111, pp.2784-2793, 2011.

[115] Jing. S. C., Shang. D. H., Determination of haloethers in water with dynamic hollow fiber liquid-phase microextraction using GC-FID and GC-ECD. Talanta vol.71, pp.882-890, 2007.

[116] Mousa, A., Basheer, C. Al-Arfaj, A.R., Application of electro-enhanced solid-phase microextraction for determination of phthalate esters and bisphenol A in blood and seawater samples. Talanta vol.115, pp.308-315, 2013.

[117] Loeppky RN, Micheljda CJ. Nitrosamines and related N-Nitroso compounds: chemistry and biochemistry. Washington, DC: ACS, 1994.

[118] O'Neill IK, Borstel RCV, Miller CT, Long J, Bartsch H. N-Nitroso Compounds: occurrence, biological effects and relevance to human cancer, IARC Scientific Publication No. 57. Oxford University Press: Lyon, 1984.

[119] US EPA. N-nitrosodimethylamine CASRN 62-75-9, Integrated Risk Information Service (IRIS) Substance File, 1997.

[120] California Department of Health Services. California drinking water: NDMA-related activities, 2000.

[121] Mills AL, Alexander M. Factors affecting dimethylnitrosamine formation in samples of soil and water. J Environ Qual, vol.5, pp.437-441, 1976.

[122] Jobb DB, Hunsinger RB, Meresz O, Taguchi VY. A study of occurrence and inhibition of formation of N-nitrosodimethylamine (NDMA) in the Ohsweken water supply. In: Water quality technology conference. Toronto, Ont: AWWA, pp.103–32, 1992.

[123] Challis BC, Kyrtopoulos SA. Rapid formation of carcinogenic nitrosamines in aqueous alkaline solutions. Br J Cancer; vol.35, pp.693–696, 1977.

[124] Williams DHL. Nitrosation. New York: Cambridge University Press, 1988.

[125] Ayanaba A, Alexander M. Transformations of methylamines and formation of a hazardous product, dimethylnitrosamine in samples of treated sewage and lake water. J Environ Qual, vol.3, pp.83–89, 1974.

[126] Graham JE, Andrews SA, Farquhar GJ, Meresz O. Factors affecting NDMA formation during drinking water treatment. In: Water quality technology conference. New Orleans, LA: AWWA, pp.757–772, 1995.

[127] Weerasooriya SVR, Dissanayake CB. The enhanced formation of N-nitrosamines in fulvic-acid mediated environment. Toxicol Environ Chem; vol.25, pp.57–62, 1989.

[128] Sacher F, Lenz S, Brauch HJ. Analysis of primary and secondary aliphatic amines in waste water and surface water by gas chromatography-mass spectrometry after derivatization with 2,4-dinitrofluorobenzene or benzenesulfonyl chloride. J Chromatogr A, vol.764, pp.85–93, 1997.

[129] Smith TA. The occurrence, metabolism and functions of amines in plants. Bio Rev, vol.46, pp.201–241, 1971.

[130] Isaac RA, Morris J. Transfer of active chlorine from chloramine to nitrogenous organic compounds. 1. Kinetics. Environ Sci Technol, vol.17, pp.738–42, 1983.

[131] Yoon J, Jensen JN. Distribution of aqueous chlorine with nitrogenous compounds: chlorine transfer from organic Chloramines to ammonia. Environ Sci Technol, vol.27, pp.403–409, 1993.

[132] Ferriol M, Gazet J, Adad MS. Chlorine transfer from chloramine to amines in aqueous medium. 1. Reaction between chloramine and methylamine. Inorg Chem, vol.28, pp.3808–3813, 1989.

[133] Ferriol M, Gazet J, Adad MS. Kinetics and mechanisms of chlorine transfer from chloramine to amines in aqueous medium. Int J Chem Kinet, vol.23, pp.315–29, 1991.

[134] Yagil G, Anbar M. The kinetics of hydrazine formation from Chloramine and ammonia. J Am Chem Soc, vol.84, pp.1797–1803, 1962.

[135] Randolph CL, Meyer RE. 1,1-Dimethylhydrazine. US Patent 3050560, USA, 1962

[136] Castegnaro M, Brouet I, Michelon J, Lunn G, Sansone EB. Oxidative destruction of hydrazines produces Nnitrosamines and other mutagenic species. Am Ind Hyg Assoc , vol.47, pp.360–364, 1986

[137] Streitwieser, A., Heathcock, C.H., Kosower, E.M., Introduction to Organic Chemistry, fourth ed. International ed. Macmillan Publishing Com, New York, NY, ISBN 0-02-946482-X, 1992

[138] Nieuwenhuijsen, M. J., Martinez, D., Grellier, J., Bennett, J., Best, N., Iszatt, N., Toledano, M. B., Chlorination disinfection by-products in drinking water and congenital anomalies: review and meta-analyses, Ciência & Saúde Coletiva, vol.15, pp.3109-3123, 2010.

[139] Richardson, S. D., Plewa, M. J., Wagner, E. Schoeny, D., R., DeMarini, D. M., Occurrence, genotoxicity, and carcinogenicity of regulated and emerging disinfection by-products in drinking water: a review and roadmap for research, Mutation Res./Rev. Mutation Res. Vol.636, pp.178-242, 2007.

[140] Krasner, W., Richardson, D., Thruston, D., The occurrence of disinfection by-products (DBPs) of health concern in drinking water: results of a nationwide DBP occurrence study, Jr. 2002.

[141] Sadiq, R., Rodriguez, M. J., Disinfection by-products (DBPs) in drinking water and predictive models for their occurrence: a review, Sci. Tot. Environ. Vol.321, pp.21-46, 2004.

[142] Villanueva, C. M., Cantor, K. P., Grimalt, J. O., Malats, N., Silverman, D., Tardon, A., Kogevinas, M., Bladder cancer and exposure to water disinfection by-products through ingestion, bathing, showering, and swimming in pools, Am. J. Epidemiol. Vol.165, pp.148-156, 2007.

[143] Jelena, R., Maria J., Yang, M., Wolfgang, G., Jurg, K., Reductive electrochemical remediation of emerging and regulated disinfection byproducts, Water Res. Vol.46 pp.1705-1714, 2012.

[144] Chin, A., Bérubé, P. R., Removal of disinfection by-product precursors with ozone-UV advanced oxidation process, Water Res. Vol.39, pp.2136-2144, 2005.

[145] Yang, W., Dong, L.L., Cui, X., Liu, J., Liu, Z., Huo M., Application of ultrasound and quartz sand for the removal of disinfection byproducts from drinking water, Chemosphere. Vol.101, pp.34-40, 2014.

[146] Sentana, M., Rodriguez, E., Prats, D., Effect of pressure and pH over the removal of disinfection by-products using nanofiltration membranes in discontinuous systems, Desal. Water Treat. Vol.23, pp.3-12, 2013.

[147] Maria, J.F., Julien, R., Francois, X.A., Maxime, R., Juorg, K., Wolfgang, G., Fate of N-nitrosodimethylamine, trihalomethane and haloacetic acid precursors in tertiary treatment including biofiltration, Water Res. Vol.45, pp.5695-5704, 2011.

[148] Abaliwano, J. K., Ghebremichael, K. A., Amy, G. L., Application of Purified Moringa Oleifera Coagulant for Surface Water Treatment; Water Mill Working Paper Series no. 5; UNESCO-IHE Institute for Water Education: Delft, Netherlands. 2008.

[149] Sutherland, J. P., Folkard, G. K., Mtawali, M. A., Moringa oleifera as a natural coagulant. Grant, Proceedings of the 20th WEDC Conference, Colombo, Sri Lanka. pp.297-299, 1994.

[150] Bergman, E., Matsinhe, M., Pearson, N., Arnoldsson, K.M., Assessment of Drinking Water Treatment Using Moringa oleifera Natural Coagulant. VATTEN Edition, vol.64 pp.137-150, 2008.

[151] Suarez, M., Entenza, J. M., Doerries, C., Meyer, E., Bourquin, L., Sutherland, J., Marison, I., Moreillon, P., Mermod, N., Expression of a plant-derived peptide harboring water-cleaning and antimicrobial activities, Biotechnol. Bioeng. Vol.81, pp.13-20, 2003.

[152] Bhatti, H.N., Mumtaz, B., Hanif, M. A., Nadeem, R., Removal of Zn(II) ions from aqueous solution using Moringa oleifera Lam. (horseradish tree) biomass, Process Biochem. Vol.42, pp.547–553, 2007.

[153] Igwe, J. C., Ogunewe, D. N., Abia, A. A., Competitive adsorption of Zn(II), Cd(II), and Pb(II) ions from aqueous and non-aqueous solutions by maize cob and husk, Afr. J. Biotechnol. Vol.4, pp.1113-1116, 2005.

[154] Rajeswari, M., Pushpa, A., Pavithra, S., Priya, G., Sandhya, R., Pavithra G. M., Continuous Biosorption of Cadmium by Moringa olefera in a Packed Column, Biotechnol. Bioprocess Eng. Vol.18, pp.321-325, 2013.

[155] Mike, A., Joana, P.C., Pereira, J.W., Meulepas, N.L., Kinetics modelling of Cu(II) biosorption on to coconut shell and Moringa oleifera seeds from tropical regions Lens, Environ. Technol. Vol.33, pp.409-417, 2012.

[156] Megat, J., Moringa oleifera seeds as a flocculant in waste sludge treatment, Int. J. Environ. Stud. Vol.58, pp.185-195, 2001.

[157] Suleyman, A., Muyibi, L., Evison, M., Moringa oleifera seeds for softening hardwater, Water Res. Vol.29, pp.1099-1105, 1995.

[158] USEPA, National primary drinking water regulations: stage 2 disinfectants and disinfection by products rule. Federal Register. Vol.71, pp.387-493, 2006.

[159]USEPA.http://water.epa.gov/scitech/swguidance/standards/upload/_10_12_criteria _ambientwqc_haloethers80.pdf.2001

[160] Water Environments. Guidelines for Safe Recreational-water Environments Final Draft for Consultation Vol. 2: Swimming Pools, Spas and Similar Recreational-water Environments. 2000

[161] WHO/SDE/WSH/03.04/64.http://www.who.int/water_sanitation_health/dwq/chemicals/ en/trihalomethanes.pdf. 2004.

[162] Pal, S., Kyeong-Hee, L., Jong-Uk, K., Seung-Hee, H., Song, J.M., Adsorption of cyanuric acid on activated carbon from aqueous solution: effect of carbon surface modification and thermodynamic characteristics, J. Colloid Interface Sci. vol.303, pp.39-48, 2006.

[163] Anwar, F., Rashid, U., Physico-chemical characteristics of Moringa oleifera seeds and seeds oil from a wild provenance of Pakistan, Pak. J. Bot. vol.39, pp.1443-1453, 2007.

[164] Raghuvanshi, S. P., Singh, R. C., Kaushik, P., kinetics study of methylene blue dye bioadsorption on baggase, Appl. Ecol. Environ Res. Vol.2, pp.35-43, 2004.

[165] Jose, T., Oliveira, S., Vasconcelos, L., Cavada, B., Moriera, R., Compositional and nutritional attributes of seeds from the multipurpose tree Moringa oleifera Lamarck, J. Sci. Food Agri. Vol.79, pp.815-820, 1999.

[166] Makkar, H., Becker, K., Nutrients and antiquality factors in different morphological parts of Moringa oleifera tree, J. Agric. Sci. Camb. Vol.128, pp.311–322, 1997.

[167] Ndabigengesere, A., Narasiah, K. S., Talbot, B. G., Active agents and mechanism of coagulation of turbid waters using Moringa oleifera, Water Res. Vol.29, pp.703-710, 1995.

[168] Gassenschmidt, U., Jany, K. D., Tauscher, B., Niebergall, H., Isolation and characterization of a flocculating protein from Moringa oleifera Lam, Biochim. Biophys. Acta. Vol.1243, pp.477-481, 1995.

[169] Muyibi, S., Evison, L., Moringa oleifera seeds for softening hard water. Water Res. Vol.29, pp.1099-1104, 1995.

[170] Okuda, T., Baes, A., Nishijima, W., Okada, M., Coagulation mechanism of salt solution-extracted active component in Moringa oleifera seeds, Water Res. Vol.35, pp.830-834, 2001.

[171] Ghebremichael, K. A., Moringa Seed and Pumice as Alternative Natural Materials for Drinking Water Treatment. Ph.D Thesis. KTH Royal Institute of Technology, Stockholm, November. 2004

[172] Larous, S., Meniai, A.H., Lehocine, M.B., Experimental study of the removal of copper from aqueous solutions by adsorption using sawdust, Desalination vol.185, pp.483–490, 2005

[173] Bedient, P.H., Rifai, H.S., Newell, C.J., Ground Water Contamination: Transport and Remediation. Prentice Hall, Englewood Cliffs, NJ. 1994

[174] Lagergren, S., About the theory of so-called adsorption of solution substances K. Sven. Vetenskapsakad. Handl. Vol.24, pp.1-39, 1898.

[175] Ho, Y.S., Review of second-order models for adsorption systems, J. Hazard. Mater. Vol.136, pp.681-689, 2006.

[176] Webber, T.N., Chakravarti, R.K., Pore and solid diffusion models for fixed bed adsorbers, J. Am. Inst. Chem. Eng. Vol.20, pp.228-238, 1974.

[177] Lou, C., Tseng, B., Wu, C., Han, Y. Chen, H., Removal of disinfection by-products in raw water using a biological powder-activated carbon system, J. Environ. Sci. Health, Part A, vol.47, pp.1478–1485, 2012.

[178] Lou, C., Chang, W. Huang, E., Effective removal of disinfection by-products and assimilable organic carbon: An advanced water treatment system, J. Hazard. Mat. Vol.172, pp.1365–1371, 2009.

VITAE

Name	ABDULNASER KHALED ALSHARAA
Nationality	SYRIAN
Date of Birth	01/03/1984
Email	abdnacero6@gmail.com
Address	Chemistry Department, KFUPM, Dhahran, Saudi Arabia

Academic Background:

 (Jun, 2005) BSc. in Applied Chemistry, Department of Chemistry, Faculty of Science, Damascus University, Syria.

 (Oct, 2008- Jun, 2010) Research Assistant and MS. Student at the Department of Chemistry, Faculty of Science, KFUPM, KSA.

 (Sep. 2013- May, 2016) Lecturer B and PhD student, KFUPM, KSA.

 Published papers:

1. Single-step microwave assisted headspace liquid-phase microextraction of trihalomethanes and haloketones in biological samples, **Abdulnaser Alsharaa**, Basheer Chanbasha and Muhammad Sajid. **Journal of chromatography B**. **2015**, 1007, 43-48.

2. Flow assisted electro-enhanced solid-phase microextraction for the determination of haloethers in water samples, **Abdulnaser Alsharaa**, Basheer Chanbasha, Mousa Amayreh and Muhammad Sajid, **Chromatographia**. **2015**, 1-6.

 Submitted papers:

1. Removal of haloethers, trihalomethanes and haloketones from water using Moringa olifera seeds
   Abdulnaser Alsharaa, Chanbasha Basheer, Salawu Omobayo Adioc, Khalid Alhooshani and Hian Kee Lee (submitted to **International Journal of Environmental Science and Technology journal**).

2. Determination of Haloacidic Acids in Water using Layered Double Hydroxides as Sorbent in Dispersive Solid-Phase Extraction followed by Liquid Chromatography-Tandem Mass Spectrometric Analysis
   Abdulnaser Alsharaa and Basheer Chanbasha, Khalid Alhooshani and Hian Kee Lee (Submitted to J**ournal of Separation Science)**.

 Submitted Patent:

1. Chanbasha, B., Abdulnaser Alsharaa, Flow-assisted Electro-enhanced Solid Phase Microextraction.

2. Chanbasha, B., Abdulnaser Alsharaa, Single-Step Microwave Assisted Headspace Liquid-Phase Microextraction.

 Conference:

1. Poster Presentations, April, 2014: Flow assisted electro-enhanced solid-phase microextraction for the determination of haloethers in water samples, The 5th Saudi Student Conference 2014 (Riyadh, Saudi Arabia). I got 7th prize for nice scientific presentation from ministry of education.